

University of Warwick institutional repository: <http://go.warwick.ac.uk/wrap>

**A Thesis Submitted for the Degree of PhD at the University of Warwick**

<http://go.warwick.ac.uk/wrap/57669>

This thesis is made available online and is protected by original copyright.

Please scroll down to view the document itself.

Please refer to the repository record for this item for information to help you to cite it. Our policy information is available from the repository home page.

## Library Declaration and Deposit Agreement

### 1. STUDENT DETAILS

Please complete the following:

Full name: MICHAEL KERR

University ID number: 0859190

### 2. THESIS DEPOSIT

2.1 I understand that under my registration at the University, I am required to deposit my thesis with the University in BOTH hard copy and in digital format. The digital version should normally be saved as a single pdf file.

2.2 The hard copy will be housed in the University Library. The digital version will be deposited in the University's Institutional Repository (WRAP). Unless otherwise indicated (see 2.3 below) this will be made openly accessible on the Internet and will be supplied to the British Library to be made available online via its Electronic Theses Online Service (ETHOS) service.

[At present, theses submitted for a Master's degree by Research (MA, MSc, LLM, MS or MMedSci) are not being deposited in WRAP and not being made available via EthOS. This may change in future.]

2.3 In exceptional circumstances, the Chair of the Board of Graduate Studies may grant permission for an embargo to be placed on public access to the hard copy thesis for a limited period. It is also possible to apply separately for an embargo on the digital version. (Further information is available in the *Guide to Examinations for Higher Degrees by Research*.)

2.4 If you are depositing a thesis for a Master's degree by Research, please complete section (a) below. For all other research degrees, please complete both sections (a) and (b) below:

#### (a) Hard Copy

I hereby deposit a hard copy of my thesis in the University Library to be made publicly available to readers (please delete as appropriate) EITHER immediately ~~OR after an embargo period of~~ ..... months/years as agreed by the Chair of the Board of Graduate Studies.

I agree that my thesis may be photocopied. YES / ~~NO~~ (Please delete as appropriate)

#### (b) Digital Copy

I hereby deposit a digital copy of my thesis to be held in WRAP and made available via ETHOS.

Please choose one of the following options:

EITHER My thesis can be made publicly available online. YES / ~~NO~~ (Please delete as appropriate)

OR My thesis can be made publicly available only after.....[date] (Please give date)  
YES / NO (Please delete as appropriate)

OR My full thesis cannot be made publicly available online but I am submitting a separately identified additional, abridged version that can be made available online.  
YES / NO (Please delete as appropriate)

OR My thesis cannot be made publicly available online. YES / NO (Please delete as appropriate)

### 3. GRANTING OF NON-EXCLUSIVE RIGHTS

Whether I deposit my Work personally or through an assistant or other agent, I agree to the following:

Rights granted to the University of Warwick and the British Library and the user of the thesis through this agreement are non-exclusive. I retain all rights in the thesis in its present version or future versions. I agree that the institutional repository administrators and the British Library or their agents may, without changing content, digitise and migrate the thesis to any medium or format for the purpose of future preservation and accessibility.

### 4. DECLARATIONS

(a) I DECLARE THAT:

- I am the author and owner of the copyright in the thesis and/or I have the authority of the authors and owners of the copyright in the thesis to make this agreement. Reproduction of any part of this thesis for teaching or in academic or other forms of publication is subject to the normal limitations on the use of copyrighted materials and to the proper and full acknowledgement of its source.
- The digital version of the thesis I am supplying is the same version as the final, hard-bound copy submitted in completion of my degree, once any minor corrections have been completed.
- I have exercised reasonable care to ensure that the thesis is original, and does not to the best of my knowledge break any UK law or other Intellectual Property Right, or contain any confidential material.
- I understand that, through the medium of the Internet, files will be available to automated agents, and may be searched and copied by, for example, text mining and plagiarism detection software.

(b) IF I HAVE AGREED (in Section 2 above) TO MAKE MY THESIS PUBLICLY AVAILABLE DIGITALLY, I ALSO DECLARE THAT:

- I grant the University of Warwick and the British Library a licence to make available on the Internet the thesis in digitised format through the Institutional Repository and through the British Library via the EThOS service.
- If my thesis does include any substantial subsidiary material owned by third-party copyright holders, I have sought and obtained permission to include it in any version of my thesis available in digital format and that this permission encompasses the rights that I have granted to the University of Warwick and to the British Library.

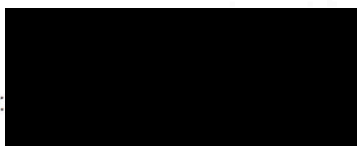
### 5. LEGAL INFRINGEMENTS

I understand that neither the University of Warwick nor the British Library have any obligation to take legal action on behalf of myself, or other rights holders, in the event of infringement of intellectual property rights, breach of contract or of any other right, in the thesis.

---

*Please sign this agreement and return it to the Graduate School Office when you submit your thesis.*

Student's signature:



Date: 11-JULY-2013





The role of adenosine in the modulation of  
synaptic transmission and action potential  
firing of thick-tufted layer 5 pyramidal  
neurons

Michael Kerr

A thesis submitted for the degree of Doctor of Philosophy  
University of Warwick, Systems Biology Doctoral Training Centre  
March 2013

# Contents

<b>Chapter 1. Introduction</b>	<b>1</b>
1.1 Neocortex	1
1.1.1 Neocortical Microcircuit	4
1.1.2 Pyramidal Neurons	10
1.1.3 Cortical Synaptic Plasticity	12
1.1.4 Cortical Network Dynamics	15
1.1.5 Neuromodulators in the Neocortex	17
1.2 Adenosine	18
1.2.1 Regulation of Adenosine Concentration	18
1.2.2 Adenosine Receptors	21
1.2.3 Physiological and Pathophysiological roles of Adenosine	23
1.3 Thesis Outline	27
<b>Chapter 2. Methods</b>	<b>29</b>
2.1 Electrophysiology	29
2.1.1 Slice Preparation	29
2.1.2 Intracellular Recording	30
2.1.3 Biosensors	31
2.1.4 Drugs	32
2.2 Histology	33
2.3 Analyses and Modelling	34
2.3.1 Deconvolution	34
2.3.2 Model of Synaptic Dynamics	34
2.3.3 Mean Variance Analysis	35
2.3.4 Measuring Asynchronous EPSPs in Strontium	36
2.3.5 Concentration Response Curves	37
2.3.6 Dynamic I-V Measurement	38
2.3.7 Electrode Filter	41

<b>Chapter 3. Characterisation of adenosine mediated suppression of mono-synaptic transmission between thick-tufted layer 5 pyramidal neurons of the juvenile rat somatosensory cortex</b>	<b>43</b>
3.1 Introduction	43
3.2 Results	45
3.2.1 Identification of neurons and mono-synaptic connections	45
3.2.2 Suppression of EPSPs by adenosine through A <sub>1</sub> R activation	47
3.2.3 Adenosine transforms synaptic dynamics	52
3.2.4 Effects of adenosine on binomial parameters	56
3.3 Discussion	69
<b>Chapter 4. Adenosine A<sub>1</sub> receptor activation underlies the developmental shift at layer 5 pyramidal cell synapses and is a key determinant of mature synaptic strength</b>	<b>74</b>
4.1 Introduction	74
4.2 Results	77
4.2.1 Characteristics of connections across development	77
4.2.2 Suppression of EPSPs by adenosine and detection of tone by 8-CPT	79
4.2.3 Adenosine controls the synaptic dynamics observed at these connections	83
4.2.4 Effects of A <sub>1</sub> R activation on EPSP variability and reliability	87
4.2.5 Estimating A <sub>1</sub> R activation by endogenous adenosine	92
4.2.6 Variability in baseline A <sub>1</sub> R activation	98
4.3 Discussion	100
<b>Chapter 5. Characterisation of the post-synaptic suppression of thick-tufted layer 5 pyramidal neurons by adenosine using naturalistic current injection and dynamic I-V curves</b>	<b>105</b>
5.1 Introduction	105
5.2 Results	108
5.2.1 Calculation of dynamic I-V curve and rEIF parameters	108
5.2.2 Effects of adenosine on sub-threshold neuronal properties	113
5.2.3 Effects of adenosine on firing and action potentials	118

5.2.4 Action potential parameters	121
5.2.5 Action potential bursting	122
5.2.6 Increase in endogenous activation of A <sub>1</sub> receptors during development	127
5.2.7 Dendritic current injection	127
5.2.8 I <sub>h</sub> sag reduction in adenosine	132
5.2.9 Action potential back propagation	133
5.3 Discussion	137
<b>Chapter 6. General Discussion</b>	<b>141</b>
6.1 Adenosine and sleep in the neocortex	142
6.2 Adenosine and homeostatic modulation	145
6.3 Tonic and phasic A <sub>1</sub> receptor activation	146
6.4 Modelling the effects of neuromodulation	148
<b>Chapter 7. Conclusions and Future Perspectives</b>	<b>150</b>
7.1 Conclusions	150
7.2 Future perspectives	152
<b>8. References</b>	<b>157</b>

## Tables

Table 1.1 Adenosine receptors in the brain	22
Table 3.1 Summary of adenosine and 8-CPT effects of thick tufted pyramidal neuron membrane potential and EPSP parameters	48
Table 5.1 Measured action potential parameters in each pharmacological manipulation	122

## Figures

Figure 1.1 Anatomy of neocortex	3
Figure 1.2 Neocortical microcircuit diagram	8
Figure 1.3 Structure of pyramidal neurons	11
Figure 1.4 Cortical synaptic dynamics	13

Figure 1.5 Cortical slow oscillation	16
Figure 1.6 Pathways of adenosine metabolism	20
Figure 3.1 Identification of thick tufted layer 5 pyramidal neurons	47
Figure 3.2 Summary of suppression of EPSPs by adenosine	49
Figure 3.3 Pharmacology of adenosine mediated EPSP suppression	52
Figure 3.4 Effects of adenosine on synaptic dynamics	55
Figure 3.5 Suppression by adenosine is mediated by a reduction in probability of transmitter release	58
Figure 3.6 Adenosine causes increased EPSP variability and failures	61
Figure 3.7 Mean variance analyses of effects of adenosine	64
Figure 3.8 Adenosine has no significant impact on aEPSP amplitude	66
Figure 3.9 Analysis of strontium experiments reveals deviation from binomial release statistics in adenosine	68
Figure 4.1 The characteristics of synaptic transmission at 3 stages of post-natal development	79
Figure 4.2 Effects of applied and endogenous adenosine on synaptic transmission at each stage of development	81
Figure 4.3 Increased A <sub>1</sub> R activation underlies the developmental shift from depression to facilitation at synapses between thick-tufted layer 5 pyramidal neurons	86
Figure 4.4 A <sub>1</sub> R activation determines variability and reliability at mature layer 5 pyramidal synapses	90
Figure 4.5 Endogenous adenosine concentration at synapses increases during development	94
Figure 4.6 Use of enzymatic biosensors to detect endogenous extracellular adenosine	96
Figure 4.7 No significant difference was detected in the concentration of adenosine between juvenile and mature slices	97
Figure 4.8 Basal A <sub>1</sub> R activation varies significantly between synapses within same individual and with the same slice	99
Figure 5.1 Protocol for the generation of the dynamic I-V curve	111
Figure 5.2 Measurement of post-spike refractory properties in control conditions	112



Figure 5.3 Summary of parameter changes in adenosine and 8-CPT in the rEIF model	115
Figure 5.4 Calculation of input resistance	117
Figure 5.5 Summary of adenosine-mediated suppression of firing	120
Figure 5.6 Adenosine modulation of action potential burst firing	126
Figure 5.7 Effects of endogenous adenosine tone across development	129
Figure 5.8 Increased suppression of firing by adenosine for current injected from the apical dendrite	131
Figure 5.9 Adenosine reduction of $I_h$ sag at soma and apical dendrite	133
Figure 5.10 Increased attenuation of back-propagating action potentials (BAPs) in adenosine	136

## **Acknowledgements**

First and foremost I would like to express my sincere gratitude to my supervisors Dr Magnus Richardson and Dr Mark Wall for their continual support and guidance throughout my PhD, making the whole process as enjoyable as it has been valuable. I would like to thank my PhD committee members Professor Nicolas Dale, Dr Marco Van den Top and Professor Nigel Stocks for their helpful advice.

I would also like to thank the Warwick Systems Biology DTC for giving me the opportunity to undertake the project. It has been a fantastic experience to spend time working at the Systems Biology DTC and School of Life Sciences and I would like to thank those in the lab and office who I have had the privilege of both getting to know and collaborating with during my time at Warwick.

Finally I would like to thank my family for their patience and support while I have been writing this thesis.

## **Declaration**

I, Michael Kerr, hereby declare that all of the work in this thesis is my own unless otherwise stated in the text or figure legends. None of this work has been previously submitted for any degree at this or any other institution. All sources of information used in the preparation of this thesis are indicated by references.

## Abstract

The actions of many neuromodulators induce changes in synaptic transmission and membrane excitability, and many of these effects are well documented in neurons across the CNS. Adenosine acts as a powerful modulator across the CNS and while its actions have been characterised in some neurons in the neocortex, its effects on excitatory transmission in layer 5 remain unstudied. Adenosine has been implicated in the modulation of spontaneous activity generated in the layer 5 excitatory network, thus understanding its actions in this area are of substantial importance.

This study used a combined approach of paired intracellular recordings and quantitative modelling to investigate the actions of adenosine on thick-tufted layer 5 pyramidal neurons in the rat somatosensory cortex.

Adenosine was found to powerfully suppress synaptic transmission between these neurons and the changes in synaptic dynamics could be precisely captured as a change only in probability of release in a simple phenomenological model. Recordings conducted at three post-natal ages provide evidence that an increased tone of endogenous adenosine is responsible for the previously described developmental shift in short-term dynamics and reliability at this synapse. The data illustrates both that this endogenous activation of A<sub>1</sub> receptors is highly heterogeneous, with variation between neighbouring synapses, and that it plays a significant role in EPSP parameters observed at mature connections.

An investigation into adenosine's post-synaptic actions using an approach that measures the neurons' I-V response to naturalistic current inputs demonstrates how adenosine's actions on membrane excitability translate to a strong suppression of spiking. Simultaneous dendritic and somatic recordings demonstrate that this effect is enhanced when current is injected from the dendrite and that back-propagating bursts of action potentials are selectively suppressed by adenosine. As a whole the work illustrates that the effects of adenosine can be well captured by mathematically tractable quantitative models.

## Abbreviations

<b>5-HT<sub>1</sub></b>	5-Hydroxytryptamine (1) receptor
<b>8-CPT</b>	8-cyclopentyltheophylline
<b>A<sub>1</sub>R</b>	adenosine A <sub>1</sub> receptor
<b>A<sub>2A</sub>R</b>	adenosine A <sub>2A</sub> receptor
<b>ABC</b>	avidin-biotin complex
<b>aCSF</b>	artificial cerebrospinal fluid
<b>ADO</b>	adenosine (biosensor)
<b>ADA</b>	adenosine deaminase
<b>aEPSP</b>	asynchronous excitatory post-synaptic potential
<b>AK</b>	adenosine kinase
<b>AMPA</b>	alpha-amino-3-hydroxy-5-methyl-4-isoxazolepropionic acid
<b>ATP</b>	adenosine 5' triphosphate
<b>BAP</b>	back-propagating action potential
<b>CA1</b>	<i>Cornu Ammonis</i> 1 (Hippocampus)
<b>cAMP</b>	cyclic adenosine 5' monophosphate
<b>CNS</b>	central nervous system
<b>CNT</b>	concentrative nucleoside transported
<b>CPA</b>	N <sup>6</sup> -cyclopentyladenosine
<b>CNQX</b>	6-cyano-7-nitroquinoxaline-2,3-dione
<b>CSF</b>	cerebrospinal fluid
<b>CV</b>	coefficient of variation
<b>DAB</b>	diaminobenzidine
<b>EEG</b>	electroencephalography
<b>EGTA</b>	ethylene glycol tetraacetic acid
<b>EIF</b>	exponential integrate-and-fire
<b>ENT</b>	equilibrative nucleoside transporter
<b>EPSC</b>	excitatory post-synaptic current
<b>EPSP</b>	excitatory post-synaptic potential



<b>GABA</b>	gamma-aminobutyric acid
<b>GABA<sub>A</sub></b>	gamma-aminobutyric acid receptor A
<b>GABA<sub>B</sub></b>	gamma-aminobutyric acid receptor B
<b>GIRK</b>	G-protein coupled inwardly rectifying potassium channel
<b>GPCR</b>	G-protein coupled receptor
<b>HCN</b>	hyperpolarisation-activated cyclic-nucleotide gated channel
<b>HEPES</b>	4-(2-hydroxyethyl)-1-piperazineethanesulfonic acid
<b>INO</b>	inosine (biosensor)
<b>I<sub>h</sub></b>	hyperpolarisation activated current
<b>IPSP</b>	inhibitory post-synaptic potential
<b>IR-DIC</b>	infra-red differential interference contrast
<b>I-V</b>	current-voltage
<b>LTD</b>	long-term depression
<b>LTP</b>	long-term potentiation
<b>M<sub>1</sub></b>	muscarinic receptor (1)
<b>mGluR</b>	metatropic glutamate receptor
<b>mRNA</b>	messenger ribonucleic acid
<b>NMDA</b>	N-methyl D-aspartic acid
<b>PBS</b>	phosphate buffer solution
<b>PPR</b>	paired-pulse ratio
<b>rEIF</b>	refractory exponential integrate-and-fire
<b>sEPSP</b>	spontaneous excitatory post-synaptic potential
<b>SK</b>	small conductive calcium-activated potassium channel
<b>STSD</b>	short-term synaptic depression
<b>TBS</b>	tris buffer solution
<b>TTL5</b>	thick-tufted layer 5
<b>V1</b>	primary visual cortex
<b>V2</b>	visual area 2



# 1. Introduction

This thesis seeks to further our understanding of the actions of adenosine in the neocortex. Adenosine is produced and acts across many regions of the brain, and while its actions have been well studied in many areas, precisely how it modulates activity in the neocortex remains unclear. I have focused my research on how adenosine can alter the excitability and synapses of the thick-tufted layer 5 pyramidal neuron. In doing so I aim to demonstrate how an understanding of neuromodulation is best achieved by considering it in the context of the history dependent synaptic dynamics and firing outputs of neurons. I have also studied the degree to which these neuromodulatory effects can be applied to simple, mathematically tractable models and thus considered using a systems approach to the resultant network effects.

The introduction will review aspects of neurophysiology and pharmacology that are of interest to the work outlined in the body of the thesis, beginning with an overview of the architecture and functions of the mammalian neocortex, with particular focus on the pyramidal neurons found in layer 5. This will be followed by an overview of the actions of adenosine in the central nervous system. Finally I will outline the body of research contained in the thesis.

## 1.1 Neocortex

In evolutionary terms the neocortex is the newest part of the mammalian brain. Although its origins can be traced to amniotes in the Carboniferous

period, it emerged as a 6-layered sheet in small mammals in the end-Triassic period. Since then it has undergone expansion in size and complexity in many mammalian clades, culminating in the heavily convoluted structure seen in humans today (Rakic, 2008).

The neocortex is vital for many higher cognitive processes such as perception, the generation of motor commands, memory storage and reasoning. As a result of these broad functions, abnormalities in the neocortex are associated with a range of neurophysiological disorders such as schizophrenia, autism, epilepsy and Alzheimer's disease. Nevertheless, in spite of this functional diversity it remains relatively structurally homogenous in humans. This homogeneity, whilst implying evolutionary constraints also suggests a significant adaptive value for the layered sheet structure (Karlen and Krubitzer, 2006).

Whilst anatomical studies of neuronal morphologies have a long history – most famously Cajal's Golgi stains (fig 1.1c, Cajal, 1911) – other aspects of cortical architecture have been revealed only with the advancement of intracellular electrophysiological techniques in the latter part of the 20<sup>th</sup> century. The ubiquity of neocortical morphology between species has meant that the organisation of the neocortex – in terms of neuronal subtypes, their connectivity and electrophysiological properties has been studied utilising a variety of animal models. Thus, although Vernon Mountcastle first proposed the columnar organisation of sensory cortices based on studies in cats (Mountcastle *et al.*, 1957), recent work has been largely focused on rodents (Markram, 2006).

Much of the focus on cortical architecture draws on the concept of the cortical column, defined by Mountcastle as “an elementary unit of organisation in the somatic cortex made up of a vertical group of cells extending through all the cellular layers.” This observation was given an apparent confirmation in the visual cortex by Hubel and Weisel (Hubel and Wiesel, 1962). They saw that, at a given site, recorded cells invariably had the same receptive field orientation. Together these studies established the quantal nature of columnar organisation. Since these pioneering studies the column has remained central to descriptions of cortical architecture even as its definition has broadened continually.

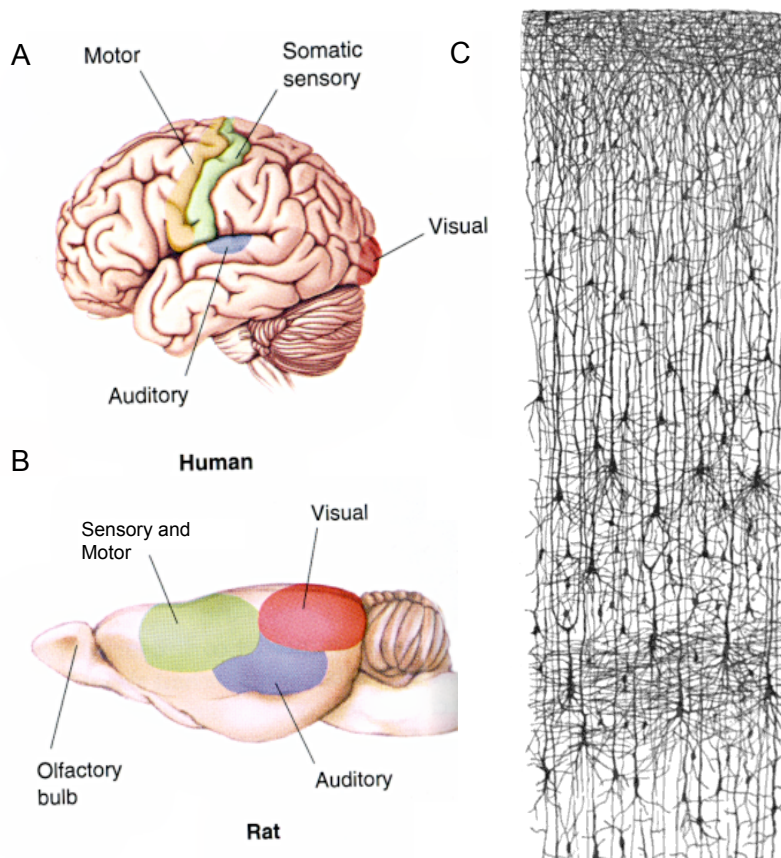


**Fig 1.1** (A and B) Illustrations of regions of sensory and motor cortex in the human (A) and rat (B) brain (Bear & Connors, 2006). (C) A Golgi stain demonstrating the distinctive neuronal architecture of neocortex (human infant, Cajal, 1911).



While the barrel cortex in rats, where individual whiskers map precisely to discrete cortical regions, presents a striking example of modular organisation, recent reviews have questioned whether any discrete functionality exists in columns in other regions of the cortex (Horton and Adams, 2005). Others have suggested that while functional columns do exist they are impressively diverse in terms of size, neuronal composition, connectivity and function (Rakic, 2008), with the concept perhaps persisting mainly because it appeals to a basic desire to find organising principals in the brain.

Despite the ongoing debate regarding columns there does however remain an impressive array of canonical elements in cortical microcircuit architecture (Silberberg *et al.*, 2002), the most obvious canonical feature being the layered structure. It is these elements, detailed below, that make the study of microcircuit function so broadly important to cortical neuroscience in general.

### 1.1.1 The neocortical microcircuit

The neocortex is generally divided into six layers. The degree of distinction between individual layers in general depends on the particular cortical region in question.

**Layer 1:** The most superficial layer of the neocortex is only sparsely populated by neuronal somata, the vast majority of which are GABAergic (Hestrin and Armstrong, 1996). Dendritic tufts from some types of pyramidal neurons in deeper layers bifurcate in layer 1 and these receive

inhibitory inputs from an array of interneuron subtypes, in particular Martinotti neurons whose ascending axons arborize horizontally in layer 1. Excitatory axons in this layer come both from other cortical areas as well as a significant number from the thalamus (Rubio-Garrido *et al.*, 2009). Also abundant in this layer are astrocytes that exhibit frequent spontaneous asynchronous  $\text{Ca}^{2+}$  activity, distinct from the synchronous activity seen in other layers (Takata and Hirase, 2008).

**Layer 2/3:** The distinction between layers 2 and 3 is strong only in the primary visual cortex (V1), where cells in layer 3 show much stronger spatial and directional selectivity (Gur and Snodderly, 2008). Layer 2 also has a much larger population of stellate cells that project only locally, in contrast to the large population of pyramidal neurons projecting to V2 in layer 3 (Lund, 1973). In other sensory regions layer 2/3 receives strong feed-forward excitatory input from layer 4. The excitatory neurons in layer 2/3 from recurrent sub-networks based on common layer 4 inputs (Yoshimura *et al.*, 2005). Different sub-networks then provide converging feed-forward inputs onto pyramidal neurons in layer 5 (Kampa *et al.*, 2006).

**Layer 4:** Although neurons in all layers of the neocortical sensory areas receive thalamic inputs, most occur within layer 4, and this layer is absent in the motor cortex. It is in layer 4 of the rodent somatosensory cortex where barrels are most prominent, each barrel containing neurons with sharp receptive fields that respond to the stimulation of a single whisker (Simons, 1978). Spiny stellate neurons are the predominant excitatory neuron in this layer. These neurons predominantly target pyramidal neurons in layer 2/3,

with a typical connection probability of 0.1 (Feldmeyer *et al.*, 2002), despite the large distance. Thalamic inputs occur with higher probability and greater efficacy onto fast-spiking interneurons in layer 4, compared to stellate neurons. This inhibition feeds forward onto the stellate cells and causes the circuitry in this layer to be particularly sensitive to the precise timing of firing in thalamic neurons (Bruno and Simons, 2002).

**Layer 5:** Layer 5 pyramidal neurons provide the major intra and sub-cortical outputs in the sensory cortices. The layer is sometimes segregated into layer 5a and 5b, and in some cortical regions there is a clear distinction based on neuronal inputs and morphology. Layer 5a pyramidal neurons receive thalamic input, tend not to exhibit spike adaptation, and project mainly to intra-cortical targets. Layer 5b pyramidal neurons are located deeper within layer 5 and send axonal projections to sub-cortical targets (pons, superior colliculus, spinal cord and striatum). The two classes also exhibit differing apical dendrite morphologies. Layer 5b neurons have thicker apical dendrites and branch extensively in layer 1, and are commonly referred to as thick-tufted layer 5 pyramidal neurons in the literature (Romand *et al.*, 2011). Similar to layer 4 and 2/3, the excitatory neurons in layer 5 form recurrent connections with each other (Nicoll & Blakemore, 1990). Both the connectivity and synaptic strengths are non-random (Perin *et al.*, 2011), though as yet little is understood regarding the functionality of these assemblies. Pyramidal neurons in layer 5 seem to have the highest spontaneous and evoked mean firing rates among excitatory neurons in the sensory cortices (Barth and Poulet, 2012).

**Layer 6:** The deepest cortical layer, 6, is perhaps also the least well understood. The neuronal population in this layer is relatively more heterogeneous than other layers (Chen *et al.*, 2009; Thomson, 2010). Layer 6 neurons receive significant monosynaptic thalamic input and in the primary sensory cortices neurons located in layer 6 provide projections to the thalamic reticular nucleus (Sherman & Guillery, 2005). However layer 6 also contains a significant amount of neurons providing outputs to the claustrum, superior colliculus and other nuclei in the thalamus (Briggs, 2010).

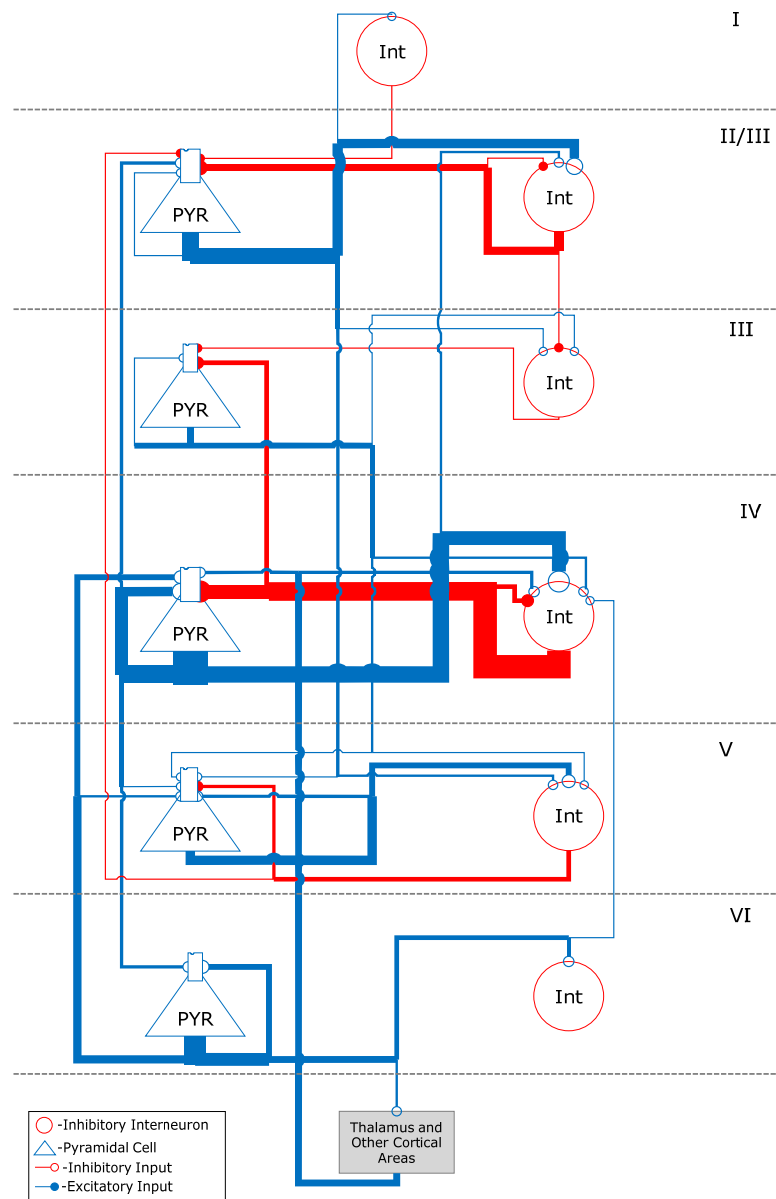


**Fig 1.2** Simplified canonical diagram of the neocortical microcircuit, illustrating the relative weighting of each canonical pathway (Yuste, 2012).

**Inhibitory interneurons:** The above summary mainly details the major excitatory circuitry in the neocortex. The GABAergic interneurons of the neocortex, despite only accounting for ~10 % (Meyer *et al.*, 2011) of the total neuron count, exhibit striking diversity in their morphological, electrophysiological and molecular properties (Markram *et al.*, 2004). In



broad terms these interneurons can be classified according to where they form synapses on excitatory neurons (soma, dendrite or axonal initial-segment), by their spiking properties (e.g. fast-spiking or adapting), and by their expression of various peptides and calcium binding proteins (e.g. somatostatin or parvalbumin). There is, to some extent, overlap in these classification methods. For example cells with a basket cell morphology target the soma of excitatory neurons, exhibit fast-spiking and express parvalbumin (Markram *et al.*, 2004); whereas cells with a Martinotti morphology target the distal apical dendrite of pyramidal neurons, exhibit low-threshold spiking with adaptation, and express somatostatin (Wang *et al.*, 2004). These two broad classes form gap-junction coupled networks (Wang *et al.*, 2004) that can promote synchronised oscillatory activity in other populations of cortical neurons (Beierlein *et al.*, 2000). In spite of several recent innovative studies (Packer and Yuste, 2011; Katzel *et al.*, 2011) there still remains much research to be done to elucidate the degrees to which interneuron classes create canonical synaptic pathways in the neocortex.

**Canonical circuit:** Despite the diversity in function across areas such as the primary sensory, motor and pre-frontal cortices it is striking that many elements of neuronal morphology and circuitry remain preserved across the neocortex. The development of techniques such as paired-intracellular recordings, uncaging glutamate and electron microscope reconstructions (Thomson and Lamy, 2007) have confirmed the presence of certain connectivity rules that are preserved across cortical regions and species.

This cross-region and species similarity suggests that elements of the circuit possess a general-purpose efficiency for certain processes. The concept of a canonical microcircuit has become firmly established and has been subject to several reviews (Lubke and Feldmeyer, 2007; Defelipe *et al.*, 2012), although further research is required on several aspects, particularly interneuron and cross-region connectivity patterns.

### 1.1.2 Pyramidal Neurons

Just as the ubiquity of the layered microcircuit across functionally diverse cortical areas and different species indicates a significant adaptive value in its structure, the presence of neurons with a distinct pyramidal morphology in the cortex, hippocampus and amygdala as well as their preservation in birds and reptiles (Spruston, 2008) suggest a special adaptive value in the characteristic structure. The pyramidal neurons, alongside the Purkinje neuron in the cerebellum, are perhaps the most extensively studied neurons in the CNS and thus the intricacies of how pyramidal cells integrate and respond to their diverse inputs are increasingly well understood.

A single axon emanates from the base of the soma making glutamergic synapses onto local and long-range targets. The dendrites are subdivided into a number of relatively short basal dendrites and a long apical dendrite that forms a distal tuft (fig 1.3). The relative lengths of these structures can vary by brain area (Spruston, 2008), however the broadly conserved morphology points to particular computational, energetic and/or anatomical advantages associated with the structure. The dendrites of pyramidal neurons are highly specialised to receive and perform

computations on synaptic inputs (London and Hausser, 2005) and both apical and basal dendrites are electrically active and capable of generating NMDA and  $\text{Ca}^{2+}$  spikes (Schiller *et al.*, 2000; Kampa *et al.*, 2006).

The basal and tuft dendrites receive inputs from distinct regions, while the active dendritic properties facilitate coincidence detection as inputs to the same dendritic branch summate sigmoidally (Polsky *et al.*, 2004). Dendrites in pyramidal neurons also express a range of ion channels (HCN, GIRK and various  $\text{Ca}^{2+}$ -channels) at levels that increase with distance from the soma (Takigawa and Alzheimer, 1999; Berger *et al.*, 2001; Schiller *et al.*, 1997). These channels further allow the dendrites to act as specialised neuronal compartments and can be activated and inhibited by a variety of neuromodulators. In summary, these factors mean that the integration of inputs in pyramidal neuron dendrites follows a series of complex rules that depend on location, timing and the background modulatory environment.

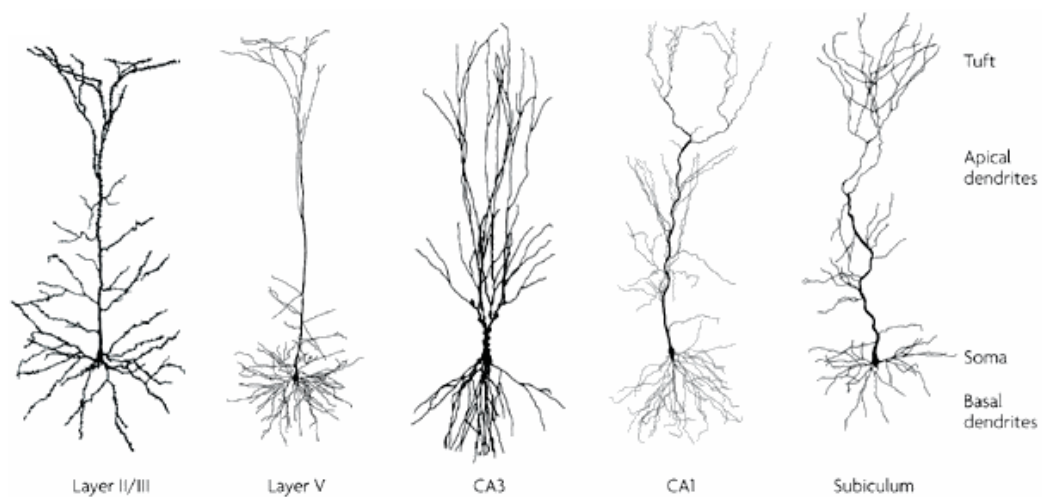


**Fig 1.3** The structure of pyramidal neurons across different brain regions. The full vertical length of each cell from left to right is: unknown,  $1180\mu\text{m}$ ,  $580\mu\text{m}$ ,  $730\mu\text{m}$  and  $790\mu\text{m}$  (Spruston, 2008).

### 1.1.3 Cortical synaptic plasticity

Individual synapses in the cortex exhibit similarly complex history dependence over time scales from milliseconds to years (Zucker and Regehr, 2002). Long-term changes in synaptic strength (LTP, LTD) can involve a large number of mechanisms and are governed by a number of rules that depend on the timing of pre and post-synaptic depolarisations (Caporale and Dan, 2008), and generally require post-synaptic calcium influx (Sjostrom and Nelson, 2002).

In pyramidal neurons the sign of synaptic plasticity (depression or potentiation) can be dependent both on the pattern of post-synaptic action potentials that back-propagate into the dendrites as well as the dendritic location of the synapse (Letzkus *et al.*, 2006). These changes must be carefully regulated across different synapses to avoid runaway changes in activity – a process achieved by homeostatic plasticity, which is a negative feedback mechanism that allows neurons to offset excess excitation or inhibition by adjusting synaptic strengths (Pozo and Goda, 2010). A net downscaling of cortical synapses in response to potentiation during wakefulness may be an important function of sleep (Tononi and Cirelli, 2006).

Short-term changes in synaptic strength (in this thesis referred to as synaptic dynamics) involve the progressive strengthening (facilitation) or weakening (depression) of synaptic transmission over millisecond to tens of

second timescales (Zucker & Regehr, 2002). Depression is often attributed to a depletion in the availability of readily releasable vesicles, and while this depletion is perhaps the dominant component of depression at many cortical synapses a number of other mechanisms can occur, for example receptor desensitisation or metabotropic receptor activation.

Facilitation is thought to depend on the pre-synaptic build up of  $Ca^{2+}$ -ions, causing increased transmitter release. The removal of these ions by different mechanisms over different time scales may result in the various time courses of facilitation that have been observed (facilitation, augmentation, potentiation). Facilitatory processes are common at many cortical synapses but are often masked by strong synaptic depression (Thomson & Lamy, 2007).

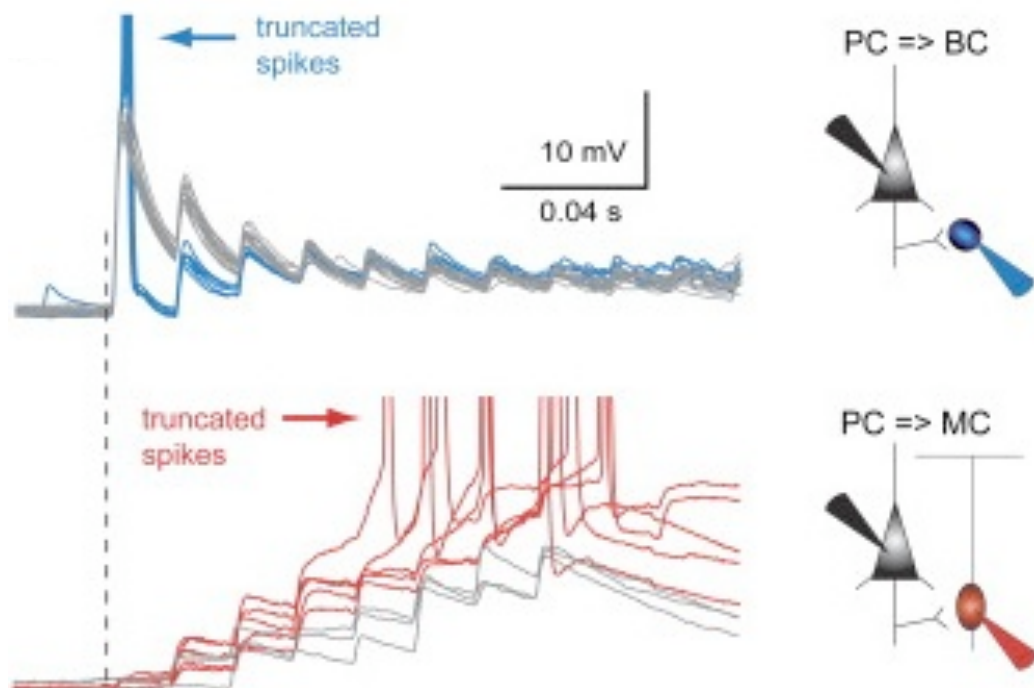


**Fig 1.4** Monosynaptic connections between a layer 5 pyramidal cell (PC) and a basket cell (BC, top) and a Martinotti cell (MC, bottom), illustrating characteristic synaptic dynamics (depression, top and facilitation, bottom). Note the contrasting positions of truncated action potentials within the post-synaptic responses (Silberberg and Markram, 2007).

The expression of synaptic dynamics confers information regarding the temporal structure of pre-synaptic activity, and by varying the relative contributions of depression and facilitation processes a synapse may be able to optimise its transmission of information to specific frequencies (Fuhrmann *et al.*, 2002). The dominance of facilitation or depression at a synapse is mainly governed by the initial transmitter release probability. Synapses with a high probability of transmitter release can rapidly deplete their readily releasable vesicles and thus mask facilitatory processes. The relative expressions of facilitation and depression at cortical synapses typically depend on the identities of both the pre and post-synaptic neuron (Markram *et al.*, 1998). The synaptic dynamics expressed between neurons are, however, not fixed and can be regulated by a variety of neuromodulators that affect pre-synaptic release machinery (Gil *et al.*, 1997). On top of this ongoing modulation the dynamics at various cortical synapses have been observed to change with post-natal development (Feldmeyer and Radnikow, 2009), and this process can occur to different degrees and at different times across synapses and cortical areas (Williams and Atkinson, 2007; Cheetham and Fox, 2010). It has been suggested that, in layer 5 of the neocortex, this developmental shift (a decrease in short-term depression) helps enable neurons to generate sustained periods of network up-states. Interestingly the development of high-amplitude slow-oscillations, which are characterised by alternating periods of synchronised hyperpolarised down-states and depolarised up-states coincides, in rats,

with this decline in synaptic depression at layer 5 synapses (Gvilia *et al.*, 2011).

#### 1.1.4 Cortical network dynamics

A striking feature of the neocortex is the characteristic slow oscillatory activity (<1 Hz) observed in cortical neurons during sleep and anaesthesia (often referred to as up- and down-states, fig 1.5). This has been subject to widespread experimental (Sanchez-Vives and McCormick, 2000) and theoretical interest (Compte *et al.*, 2003) in recent years, and has been demonstrated to play an important role in memory consolidation (Marshall *et al.*, 2006; Diekelmann and Born, 2010). It has been observed that the oscillation can be generated in isolated cortex and arises first in layer 5 (Sanchez-Vives and McCormick, 2000).

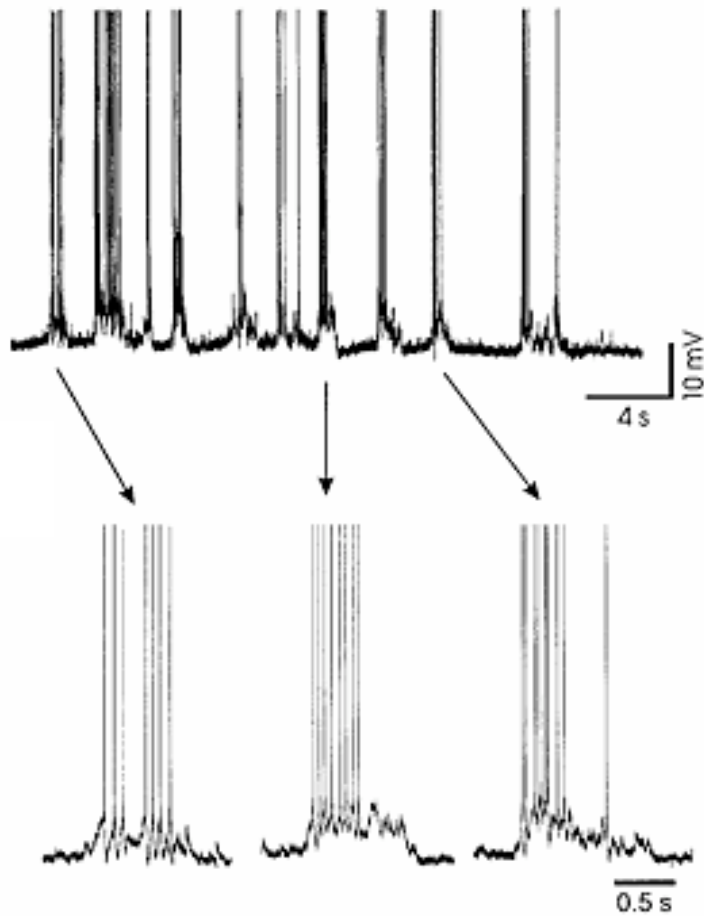


**Fig 1.5** *In vivo* intracellular recordings from cat layer 5 pyramidal neurons during halothane anaesthesia illustrating the characteristic slow oscillation (Sanchez-Vives & McCormick, 2000).

While the mechanisms through which the up-states are generated and terminated are not yet fully understood, it appears that some of the elements of the layer 5 circuit (high levels of recurrent connections, neurons that fire action potential bursts and ephaptic interactions) aid in the generation of these oscillatory rhythms. However these elements also make this circuit particularly vulnerable to epileptic activity (McCormick and Contreras, 2001). Other mechanisms that may be important in the dynamics of the slow oscillation include thalamic interactions (Crunelli *et al.*, 2011),



brain-stem neuromodulatory influences (Constantinople and Bruno, 2011) and neuron-glia interactions (Poskanzer and Yuste, 2011).

### 1.1.5 Neuromodulators in the cortex

Chemicals that act in a diffuse manner and exert actions on multiple neurons are known as neuromodulators and play a vital role in cortical function.

Modulators exert a variety of actions on synaptic transmission and neuronal excitability in order to regulate the balance of excitation/inhibition, gate information flow, enhance signal-noise ratios and regulate the threshold for long-term synaptic changes (Hasselmo, 1995; Seol *et al.*, 2007). These actions have a variety of downstream actions on behavioural processes such as arousal, attention, cognition and emotion (Gu, 2002). The actions that these chemicals exert on neurons mean that an array of properties of neurons in the circuit, such as spike adaptation, synaptic dynamics, resting potential and spiking threshold, can be largely context dependent.

Cortical modulators can be broadly divided between those that are released from axons originating in sub-cortical centres (acetylcholine, noradrenaline, serotonin, dopamine and histamine) and those that are released endogenously from cortical neurons or glia (endocannabinoids, neuropeptides, purines, glutamate – via mGluRs and GABA – via GABA<sub>B</sub>Rs). There is abundant data on the neuronal actions of many of these chemicals at the cellular level, as well as their effects on neuronal activity patterns at larger scales (EEG) and on behaviour (Noudoost and Moore, 2011).

However it remains a significant challenge to understand how their effects

on synaptic transmission and excitability at the single neuronal level are integrated by the cortical circuit to alter emergent activity patterns.

### 1.2 Adenosine

Adenosine acts as a potent modulator of both normal and pathological processes throughout the mammalian central nervous system (Boison, 2006). The neuroprotective (via A<sub>1</sub> receptor activation) release of adenosine in response to ischemia and epilepsy is well documented (Dale and Frenguelli, 2009) and adenosine has been frequently recorded at physiologically significant tonic concentrations in the extracellular space in different brain regions (Dunwiddie and Diao, 1994; Latini and Pedata, 2001). The basal extracellular concentration of adenosine has been estimated pharmacologically and by microdialysis; and appears to be dynamically maintained somewhere in the region of 25-250 nM (Dunwiddie and Masino, 2001), which suggests significant tonic activation of the high affinity A<sub>1</sub> and A<sub>2A</sub> receptors. This tone is also evident from the psychoactive effects of the non-specific adenosine receptor antagonist caffeine.

#### 1.2.1 regulation of adenosine concentration

Adenosine may be formed intracellularly by the dephosphorylation of AMP, and this intracellular concentration is tightly regulated by the actions of the enzymes adenosine deaminase (ADA) and, predominantly in glial cells, adenosine kinase (AK), which rapidly metabolise adenosine to inosine and AMP respectively. In normal conditions the phosphorylation of adenosine by AK is the dominant route by which adenosine is metabolised and subtle

changes in the activity of AK can have significant effects on the resultant extracellular concentration of adenosine due to the action of nucleoside transporters (Boison, 2006).

Intracellular adenosine can be transported to the extracellular space by equilibrative nucleoside transporters (ENTs, down the concentration gradient), while concentrative transporters (CNTs), can actively transport adenosine back into the cell (Craig and White, 1993; Cass *et al.*, 1998). ENTs tend to act to rapidly equilibrate the intra and extracellular concentrations of adenosine. Recent evidence suggests that the rapid transport of adenosine through ENTs on post-synaptic neurons during action potential firing may play a role in short-term synaptic plasticity (Lovatt *et al.*, 2012).

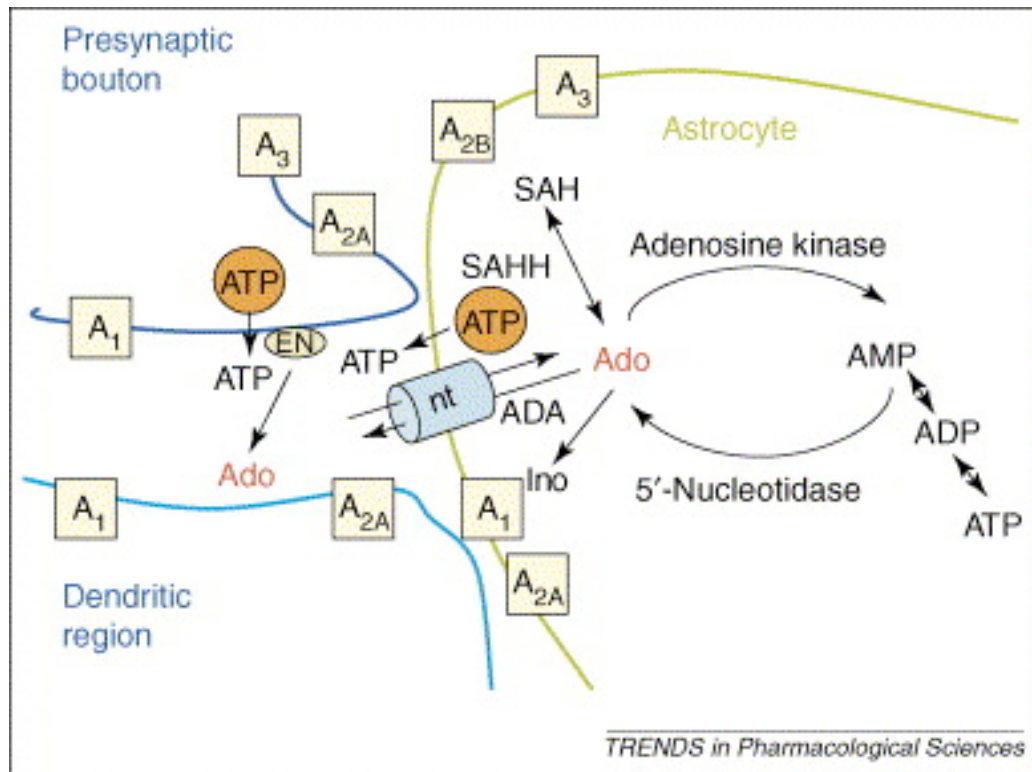


**Fig 1.6** Selected pathways of adenosine metabolism. Under physiological conditions the activity of adenosine kinase largely controls the intracellular concentration of adenosine. Intracellular and extracellular concentrations of adenosine equilibrate rapidly via nucleoside transporters, which are expressed ubiquitously (nt, shown on astrocytes). Thus, the extracellular concentration of adenosine depends largely on its intracellular metabolism. In addition, the extracellular cleavage of ATP that is released from either neurons or astrocytes (orange circles) by ectonucleotidases (EN) contributes to the formation of adenosine (Boison, 2006).

Adenosine can also arrive in the extracellular space via the dephosphorylation of adenine nucleotides (generally ATP that is exocytosed from neurons and glial cells – Edwards *et al.*, 1992; Pankratov *et al.*, 2006; Pangrsic *et al.*, 2007, or released via hemichannels – Stout *et al.*, 2002) by ectonucleotidases (Cunha and Sebastiao, 1991). The ectonucleotidases that catabolise ATP to adenosine are mostly membrane bound with their active site facing the extracellular space (Zimmermann, 2000). There is also some evidence for a mechanism of adenosine release strongly resembling direct exocytotic release (Wall & Dale, 2008).

### 1.2.2 Adenosine Receptors

There are currently 4 recognised adenosine receptors (ARs, or sometimes referred to as P1Rs), and these have been named  $A_1$ ,  $A_{2A}$ ,  $A_{2B}$  and  $A_3$ . They are all transmembrane spanning G-protein coupled receptors (GPCRs).

The  $A_1$  receptor is the most abundant and widespread in the CNS, with high levels of immunohistochemistry staining in many regions of the brain, including the neocortex, hippocampus and thalamus (Ochiishi *et al.*, 1999). Both pre and post-synaptic terminals show strong staining in cortical and hippocampal neurons. The  $A_{2A}$  receptor exhibits strong expression only in the striatum (Svenningsson *et al.*, 1999), but is also expressed at lower levels (that remain pharmacologically significant, Cunha *et al.*, 1994) in other regions such as the neocortex, hippocampus and nucleus accumbens (Ralevic and Burnstock, 1998).  $A_{2A}$  receptors are often tightly coupled to receptors from other modulatory systems (Canals *et al.*, 2003).  $A_{2B}$  receptors are widely expressed in the CNS, but at very low levels. They are found on most cells but require high concentrations of adenosine to evoke a response. The  $A_3$  receptor is also expressed widely but at low levels and thus its physiological roles remain enigmatic (Gessi *et al.*, 2008).

$A_1$  and  $A_3$  receptors are coupled to  $G_{i/o}$  proteins and through this signalling pathway inhibit adenylate cyclase and decrease intracellular cAMP levels (Blazynski, 1987).  $A_{2A}$  and  $A_{2B}$  receptors couple to  $G_s$  proteins activating adenylate cyclase, thus increasing intracellular cAMP (Dunwiddie and Masino, 2001). Due to the rapid metabolism of adenosine even in isolated biological membranes it is has proved difficult to obtain affinity data for

adenosine receptors by direct binding studies. Even using isolated membrane preparations, adenosine is rapidly metabolised and produced endogenously, which confounds measurements (Fredholm, 2010). If measurements are taken from functional assays they remain influenced by receptor number as well as the type of response that is measured.

Estimated affinities for each receptor are detailed in table 1 (Dunwiddie and Masino, 2001). However when affinities are compared at similar receptor densities, in most cases the A<sub>1</sub>, A<sub>2A</sub>, and A<sub>3</sub> receptors are recorded with similar affinities, whereas the A<sub>2B</sub> receptor is approximately 50 times less potent in altering cAMP levels (Fredholm *et al.*, 2001). If however the activation of MAP kinase is measured the affinities of each receptor appear equipotent (Schulte and Fredholm, 2000).

Receptor	Affinity for adenosine	G-protein	Intracellular transduction	Physiological actions in the brain	Distribution in brain
A <sub>1</sub>	~70nM	G <sub>i</sub> and G <sub>o</sub>	Adenyl cyclase ↓ GIRKs ↑ Ca <sup>2+</sup> -channels ↓ PLC ↑	Inhibits synaptic transmission  Hyperpolarises neurons	Widespread
A <sub>2A</sub>	~150nM	G <sub>s</sub> and G <sub>oif</sub>	Adenyl cyclase ↑ Ca <sup>2+</sup> -channels ↓ Ca <sup>2+</sup> -channels ↑ (?)	Facilitation of transmitter release  Inhibition of transmitter release	Primary striatum  Olfactory tubercle  Nucleus accumbens
A <sub>2B</sub>	~5100nM	G <sub>s</sub>	Adenyl cyclase ↑ PLC ↑	Increases cAMP in brain slices  Modulation of Ca <sup>2+</sup> channel function (?)	Widespread
A <sub>3</sub>	~6500nM	G <sub>i</sub> and G <sub>q</sub>	Adenyl cyclase ↓ PLC ↑ Intracellular Ca <sup>2+</sup> ↑	Uncouples A <sub>1</sub> , mGlu receptors (?)	Widespread

**Table 1.1** Adenosine receptors in the brain. GIRKs, G-protein coupled receptors. PLC, phospholipase C (Dunwiddie and Masino, 2001).

The work in this thesis concerns actions of adenosine at the A<sub>1</sub> receptor thus a more in depth account of its actions and physiological relevance at this receptor will be detailed. Besides inhibiting adenylyl cyclase, activation of the A<sub>1</sub> receptor inhibits multiple sub-types (both conotoxin and agatoxin sensitive) of voltage-gated Ca<sup>2+</sup>-channels (McCool and Farroni, 2001). At pre-synaptic terminals, this reduction in Ca<sup>2+</sup> influx causes a reduction in neurotransmitter release. These actions have been documented in neurons that release a variety of transmitters including glutamate, GABA and acetylcholine. A<sub>1</sub> receptor activation can also activate potassium channels – most commonly G-protein coupled inwardly rectifying potassium (GIRK) channels (Trussell and Jackson, 1985), but also SK-channels (Clark *et al.*, 2009) and ATP-sensitive potassium channels (Kawamura *et al.*, 2010). These actions act to reduce membrane excitability by hyperpolarising neurons and reducing input resistance. A<sub>1</sub> receptor activation has also been reported to inhibit non-selective hyperpolarisation activated cation (HCN) channels via the cAMP pathway (Li *et al.*, 2011). Through these actions A<sub>1</sub> receptor activation is associated with a reduction in neuronal activity across the brain.

### 1.2.3 Physiological and pathophysiological roles of adenosine

The release of large amounts of adenosine during ischemic episodes and during seizures is now well documented (Dale & Frenguelli, 2009). Given adenosine's predominantly inhibitory actions and because the intracellular concentration of adenosine is tightly linked to the energy expenditure of cells it is well placed to act as a protective response mechanism against

energetic stresses (Cunha, 2005). A decrease in intracellular ATP in response to increased energy expenditure will lead to an increase in intracellular adenosine and this adenosine can rapidly exit the cell through ENTs where it can bind to A<sub>1</sub> receptors to reduce activity in both the cell releasing adenosine and neighbouring cells. The intracellular concentration of ATP is many times higher than that of adenosine, meaning that small energy changes can result in significant changes in the concentration of adenosine. This allows adenosine to act as a homeostatic modulator. In cases of extreme stress adenosine can act as a neuroprotective agent against excitotoxicity in this manner (de Mendonca *et al.*, 2000).

Due to its tight coupling to cellular energy use adenosine is well placed to act as a general modulator of neural activity across the brain. The ubiquitous nature of the adenosine system has allowed researchers to identify roles for adenosine in the modulation of locomotion, respiration, sleep homeostasis and neuroprotection from excitotoxicity (Dunwiddie and Masino, 2001), and recently, modulatory roles in the development of various neurological diseases such as epilepsy, Parkinson's, schizophrenia, chronic pain and Alzheimer's (Boison, 2008).

Of particular interest in the neocortex are adenosine's actions in the modulation of slow wave activity and sleep homeostasis (Bjorness *et al.*, 2009). In rodents, the concentration of extracellular adenosine rises in various brain regions during the dark (active) cycle and in response to sleep deprivation (Huston *et al.*, 1996; Porkka-Heiskanen *et al.*, 1997, Schmitt *et al.*, 2012), and this increase in extracellular adenosine, via A<sub>1</sub> receptor



activation, is known to modulate the power of slow wave activity during sleep (Fellin *et al.*, 2009).

The large amplitude slow waves observed in EEG recordings result from high levels of synchronisation of the activity of individual neurons as they alternate between short bursts of increased synaptic input and spiking, and periods of hyperpolarisation resulting from a sudden cessation of significant synaptic input. These alternating patterns of “on” and “off” (or up and down) activity have been observed to occur in individual cortical neurons in awake rats (Vyazovskiy *et al.*, 2011). The down-states increase in frequency and duration in response to sleep deprivation, and result in performance impairments. These results have provided further evidence supporting the view that sleep is a phenomenon with local as well as global characteristics.

The role that extracellular adenosine may play in these activity transformations is not fully understood at present. Activation of the A<sub>1</sub> receptor has been shown to increase EEG slow wave power in a manner similar to that seen in response to sleep deprivation (Landolt, 2008), although other studies have suggested that A<sub>2A</sub> activation may also play a significant role (Methippara *et al.*, 2005). Fellin *et al.*, (2009) have demonstrated that A<sub>1</sub> antagonism increases slow wave power in the local field potential (LFP), whereas Poskanzer & Yuste (2011) have demonstrated 8-CPT (an A<sub>1</sub> receptor specific antagonist) application decreasing the amount of up-states seen in whole-cell recordings. These studies indicate that adenosine may play an active role in the generation of cortical up- and down-states.

It is clear that adenosine plays a wide variety of important roles in the neocortex, and while literature on its electrophysiological effects on neocortical neurons remains relatively sparse some data on adenosine's synaptic actions is available. Thalamacortical excitation onto both excitatory and inhibitory neurons in layer 4 of the neocortex is suppressed to roughly the same extent (78 and 81% respectively, at 100  $\mu$ M) by adenosine (Fontanez and Porter, 2006). While another study (Varela *et al.*, 1997) noted a 50% suppression of layer 2/3 pyramidal responses to stimulation in layer 4. These studies of adenosine's actions on local connections within the neocortex have so far been limited to observing effects of extracellular stimulation on evoked EPSPs.

With extracellular stimulation methods, while useful for studying well-defined interlaminar synaptic pathways, it is impossible to isolate specific local synaptic contacts between neighbouring neurons. For example, distinguishing the thick-tufted pyramidal neurons whose dendrite terminates in layer 1 from other smaller pyramidal neurons in layer 5. Paired intracellular recordings have previously demonstrated differing connectivity principles and electrophysiological properties between these neurons (Thomson & Lamy, 2007), so it is important to consider them as heterogeneous populations. Paired intracellular recordings also facilitate careful examination of the properties of mono-synaptic transmission, which is a key element in information processing in neuronal circuits.

Adenosine, as an endogenously produced neuromodulator that can target multiple aspects of neuronal signal processing and transmission, is well

placed to transform the manner in which information propagates in large networks of neurons. Little is understood regarding how modulators may do this at the level of the microcircuit. As well as this, the contribution of tonic adenosine to the maintenance of normal activity and plasticity or the transformation into slow wave activity is not well understood. I aimed to begin addressing these questions by investigating adenosine's actions on neural activity in layer 5.

### 1.3 Thesis Outline

This thesis will focus on how adenosine modulates the activity of thick-tufted layer 5 pyramidal neurons. I have aimed both to increase the level of detail at which the interaction of neuromodulators with neurons and the chemical synapses connecting them is studied, and to examine the extent to which the changes induced by neuromodulation can be accounted for by simple mathematically tractable models that, in the future, can be integrated into network models to facilitate understanding of the emergent dynamics.

Chapter 3 examines the effects of adenosine on synaptic transmission between thick-tufted pyramidal neurons in layer 5 of the somatosensory cortex. I used paired whole-cell patch clamp recordings on cortical slices to first categorise the effects pharmacologically, before using patterned stimulus trains to probe how adenosine impacts various parameters determined from models of synaptic dynamics and binomial analysis. I found that the synaptic effects were mediated by  $A_1$  receptor activation and could be accurately described in a model of synaptic dynamics as a change in only the parameter representing probability of release.

Chapter 4 examines how the activation of  $A_1$  receptors by endogenous adenosine affects synaptic transmission. I conducted experiments on connections at three stages of post-natal development and found that an increase in  $A_1$  receptor activation during development is responsible for the shift in synaptic dynamics and increase in EPSP variability that has previously been observed. I also demonstrate that endogenous  $A_1$  receptor activation is heterogeneous at the local synaptic level and plays a major role in determining EPSP amplitude and variability in the mature cortex.

Chapter 5 characterises the post-synaptic effects of adenosine on firing outputs from thick-tufted layer 5 pyramidal neurons. I used a noisy input to generate naturalistic firing patterns that were used to generate dynamic I-V curves and parameterise a reduced neuronal model. I demonstrate that despite a relatively small hyperpolarisation and reduction in input resistance, adenosine causes a powerful suppression of firing. This suppression is significantly increased when current is injected from the apical dendrite. I also show that adenosine causes a selective shunting of back-propagating bursts of action potentials.

Finally, a general discussion and conclusion are presented where I assess the implications of my results and discuss future perspectives.

## 2. Methods

### 2.1 Electrophysiology

#### 2.1.1 Slice preparation

Wistar rats (male, postnatal days P11-14, P18-22 or P28-32) were killed by cervical dislocation and decapitated in accordance with the UK Animals (Scientific Procedures) Act 1986. Rats were killed within one hour of the beginning of the light (sleep) period. The brain was rapidly removed, whilst washing with ice-cold aCSF, cut down the mid line, and the two sides of the brain were glued at the surface of the sagittal plane onto a petri dish. This dish was filled with cold (2-4°C) high Mg<sup>2+</sup>, low Ca<sup>2+</sup> aCSF, composed of (mM): 127 NaCl, 1.9 KCl, 8 MgCl<sub>2</sub>, 0.5 CaCl<sub>2</sub>, 1.2 KH<sub>2</sub>PO<sub>4</sub>, 26 NaHCO<sub>3</sub>, and 10 D-glucose (300 mOSM, pH 7.4 when bubbled with 95% O<sub>2</sub> and 5% CO<sub>2</sub>) and mounted at an angle of 20° on a Microm HM 650V microslicer such that the blade cut from the upper border of the neocortex towards the caudal border and towards the midline. This slicing protocol, based on Markram *et al*, (1997) was used so that slices with fully intact pyramidal-neuron apical dendrites could be obtained. The slices used in experiments corresponded to the hind-limb area of the somatosensory cortex. Slices were carefully trimmed so that only the cortex was present. Neocortical slices were stored in normal aCSF (1 mM MgCl<sub>2</sub>, 2 mM CaCl<sub>2</sub>) at 34°C for 30 minutes then stored at room temperature for 1-6 hours before recording.

### 2.1.2 Intracellular recording

A neocortical slice was transferred to the recording chamber and perfused with normal aCSF at  $32 \pm 0.5^\circ\text{C}$ . The slice was visualized using IR-DIC optics with an Olympus BX51W1 microscope and Hitachi CCD camera (Scientifica, Bedford UK). Somatosensory cortex was located from its position relative to the hippocampus under low (x40) magnification. Under high (x600) magnification whole-cell recordings were made from 2-4 large neighbouring layer 5 pyramidal neurons in the somatosensory cortex using patch pipettes (3-8 M $\Omega$ ) manufactured from thick-walled borosilicate glass (Harvard Apparatus, Edenbridge UK) and containing (mM): potassium gluconate 135, NaCl 7, HEPES 10, EGTA 0.5, phosphocreatine 10, MgATP 2, NaGTP 0.3 and biocytin 1 mgml<sup>-1</sup> (290 mOSM, pH 7.2). In some experiments Alexa-fluor 488 hydrazide (50  $\mu\text{M}$ ) was also included in the pipette solution to aid the visualisation of the apical dendrite for dendritic recordings.

Somata of recorded neurons were located at least 50  $\mu\text{m}$  below the slice surface to enable reliable morphological identification. Thick-tufted layer 5 pyramidal neurons were identified by their position in the slice (layer 5b), their large size and thick apical dendrite (measured immediately above the somata), and their characteristic current-voltage relationship. Recorded neurons were then processed using a biocytin staining protocol (2.2).

Following DAB staining the neurons were generally revealed to be of the thick-tufted pyramidal morphology. Data recorded from neurons that did

not fit the thick-tufted morphological classification was removed from further analysis.

Voltage recordings were obtained using Axon Multiclamp 700B amplifiers (Molecular Devices, USA) and digitized at 20 kHz (Axon Digidata 1440a). Data acquisition and analysis was performed using Pclamp (vers 10 Axon, Molecular Devices). Voltages were not corrected for the liquid junction potential (~10 mV).

If synaptic connectivity was detected between pairs of neurons then short trains of action potentials (8-10) at 15-50 Hz were elicited by brief current pulses in the pre-synaptic neuron, followed by a recovery test pulse 500 ms later. Unitary EPSP amplitudes were monitored for 5 minutes before recordings were taken. Stimulus trains were separated by 12 seconds and repeated 25-100 times during recording.

### 2.1.3 Biosensors

Sensors were obtained from Sarissa Biomedical Ltd (Coventry, UK). The adenosine sensor consists of three enzymes (adenosine deaminase, purine nucleoside phosphorylase and xanthine oxidase) within a matrix encasing a 50  $\mu\text{m}$  platinum electrode (Llaudet *et al.*, 2003) making it sensitive to adenosine, but also inosine and hypoxanthine. To detect a specific adenosine signal, a signal from an inosine biosensor (sensitive to both hypoxanthine and inosine) containing just the purine nucleoside phosphorylase and xanthine oxidase enzymes, was subtracted from the adenosine sensor signal.

A null sensor containing the deposition matrix, but no enzymes was also used to control for the release of non-specific electro-active interferents. Biosensors were calibrated with known concentrations of adenosine and inosine (10  $\mu\text{M}$ , typically giving a  $\sim 2$  nA response in each sensor) before the slice was placed in the perfusion chamber. The perfusion chamber consisted of a suspended grid to allow perfusion from above and below the slice. The aCSF was perfused at either 2 or 6  $\text{mlmin}^{-1}$ . The biosensors were carefully inserted (at an angle of  $70^\circ$ ) into layer 5 of the somatosensory and following a 15-minute period to allow the purines released during insertion to wash from the tissue (at an increased aCSF flow rate, 6  $\text{mlmin}^{-1}$ ). The flow rate was then reduced to 2  $\text{mlmin}^{-1}$  (to match the patch-clamp experiments) and 10 minutes was allowed for the extracellular tone to reach steady state. Following removal from the slice the signals were subtracted from the null electrode to give a total purine and an inosine signal and compared to the post experiment calibration to give estimated concentrations. Finally the total purine concentration was subtracted from the inosine concentration to produce an estimated slice adenosine concentration.

#### 2.1.4 Drugs

All drugs were prepared as concentrated stock solutions (10 – 100 mM), stored frozen, and then thawed and diluted in aCSF immediately before use. Adenosine, inosine, 8-cyclopentyltheophylline (8-CPT) and N6-cyclopentyladenosine (CPA) were purchased from Sigma (Poole, UK). Kynurenic acid was purchased from Ascent Scientific (Bristol UK). In the



strontium experiments the aCSF was modified from 2 mM CaCl<sub>2</sub>, to 1 mM CaCl<sub>2</sub> and 4 mM SrCl<sub>2</sub>.

## 2.2 Histology

Following recording the patch pipettes were carefully removed to ensure that the neurons were not damaged and the slice was immediately transferred to 4% paraformaldehyde/phosphate buffer solution and kept refrigerated overnight. Slices were then washed thoroughly (5 x 5 min washes) in phosphate buffer solution (PBS, pH 7.3), followed by several washes in tris buffer solution (TBS, pH 7.3). Slices were then incubated overnight in 1% triton/TBS in order to permeabilise cell membranes before being washed several times in TBS. Slices were then incubated for 30 minutes at room temperature in 3% hydrogen peroxide (H<sub>2</sub>O<sub>2</sub>) in methanol in order to remove endogenous peroxidase activity, before a 1% triton/TBS wash and several TBS washes. The ABC kit was mixed following the package instructions and incubated at room temperature for 30 minutes. Following the TBS washes slices were incubated in the ABC solution for 2 hours. Slices were then thoroughly washed in TBS before being submerged in the DAB reaction mixture for 1 – 3 minutes. The reactions were quenched using TBS washes under visual inspection when the dendrites became clearly visible. In some cases slices were then dehydrated using a series of ethanol/H<sub>2</sub>O mixtures, cleared using methyl salicylate and mounted on to transparent slides for further inspection.

### 2.3 Analyses and Modelling

Analyses were performed on Excel, MATLAB or R. All values are written as mean  $\pm$  standard deviation unless otherwise stated.

#### 2.3.1 Deconvolution

The paired intracellular recordings utilised trains of action potentials at frequencies of 10 – 50 Hz in order to probe the synaptic dynamics of the connections. At these frequencies the EPSPs overlap, thus in order to accurately measure the EPSP amplitudes and to facilitate the identification of release failures a voltage deconvolution technique (Richardson and Silberberg, 2008) was used to defilter the voltage trace allowing isolated signals to be cropped and reconvolved which could be used to directly measure amplitudes.

In brief, the temporal derivative of the voltage signal was defined at time step  $k = t/dt$  for time  $t$ , where  $dt$  is the unit for each step, as  $\tau(x_{k+1} - x_k)/dt + x_k = f_k$  to be consistent with the subsequent reconvolution  $x$  of a signal  $f(t)$ , which can be found through integration using the forward scheme  $x_{k+1} = x_k + dt(f_k - x_k)/\tau$ .  $\tau$  was identified using a least square optimisation of the flatness of the deconvolved trace in a 20 – 80 ms window following the recovery test EPSP.

#### 2.3.2 Model of synaptic dynamics

The depression-facilitation model in Markram *et al.*, (1998) was used. The model includes four parameters: the fraction of resources used upon arrival of an action potential ( $P$ ), the maximum available resources ( $aN$ ), recovery

from facilitation ( $\tau_F$ ), and recovery from depression ( $\tau_D$ ). Upon an action potential the fraction of resources used ( $P$ ) becomes unavailable for release and recovers with time constant  $\tau_D$ . Facilitation is included as a pulsed increase in  $P$  upon an action potential, such that the running value of  $P$  is referred to as  $p$ , which recovers with time constant  $\tau_F$ . The amplitude of the pulsed change in  $p$  was defined as  $P(1-p)$ , ensuring that  $p < 1$ . The fraction of available resources available at any time was referred to as  $R$ .

Thus,  $R$  and  $p$  for consecutive action potentials in a train can be described by

$$R_{n+1} = R_n(1 - p_n)\exp(-\Delta_t/\tau_D) + 1 - \exp(-\Delta_t/\tau_D) \quad (1)$$

$$p_{n+1} = p_n*\exp(-\Delta_t/\tau_F) + P(1 - p_n*\exp(-\Delta_t/\tau_F)) \quad (2)$$

Where  $\Delta_t$  is the time interval between the  $n$ th and  $(n+1)$ th action potentials.

Thus the synaptic response by any action potential in a train is given by

$$EPSP_n = aN*R_n*p_n \quad (3)$$

The model was fit to the data by finding the lowest mean-squared error over an exhaustive parameter search with resolutions 0.1 mV for  $aN$ , 0.02 for  $P$ , 20 ms for  $\tau_D$ , and 10 ms for  $\tau_F$ .  $\tau_D$  and  $\tau_F$  were optimised for all pharmacological manipulations simultaneously while  $aN$  and  $P$  were optimised for each manipulation separately.

### 2.3.3 Mean variance analysis

Differences in mean EPSP amplitude within trains were assumed to differ due to a reduction in effective  $p$ , as the proportional difference in  $CV^{-2}$  was found to be greater than the proportional difference in mean amplitude. A

linearised version of mean-variance analysis was used to estimate the number of independent release sites ( $N$ ) and the quantal amplitude ( $a$ ), based on simple binomial statistics. When variance/mean amplitude was plotted against mean amplitude, EPSPs differing in effective  $p$  form a straight line,  $y = Nx + a$ , with the gradient estimating the number of release sites and the  $y$ -axis intersection estimating quantal amplitude (Bremaud *et al.*, 2007). Parameters were optimised using a mean lowest-squared error approach with resolutions of 1 for  $N$  and 0.01 for  $a$ .

#### 2.3.4 Measuring asynchronous EPSPs in strontium

A modified aCSF was created that included 1 mM CaCl and 4 mM SrCl instead of the normal 2 mM CaCl. Connections were identified in normal aCSF and trains of EPSPs (~30 sweeps) were recorded in control conditions. Following this, the normal aCSF was replaced with the Sr<sup>2+</sup> aCSF. Following a 10-minute wash on period several pre-synaptic action potentials (at ~30 Hz) were elicited by short pulses of injected current. 50 – 100 sweeps, separated by 10 seconds, were recorded. EPSPs arriving within 100 ms of the final action potential were measured and if the 10-90 % rise time fell within 2 standard deviations of the evoked synchronous EPSP they were counted as asynchronous EPSPs (aEPSPs). In order to estimate signal error due to spontaneous EPSPs a 100 ms window in the post-synaptic voltage trace, before the stimulation, was also analysed in the same way. Following this, adenosine (100  $\mu$ M) was added to the modified aCSF and the process was repeated. Finally, normal (2 mM CaCl) aCSF was reapplied, with 100  $\mu$ M adenosine and allowed to wash on for 10-15 minutes to replace the Sr<sup>2+</sup>

aCSF, before trains of EPSPs were evoked (at 30 Hz) and recorded. At the end of the experiments the adenosine was washed off, and EPSP trains were rerecorded to detect any run-down.

### 2.3.5 Concentration response curves

The concentration response curves (chapter 5) for mean unitary EPSP amplitude ( $E$ ) at bath applied adenosine concentration ( $A$ ) were modelled by the logistic form  $E = E_{min} + F(A)(E_{max} - E_{min})$  where

$$F(A) = \frac{1}{1 + (A + A_T)/A_h} \quad (4)$$

is the relative amplitude. The parameters of the fit were the minimal ( $E_{min}$ ) and maximal ( $E_{max}$ ) EPSP amplitudes, the bath applied equivalent endogenous adenosine tone concentration ( $A_T$ ) and the bath-applied equivalent half activation ( $A_h$ ). As well as in CPA and 8-CPT, EPSP amplitudes were measured in control ( $A = 0$ ), and  $A = 10, 30$  and  $100 \mu\text{M}$  adenosine. CPA and 8-CPT were equivalent to  $A = -A_T$  and  $A = \infty$  respectively. The measured amplitudes for these five conditions were compared with the predictions from equation 4 for a trial parameter set  $\{E_{min}, E_{max}, A_T, A_h\}$  and the mean squared-errors between the two were minimised over an exhaustive search with resolutions:  $E_{min}, E_{max}$  voltage step  $0.02 \text{ mV}$  and  $A_T, A_h$  over a logarithmic scale from  $0.01$  to  $100$  and  $0.1$  to  $1000$  respectively with  $65$  intervals. If the best fit value of  $A_T$  was  $0.01 \mu\text{M}$  it was concluded that no measurable adenosine was present. The average half activation concentration ( $a_h$ ) was calculated using a geometric mean, and the mean relative amplitudes ( $f_T$ ) in control (due to the endogenous tone)

were calculated as the arithmetic mean of  $1/(1+A_T/A_h)$  over each of the connections measured. The equivalent mean adenosine tone is then  $a_T = a_h(1/f_T - 1)$ . The mean data points (for 0, 10 and 100  $\mu\text{M}$  adenosine) were calculated by taking geometric means over the concentrations and arithmetic means of the relative amplitudes.

### 2.3.6 Dynamic I-V

To probe the post-synaptic actions of adenosine a method was used that measures the neuronal I-V curve during ongoing firing activity (Badel *et al.*, 2008). This dynamic I-V curve was then used to parameterise a reduced neuronal model (refractory exponential integrate-and-fire, rEIF, Fourcaud-Trocme *et al.*, 2003) in control conditions, adenosine and 8-CPT (following adenosine wash).

The dynamic I-V method involves the injection of noisy current traces (generated previously, and saved as text files) into the neuron. These currents files, and the neurons voltage response can be used to calculate an average transmembrane current at any membrane potential, pre or post spike. This curve, the dynamic I-V curve, can then be used to parameterise simple spiking neuronal models (Badel *et al.*, 2008). A full account of how this process was undertaken is detailed below.

A stochastically fluctuating current trace was produced using a numerical realisation of an Ornstein-Uhlenbeck process (Uhlenbeck and Ornstein, 1930). The process was implemented twice with fast and slow (3 and 10 ms) time constants that were then summed to produce a single trace. Two

sets of variances (low,  $\sigma_{\text{fast}} = \sigma_{\text{slow}} = 0.18$  and high,  $\sigma_{\text{fast}} = 0.36$ ,  $\sigma_{\text{slow}} = 0.25$ ) and two sets of DC biases (0, 0.06 in relative units) were used to produce a total of 4 different current traces (saved as text files). These were multiplied by a factor (generally 300-1000 pA) when injected to induce neuronal firing in the desired range (1-15 Hz).

In a typical experiment 2 of these current traces were sequentially injected (with a gap between injections of 2 minutes) into the neuron under each pharmacological manipulation (control, adenosine, 8-CPT). One current file and voltage response was used to parameterise a refractory exponential integrate-and-fire (rEIF) model in the manner detailed below. The rEIF model was then used to calculate a voltage trace in response to the second current file. The prediction of this model was then compared to the actual voltage recording in response to that current file. The number of spikes that could be matched to within  $\pm 2$  ms was typically 70-90%.

In order to take into account the refractory parameters of pyramidal neurons data falling in a 200 ms window following each spike peak was removed from the initial analysis. The dynamic transmembrane current  $I_m(V, t)$  was calculated from the remainder of the voltage  $V(t)$  and injected current  $I_{\text{in}}(t)$  traces using the equation

$$I_m(V, t) + I_{\text{noise}} = I_{\text{in}}(t) - C \frac{dV}{dt} \quad (5)$$

The capacitance ( $C$ ) was calculated using a standard optimisation procedure based on the variance of the voltage ( $V$ ). This allows the calculation of the transmembrane current ( $I_m$ ) as a function of time ( $t$ ). The average

transmembrane current (1 mV bins) thus yielding the dynamic I-V curve (see fig 5.1).

$$I_d(V) = \text{Mean}[I_m(V,t)] \quad (6)$$

The dynamic I-V curve was then used to parameterise an exponential integrate-and-fire model described by

$$F(V) = \frac{1}{\tau_m} \left( E_m - V + \Delta_T \exp\left(\frac{V - V_T}{\Delta_T}\right) \right) \quad (7)$$

where

$$F(V) = -\frac{I_d(V)}{C} \quad (8)$$

These equations were integrated using an Euler scheme with a time step of 0.05 ms. The action potentials of the model appear as a rapid rise in voltage governed by the exponential term, and stopped when  $V$  reached 0 mV.

Because the downswing of the spike was not described in the model the integration was interrupted for 2 ms after detection of an action potential and reset at a voltage ( $V_{re}$ ) generally close to  $V_T$ .

The four EIF parameters correspond to the membrane time constant ( $\tau_m$ ), the resting potential ( $E_m$ ), the spike initiation threshold ( $V_T$ ) and the spike width ( $\Delta_T$ ), which controls the sharpness of the initial phase of the spike.



Refractory properties were included, according to Badel *et al.*, (2008) by making  $E_m$ ,  $1/\tau_m$  and  $V_T$  dependent on the time since the last spike. The refractory parameters were fit from a recalculation of the dynamic I-V curve using post-spike time windows of 5-10, 10-20, 20-30, 30-50, 50-100 and 100-200 ms (see fig 5.2), demonstrating that the EIF parameters recovered post spike with single exponential ( $1/\tau_m$  and  $V_T$ ) or double exponential relaxation ( $E_m$ ). The model parameters were used to calculate a voltage trace in response to the second current file. This model prediction was then tested against the experimentally measured voltage trace that occurred during the injection of that current trace (fig 5.2c & d).

### 2.3.7 Electrode Filter

It was assumed that the voltage across the electrode is a linearly filtered version of the input current  $I(t)$ . The recorded voltage ( $V_{rec}$ ) is the sum of the true membrane voltage ( $V$ ) and the electrode filter ( $V_{el}$ ). The electrode voltage ( $V_{el}$ ) is then written as a convolution integral of the current with the unknown electrode filter  $f(s)$

$$V_{rec}(t) = V(t) + V_{el}(t) = V(t) + \int_0^{\infty} f(s)I(t-s)ds \quad (9)$$

The combined electrode and membrane filter is then determined using a minimisation approach following Badel *et al.*, 2008. This combined filter is accurately described by a sum of two exponentials, one with a fast time constant (0.2 – 0.5 ms) that is due to the electrode, and one with a slower time constant (~15 ms) that is due to the membrane. The slower exponential is then subtracted to yield the electrode filter. Using this

electrode filter, the component of the voltage due to the electrode is subtracted from the recorded voltage to yield the true membrane voltage.

### **3. Characterisation of adenosine-mediated suppression of mono-synaptic transmission between thick-tufted layer 5 pyramidal neurons of the juvenile rat somatosensory cortex**

#### 3.1 Introduction

Paired intracellular recordings have, in recent years, provided much of the data on the properties of local cortical synaptic pathways including connectivity, efficacy and short-term dynamics (Thomson and Lamy, 2007). These studies also provide a wealth of data on the reliability of transmission at this key site for the processing of information (Feldmeyer *et al.*, 2006). The observed variability across synaptic pathways has led to attempts to quantify this across different connections in terms of binomial parameters (Bremaud *et al.*, 2007, Hardingham *et al.*, 2010). These parameters also play a role in the short-term dynamics observed in these pathways, which again encode information (Abbott *et al.*, 1997). These studies utilise acute slice preparations and thus present what is effectively a snapshot of the synapse, which would be under the influence of ongoing modulation *in vivo*.

Adenosine plays a vital modulatory role in many parts of the brain (Dunwiddie and Masino, 2001) and in the neocortex is known to modulate the power of delta-frequency (1-4 Hz) slow waves. As well as this, the release of adenosine in response to epileptic or ischemic excitotoxicity is known to have a neuroprotective role through the activation of A<sub>1</sub> receptors (Cunha, 2005). Although the effects of adenosine have been well characterised on synaptic pathways in areas of the brain such as the cerebellum and hippocampus using extracellular stimulation, (Wall and

Dale, 2007, Lupica *et al.*, 1992) the complex network of local synaptic connections in the neocortex have been less amenable to such investigation. Those studies that have investigated adenosine's actions in the neocortex have used extracellular stimulation to probe feed-forward thalamocortical (Fontanez and Porter, 2006) or interlaminar (Varela *et al.*, 1997) pathways. The modulation of synapses that make up the extensive intralaminar recurrent networks have not yet been investigated.

The thick-tufted pyramidal cells in layer 5 of the neocortex are characterised by a thick apical dendrite that first bifurcates and then forms tufts in layer 1. They provide cortical output to the superior colliculus, spinal cord and basal pons (Kasper *et al.*, 1994; Romand *et al.*, 2011) and play a key role in the generation of active states during the cortical slow oscillation (Chauvette *et al.*, 2010). Gliotransmitters such as adenosine are known to play an important role in modulating this activity (Fellin *et al.*, 2009), however the manner in which adenosine alters the properties of these neurons and their synapses has not been investigated.

Adenosine is known to exert both pre and post-synaptic modulatory effects on synaptic transmission (Proctor and Dunwiddie, 1987) via the A<sub>1</sub> receptor, which is highly expressed on thick-tufted layer 5 pyramidal neurons (Ochiishi *et al.*, 1999). These effects will have differing impact on short-term synaptic dynamics. A number of techniques have been utilised to dissect pre and post-synaptic modulatory effects including observing the modulator's effect on currents from bath applied neurotransmitter (Salgado *et al.*, 2011) and using puffed transmitter (Takigawa and Alzheimer, 2003).

However currents produced by these methods may not undergo the same degree of functional modulation due to their artificial time course, amplitude or location. Thus a dissection of the components of unitary EPSPs represents a more physiologically relevant alternative.

In this chapter I examine the effects of adenosine on the synaptic transmission between thick-tufted layer 5 pyramidal neurons demonstrating via a combined experimental and modelling approach that the depressant effects of adenosine are mainly mediated pre-synaptically through A<sub>1</sub> receptor activation. The shift in synaptic dynamics from prominent depression to weak facilitation can be accurately captured by a change only in the probability of release. However the results also indicate that the increased variability in transmission observed in adenosine (and possibly also in control) cannot be precisely captured by a simple model of independent binomial release.

## 3.2 Results

### 3.2.1 Identification of pyramidal neurons and monosynaptic connections

I recorded 58 connections between thick-tufted layer 5 pyramidal neurons (identified according to criteria detailed in chapter 2.1; including 12 pairs of reciprocal connections) from approximately 600 unidirectional tests. Thus around 1 in 10 pairs of neurons exhibited a synaptic connection, in line with previous studies (Markram *et al.*, 1997; Levy *et al.*, 2006). EPSP amplitudes were monitored for stability (5-10 minutes) before the stimulation protocol was recorded. Stimulation protocols consisted of a train of 5-20 pulses (at

15-50 Hz) followed by a recovery test pulse (typically after 500 ms), repeated 25-100 times, separated by 12 seconds. The running mean amplitude (for the last 10 sweeps) of EPSPs was used to monitor the stability of recordings, with recordings discarded when significant changes occurred. On rare occasions disynaptic IPSPs were evoked on top of the EPSPs and these recordings were removed from further analysis. Kynurenic acid (10 mM, non-selective glutamate receptor antagonist) abolished the EPSPs confirming that they were glutamergic ( $n = 5$ ). Connections with a latency of  $>3$  ms were not included in further analysis as they may have been disynaptic.

Evoked EPSPs had a mean amplitude of  $1.33 \pm 0.95$  mV (mean  $\pm$  std dev,  $n = 58$ ), 10-90% rise time of  $2.7 \pm 0.75$  ms, half-width of  $24.4 \pm 3.7$  ms, and a latency of  $1.7 \pm 0.6$  ms (Fig 3.1). All cells exhibited a short sag in response to hyperpolarising current steps, characteristic of the  $I_h$  current, and could be characterised as regular-spiking or intrinsically bursting according to established terminology (Connors and Gutnick, 1990). Following a biocytin and DAB staining procedure cells were found to be located in layer 5 of the somatosensory cortex and had bifurcating apical dendrites with tufts extending into layer 1, indicating they were of the thick-tufted type (Markram *et al.*, 1997).

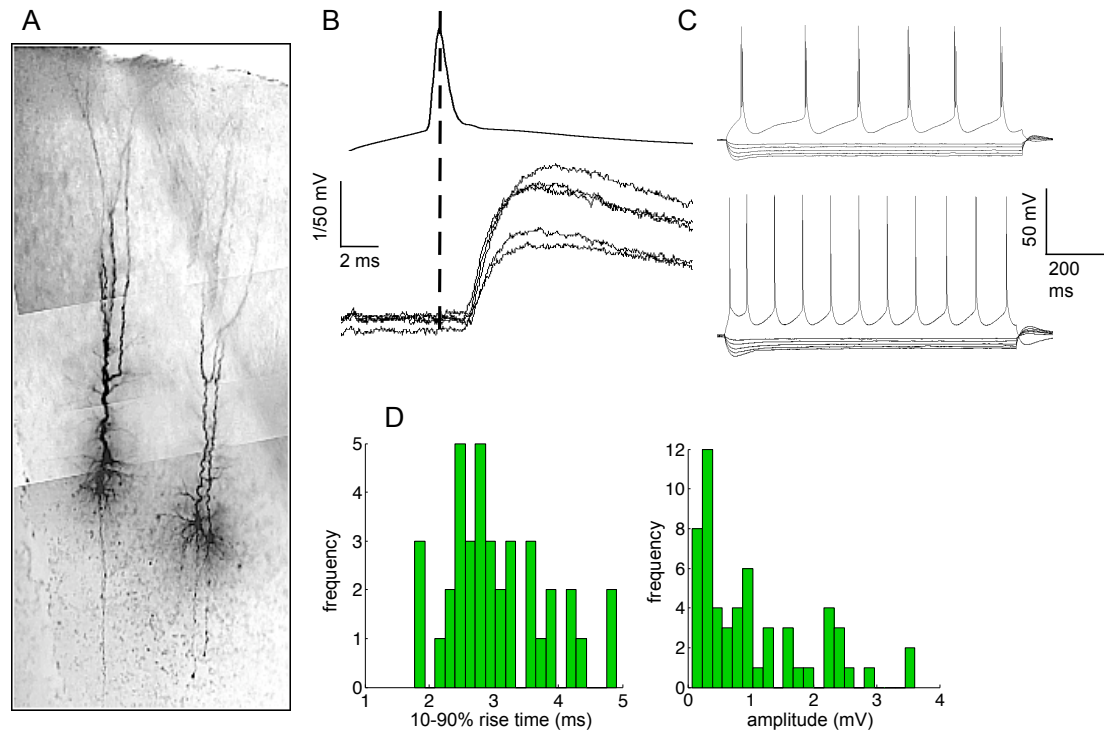


**Fig 3.1** Identification of thick-tufted layer 5 pyramidal neurons. (A) Following a biocytin and DAB staining procedure recorded neurons were found to be located in layer 5 and exhibited bifurcating apical dendrites extending to layer 1. (B) EPSPs showed a short latency (0.5 – 2 ms), demonstrating that they were monosynaptic. (C) Neurons exhibited a depolarising sag in response to negative current steps and fired action potentials in a bursting or adapting pattern. (D) Summary of EPSP rise time (10-90%) and EPSP amplitude across all connections.

### 3.2.2 Suppression of EPSPs by adenosine mediated by $A_1R$ activation

To examine the modulatory effects of adenosine 100  $\mu$ M was bath applied following the characterisation of the synapse in control conditions.

Application of adenosine caused a reduction in the amplitude of the first EPSP in all connections, resulting in a new mean amplitude of  $0.28 \text{ mV} \pm 0.24 \text{ mV}$  ( $n = 48$ ). This change was highly significant (one-tailed Wilcoxon matched pairs,  $P < 0.001$ ,  $n = 48$ ) and represents a mean reduction of 78% (relative to control). Care was taken to ensure the synapse had reached steady state following application of adenosine before recordings commenced (>5 mins). The mean amplitude of EPSPs following adenosine

(100  $\mu$ M) application, and the degree of suppression from control conditions were not significantly different from that observed following application of a high concentration of CPA (5  $\mu$ M, a non-hydrolysable A<sub>1</sub> receptor agonist), suggesting that adenosine acts through the A<sub>1</sub> receptor and that 100  $\mu$ M adenosine is close to the top of the concentration-response curve. There was no significant change in EPSP latency or rise time following application of adenosine. However there was a small but significant reduction in EPSP half-width (table 3.1).

	Control	Adenosine	8-CPT
V <sub>m</sub> (mV)	-67.2 $\pm$ 3.5	-69.1 $\pm$ 3.1	-66.5 $\pm$ 3.7
Amplitude (mV)	1.33 $\pm$ 0.95	0.28 $\pm$ 0.24	1.45 $\pm$ 1
Latency (ms)	1.7 $\pm$ 0.6	1.62 $\pm$ 0.8	1.7 $\pm$ 0.65
Rise time (ms)	2.7 $\pm$ 0.75	2.48 $\pm$ 0.78	2.5 $\pm$ 0.7
Half width (ms)	21.8 $\pm$ 3.7	16.2 $\pm$ 2.6	22.2 $\pm$ 3.1

**Table 3.1** Summary of thick-tufted layer 5 pyramidal membrane potential and EPSP parameters in control, adenosine and 8-CPT (A<sub>1</sub> receptor antagonist).

This sharpening of the decay coincided with a small (but significant, chapter 5) reduction in membrane potential (hyperpolarisation of 2-3 mV). This effect is known to be caused by the modulation of GIRK and other K<sup>+</sup>-channels (Trussell and Jackson, 1987) and is associated with a decrease in neuronal input resistance. Thus the effect on EPSP half-width could have arisen by K<sup>+</sup>-channel mediated shunting of EPSPs or a reduction NMDAR activation mediated by the hyperpolarisation.



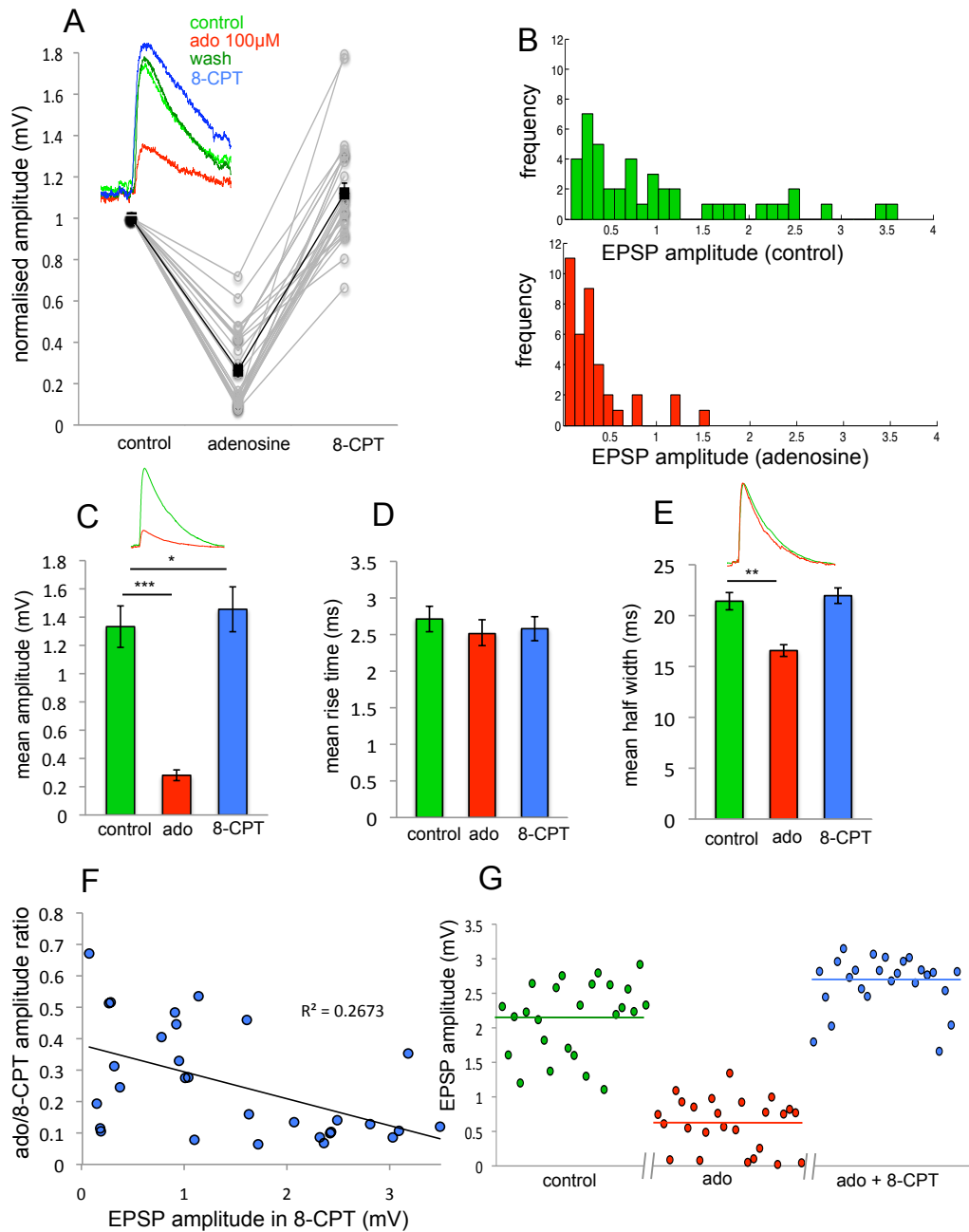


**Fig 3.2** Summary of suppression of EPSPs by adenosine. (A) Mean EPSP amplitudes in control, adenosine (100  $\mu$ M) and adenosine plus the  $A_1$ R antagonist 8-CPT (2  $\mu$ M, normalised to control). Inset shows typical EPSPs in each condition including following adenosine wash (dark green). (B) Distribution of EPSP amplitudes in control and adenosine. (C), (D), and (E) mean amplitudes, rise times and EPSP half-widths across connections in control, adenosine and 8-CPT. Adenosine induced a large reduction in amplitude, a small reduction in half-width, and no change in rise time. All effects were reversed upon application on 8-CPT (in the presence of adenosine). (F) Reduction in mean EPSP amplitude by adenosine plotted against the EPSP amplitude in 8-CPT (to remove variability in endogenous adenosine across connections). Stronger connections were more powerfully suppressed by adenosine. (G) Graph of individual EPSP amplitudes (from a single recording), demonstrating that the amplitude does not run down over the course of an experiment (breaks of  $\sim$ 5 minutes to allow manipulations to reach steady state).

In several experiments ( $n = 2$ ) adenosine was washed from the bath solution, resulting in a return in the EPSP to a similar amplitude to control (fig 3.2a inset). Application of the  $A_1$  receptor antagonist 8-CPT ( $2 \mu\text{M}$ ) in the presence of adenosine removed the reduction in EPSP amplitude and, in most experiments, increased EPSP amplitude above control (amplitude in 8-CPT =  $1.45 \pm 1 \text{ mV}$ ,  $n = 39$ ). This increase could be mediated by the activation of facilitatory adenosine receptors (such as  $A_{2A}$ ) not blocked by 8-CPT, or by the presence of an endogenous tone of adenosine that slightly suppressed (via  $A_1\text{R}$  activation) the synapse in control conditions. To investigate this I first applied 8-CPT (to block  $A_1$  receptors) and then applied adenosine (with 8-CPT still present, to activate non- $A_1$  adenosine receptors). I found no significant difference in the EPSP amplitude in 8-CPT compared to 8-CPT + adenosine (8-CPT =  $0.73 \pm 0.3$ , 8-CPT + adenosine =  $0.72 \pm 0.27 \text{ mV}$ , two-tailed Wilcoxon matched pairs,  $P = 0.79$ ,  $n = 6$ ). Thus the activation of non- $A_1$  adenosine receptors has little effect on EPSP amplitude at this synapse.

There is some evidence that suggests that activation of  $A_{2A}$  receptors may increase through cross-talk with activated  $A_1$  receptors (Sebastiao and Ribeiro, 2009). If this were the case at this synapse the presence of 8-CPT may interfere with  $A_{2A}$  activation. Thus while the previous experiments reveal that the increase in amplitude in 8-CPT was due to the blockade of endogenous  $A_1$  activation, they do not rule out the presence of functional  $A_{2A}$  receptors at the synapse. However I also observed no significant difference in EPSP amplitude between adenosine ( $100 \mu\text{M}$ ) and the  $A_1$  specific agonist

CPA (5  $\mu$ M), which was applied at a high concentration to fully activate  $A_1$  receptors (adenosine =  $0.42 \pm 0.36$ , CPA =  $0.33 \pm 0.27$ , one-tailed Wilcoxon matched pairs,  $P = 0.13$ ,  $n = 7$ ). This indicates that any activation of  $A_{2A}$  receptors by adenosine was minimal. In later experiments, based on this evidence that 8-CPT and 8-CPT + adenosine were equivalent, I applied 8-CPT following adenosine wash.

The degree of suppression observed in 100  $\mu$ M adenosine was inversely proportional (linear regression,  $R = 0.267$ ,  $P = 0.003$ ,  $n = 39$ ) to the amplitude of EPSPs measured in 8-CPT (to remove any effects of the endogenous adenosine tone). Thus stronger synapses were more sensitive to suppression by adenosine (Fig 3.2f).

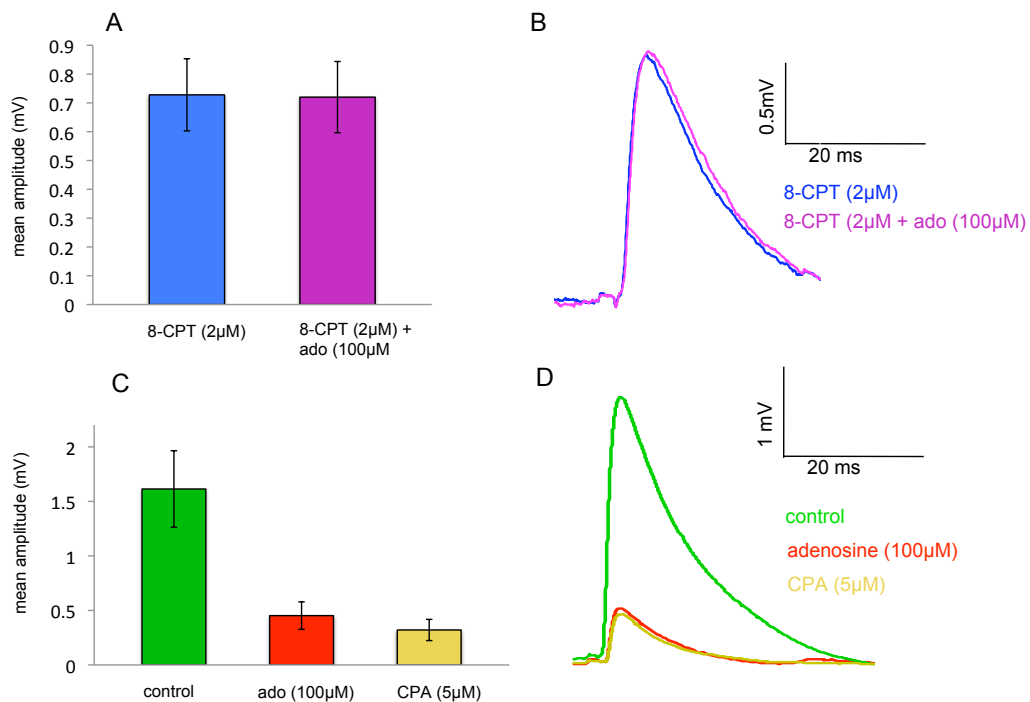


**Fig 3.3** Pharmacology of adenosine mediated EPSP suppression. (A and B) Adenosine had no effect when applied on top of  $A_1$  specific antagonist 8-CPT. (C and D) application of high concentration of non-hydrolysable  $A_1$  specific agonist CPA (5  $\mu$ M) mimicked the effects of 100  $\mu$ M adenosine.

### 3.2.3 Adenosine transforms synaptic dynamics

Synaptic connections between layer 5 pyramidal neurons in juvenile rats typically exhibited prominent short-term synaptic depression (STSD) over a variety of train frequencies (16-50 Hz) in control conditions. The mean PPR (paired pulse ratio,  $EPSP_2/EPSP_1$ ) was 0.86 at 16 Hz ( $n = 13$ ) and 0.78 ( $n = 18$ ) at 50 Hz in control conditions. This depression has been well characterised at this synapse at this stage of development and is caused by a pre-synaptic mechanism (Tsodyks and Markram, 1997). Whilst paired-pulse facilitation was sometimes observed in control conditions (in only 8 out of 58 connections), the EPSPs that followed the first pair exhibited

depression. For example at 30 Hz stimulation the mean ratio of the 8<sup>th</sup> and 1<sup>st</sup> EPSP was  $0.43 \pm 0.12$  ( $n = 13$ ).

Application of adenosine caused a marked increase in the PPR and typically converted paired-pulse dynamics from depression to facilitation regardless of the stimulation frequency (for example the PPR at 16 Hz was  $1.17 \pm 1.1$ , and at 50 Hz was  $1.45 \pm 0.67$ ). However the EPSPs later in the train still exhibited depression (although at a reduced magnitude compared to control) in adenosine. The mean ratio of the 8<sup>th</sup> and 1<sup>st</sup> EPSP in adenosine for trains at 30 Hz was  $0.77 \pm 0.32$  ( $n = 12$ ) compared to  $0.43 \pm 0.12$  in control. Facilitation is known to occur over multiple time scales at cortical synapses (Zucker and Regehr, 2002), and this was evident in my data from the amplitude of the recovery EPSP (500 ms after the end of the train) in adenosine (fig 3.4d). Whilst in control conditions the recovery EPSP was typically still depressed compared to the 1<sup>st</sup> EPSP, in adenosine it was frequently facilitated. In some connections the recovery EPSP was as much as 4 times the amplitude of the first pulse.

Application of 8-CPT abolished the changes in dynamics produced by adenosine and significantly decreased the PPR compared to control (fig 3.4b, at 50 Hz, control =  $0.76 \pm 0.34$ , 8-CPT =  $0.62 \pm 0.21$ , one-tailed Wilcoxon matched pairs,  $P = 0.02$ ,  $n = 16$ ), indicating again the role played by endogenous activation of A<sub>1</sub> receptors in control conditions. This is addressed in further detail in chapter 4.

In some experiments the paired pulse stimulations were conducted at a variety of frequencies in order to more fully characterise the time course of

short-term dynamical changes in both control conditions and adenosine. These experiments demonstrate a complex time course for the short-term dynamics (fig 3.4c), with the PPR exhibiting minima at the highest stimulation frequency (100 Hz) and also at ~3 Hz stimulation, resulting from the decay of the facilitatory component occurring more quickly than the recovery from depression. Significantly however, the overall pattern of depression and facilitation in control and in adenosine respectively, remained robust. Depression dominated at each stimulation frequency in control and in 8-CPT, and was strongest in both at 100 Hz and 3 Hz. Between these frequencies an element of facilitation was apparent, peaking between 25 and 50 Hz, although the mean PPR was still >1, indicating that the dynamics were still dominated by depression. The paired-pulse dynamics in adenosine followed a broadly similar pattern, as although the PPR was consistently increased compared to control and 8-CPT, the time course of recovery from depression and facilitation was identical (fig 3.4c).

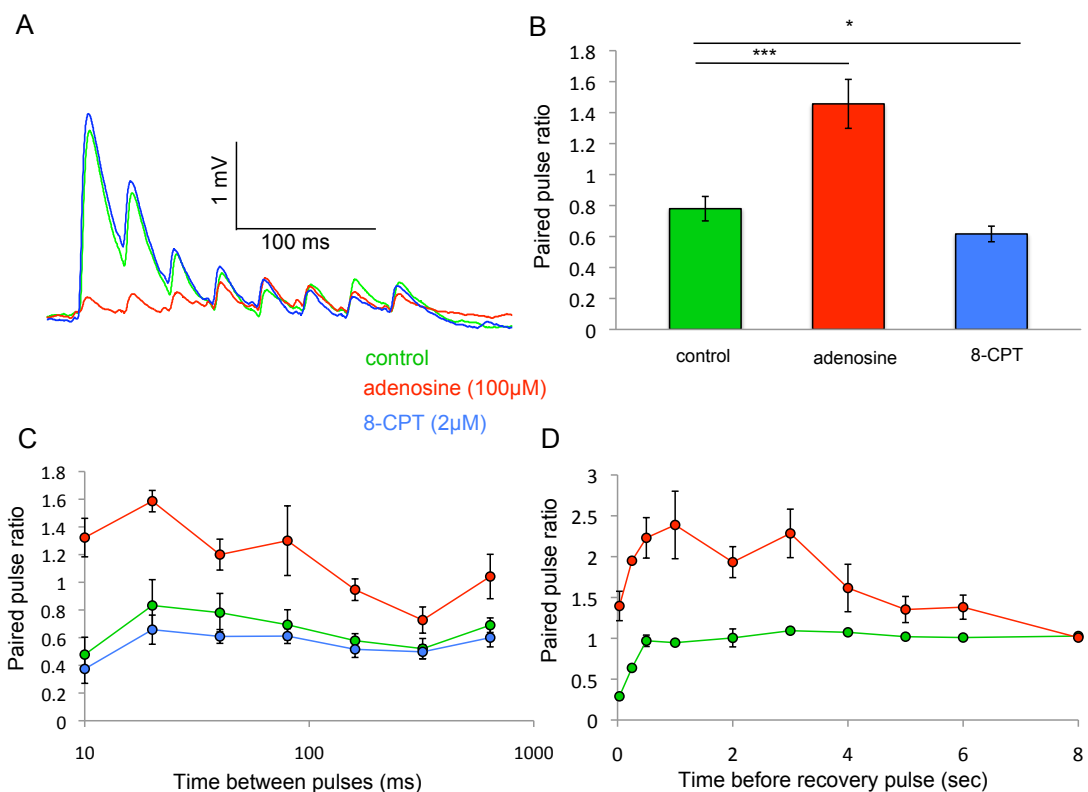


**Fig 3.4** Summary of the effects of adenosine on short-term synaptic dynamics. (A) Typical sweep-averaged EPSP trains (30 Hz) in control (green), adenosine (red) and 8-CPT (blue). (B) Mean paired-pulse ratio at 50 Hz in the three conditions. (C) Mean paired pulse ratios at a range of frequencies illustrating similar time dependence of changes between control, adenosine and 8-CPT. (D) Mean ratio of recovery test EPSP to initial EPSP illustrating the augmentation of the recovery pulse in adenosine (red), but not in control (green).

In some experiments it was notable that the recovery test EPSP (500 ms following the train) continued to exhibit prominent facilitation in adenosine. This facilitation was particularly strong after a longer train of EPSPs (20 pulses at 30 Hz), indicating that it may have been a distinct form of facilitation with a longer time constant of decay (typically 5-10 seconds), known as augmentation (Zucker and Regehr, 2002). Augmentation has previously been observed in the pre-frontal cortex of rodents (Hempel *et al.*, 2000), where excitatory connections typically exhibit a lower probability of

transmitter release, but has not been previously identified in sensory cortices (Wang *et al.*, 2006). I decided to investigate this phenomenon further so in a subset of connections I varied the time to the recovery pulse. No significant augmentation was observed in control experiments (fig 3.4d, green), however in adenosine augmentation was strongly expressed in the recovery EPSP, reaching a maximal amplitude ( $\sim 200\%$  larger than the initial EPSP,  $n = 5$ ) between 1 and 3 seconds after the EPSP train (fig 3.4d) following recovery from depression, and decaying back to the amplitude of the initial EPSP in  $\sim 8$  seconds.

#### 3.2.4 Effects of adenosine on binomial parameters

The probability of transmitter release is a key determinant of short-term dynamics at cortical synapses (Tsodyks and Markram, 1997) and the prominent short-term dynamical changes at these synapses have been used to estimate the mean probability of transmitter release and time constants of depression and facilitation in phenomenological models (Tsodyks and Markram, 1997; Varela *et al.*, 1997). Thus to further quantify the changes in dynamics observed in adenosine I used the EPSP trains to fit a deterministic model of short-term synaptic dynamics parameterised by probability of release ( $p$ ), maximal EPSP strength ( $aN$ ), and time constants ( $\tau_D$  and  $\tau_F$ ) for depression and facilitation.

The model characterises the synapse with maximal efficacy ( $aN$ ) and assumes that when an action potential arrives a fraction ( $p$ ) of available pre-synaptic resources are utilised. This utilised fraction becomes instantaneously unavailable then recovers exponentially with time constant



$\tau_D$ . Facilitation is incorporated into the model as a pulsed increase in  $p$  with each action potential, which decays with time constant  $\tau_F$ . Full details of the iteration can be found in chapter 2.3.2.

Whilst it is inevitable that some information on the underlying biophysical processes is lost in simple phenomenological modelling the aim was to capture the changes at the synapse induced by adenosine in a model that would be suitable for network level computational analysis. Given the nature of the experiments, which involved periods of recording (5–10 minutes) interspersed with periods of drug wash-on (5–10 minutes), there were limits on amount of data that could be collected in each pharmacological manipulation.

The paired-pulse experiments demonstrated that the recovery from depression and facilitation follow broadly similar time courses across the pharmacological manipulations, so I constrained these time constants to remain the same between control, adenosine and 8-CPT within each experiment, allowing just  $aN$  and  $p$  to vary freely.

The fitting procedure in general captured the changes in dynamics and mean EPSP amplitude in adenosine by a reduction only in  $p$ , the probability of release. Some very weak connections were removed from the fitting analysis because of a very low signal to noise ratio (EPSP amplitudes below 0.1 mV). In the 24 connections that were fit using the model,  $p$  reduced from  $0.42 \pm 0.08$  in control, to  $0.1 \pm 0.1$  in adenosine, while rising to  $0.47 \pm 0.09$  in 8-CPT (fig 5a). The reduction from control to adenosine was highly significant (paired one-tailed t-test,  $P < 0.001$ ,  $n = 24$ ), as was the increase in

$p$  between control and 8-CPT (paired one-tailed t-test,  $P = 0.012$ ,  $n = 24$ ). No significant change was observed for the synaptic efficacy parameter  $aN$  (control =  $4.06 \pm 2.2$  mV, adenosine =  $3.82 \pm 3.1$  mV, 8-CPT =  $3.68 \pm 2.4$  mV, paired one-tailed t-test control/adenosine,  $P = 0.68$ ,  $n = 24$ , control/8-CPT,  $P = 0.12$ ,  $n = 24$ , fig 3.5b). The fitting procedure was applied to connections stimulated in a number of patterns at different frequencies (15-50 Hz) with no significant changes in the means of fitted parameters, indicating the robustness of the approach.

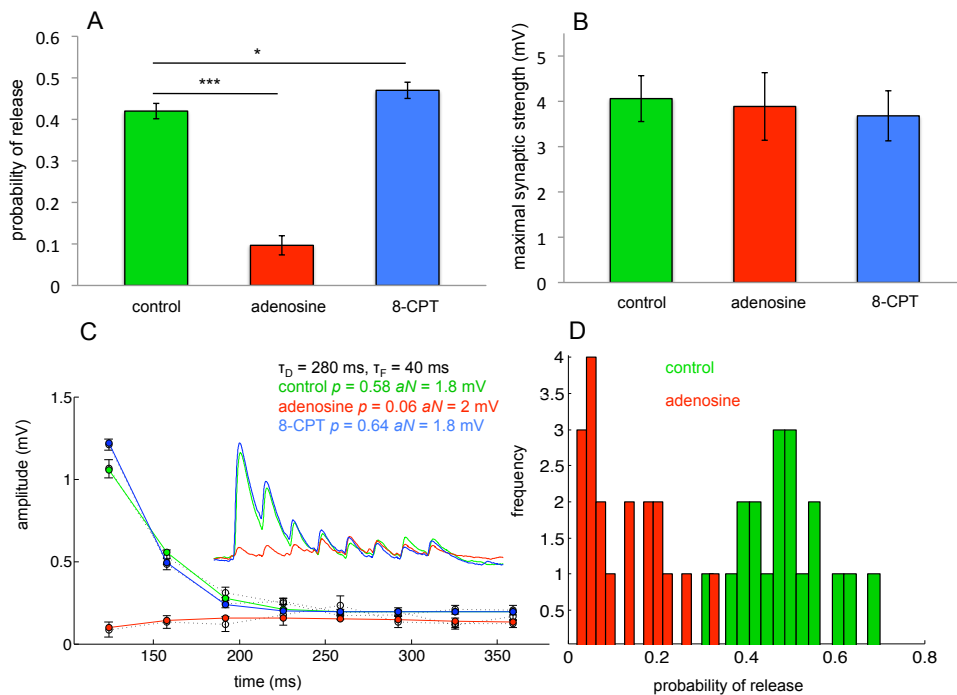


**Fig 3.5** Suppression by adenosine is mediated by a reduction in the probability of transmitter release. (A and B) Adenosine significantly reduced  $p$  (probability of release) but not  $aN$  (maximal synaptic strength) when EPSP trains were fitted to a model of synaptic dynamics. (C) Example of EPSP amplitude fits (coloured), and measured amplitudes (grey) in all three manipulations. (D) Summary of release probability for individual connections in control and adenosine.

These results suggest that the effects of adenosine are mediated pre-synaptically. To further test this suggestion I examined how the reliability of synaptic transmission (the variation in EPSP amplitude between sweeps, and rates of transmission failure) was modulated by adenosine. The coefficient of variation (CV = standard deviation/mean,  $\sigma/\mu$ ) of EPSP amplitude offers a normalised measure of variability, and because it does not depend on mean quantal amplitude can be used to determine the pre or post-synaptic locus of changes in synaptic transmission. The mean CV across connections was  $0.44 \pm 0.28$  in control,  $1.52 \pm 1.37$  in adenosine, and  $0.40 \pm 0.33$  in 8-CPT. This represents a significant increase between control and adenosine (paired one-tailed t-test,  $P < 0.001$ ,  $n = 48$ ), but no significant change between 8-CPT and control (paired one-tailed t-test,  $P = 0.18$ ,  $n = 42$ , fig 3.6a). A similar pattern was observed for the failure rate of synaptic transmission (measured for the initial EPSP). Failures of transmission were measured manually using the deconvolved voltage traces as this method allowed the clearest identification of failures. The failures for each recording were averaged and then closely examined to confirm the accuracy of the technique (fig 3.6e), i.e. that small EPSPs were not being miss-counted as failures. The mean failure rate across connections was  $0.07 \pm 0.09$  in control (comparable to previous studies, Markram *et al.*, 1997),  $0.38 \pm 0.27$  in adenosine and  $0.06 \pm 0.1$  in 8-CPT (fig 3.6b). The changes were again significant between control and adenosine (one-tailed Wilcoxon matched pairs,  $P < 0.001$ ,  $n = 48$ ) but showed no significant difference between control and 8-CPT (one-tailed Wilcoxon matched pairs,  $P = 0.22$ ,  $n = 42$ ). Analysis of the changes in EPSP amplitude and  $1/CV^2$  in control and

adenosine provides another method of determining pre or post-synaptic changes. By plotting the ratio of changes in amplitude and  $1/CV^2$  between control and adenosine, the shaded region (fig 3.6c) between the  $x = y$  diagonal and  $y = 1$  corresponds to a post-synaptic change. The vast majority of connections (44 out of 48) show a greater proportional change in  $1/CV^2$  compared to EPSP amplitude and lie within the region corresponding to a pre-synaptic change (Levy *et al.*, 2006).

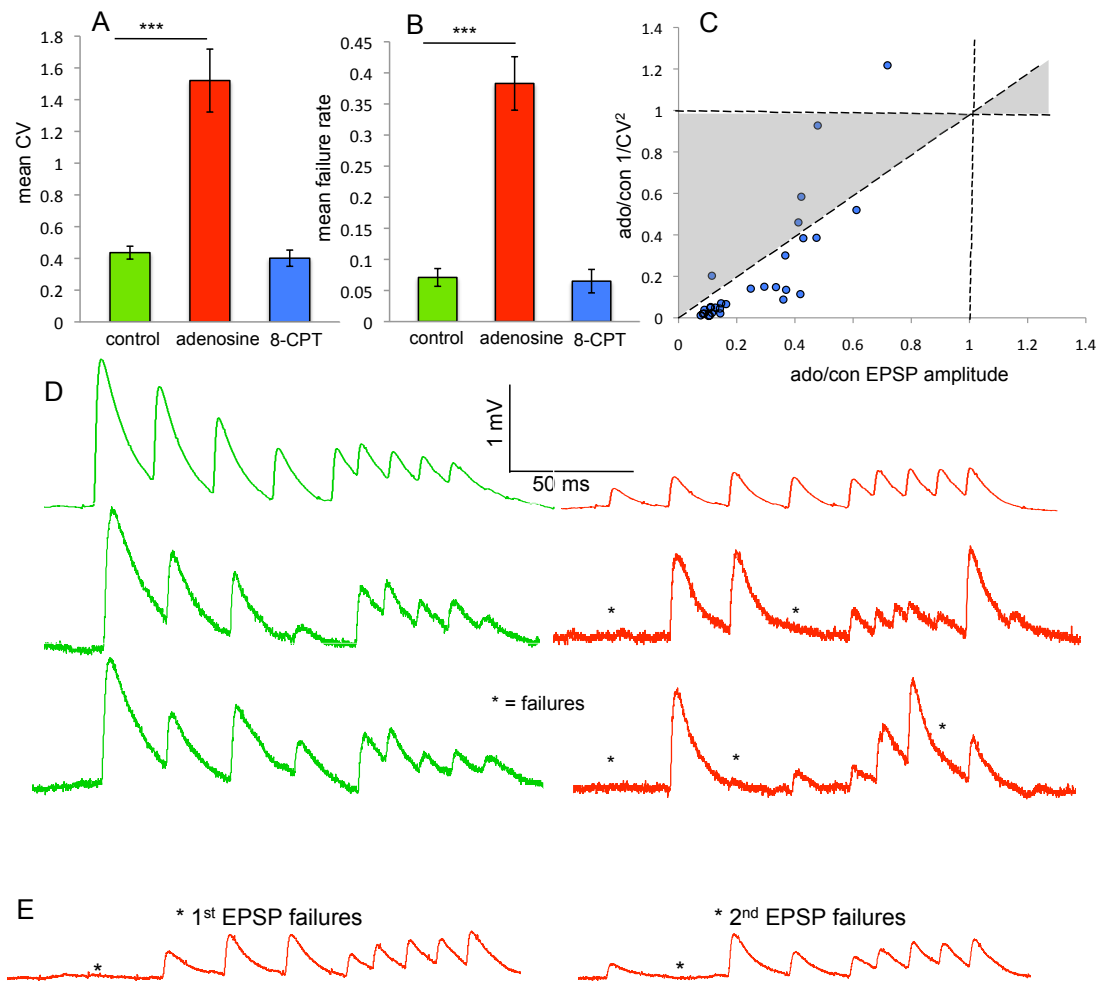


**Fig 3.6** Adenosine increases EPSP variability and failures. (A) Mean CV across connections. (B) Mean failure rate (initial EPSP) across connections. (C) Proportional reduction in  $1/CV^2$  against EPSP amplitude in adenosine indicates amplitude reduction occurs through a pre-synaptic mechanism. (D) Averaged EPSPs trains (~30 sweeps, top) and two examples of single-sweep transmission in control and adenosine illustrating noisy transmission in adenosine. (E) Sweep averaged EPSP trains in adenosine in which (left, 18 sweeps) 1<sup>st</sup> EPSPs were counted as failures, and (right, 14 sweeps) in which 2<sup>nd</sup> EPSPs were counted as failures.

In spite of the large increase in failure rate in adenosine, it was striking that the amplitude of EPSPs during successful transmission were frequently relatively large. I decided to investigate this phenomenon further by utilising a binomial model based analysis approach to further derive the parameters of synaptic transmission – specifically the quantal size ( $a$ ) and

number of independent connections ( $N$ ). I took advantage of the EPSP train data that can be shown to differ primarily by the effective probability of release ( $p$ ) when, within the train, the proportion difference in  $CV^2$  is greater than the proportional difference in mean amplitude (Bremaud *et al*, 2007). Previous experimental work has demonstrated that the synaptic dynamics at thick-tufted layer 5 pyramidal synapses are predominantly determined pre-synaptically (Markram, 1997) and in all, 21 out of 24 of the connections that transmitted at a sufficient signal-to-noise ratio fit this criterion. Care should be taken with this approach because binomial analysis places many strict assumptions on the characteristics of transmitter release such as lack of inter and intra site quantal amplitude variability and probability of release, and with this data, that the EPSP amplitudes within a train solely differ due to effective probability of transmitter release. Nevertheless this approach has previously achieved some success when applied to similar data (Bremaud *et al.*, 2007).

The variability in EPSP amplitude between sweeps is governed by the quantal nature of synaptic transmission. Assuming synaptic transmission is governed by simple binomial statistics (see discussion) the statistics of EPSP amplitude variability and failure rate can be exploited to estimate the binomial parameters of the synapse. I used these methods to fit binomial parameters to my data from the three experimental manipulations.

I used a linearised version of mean-variance analysis to plot the variance divided by mean amplitude ( $V/M$ ) against mean amplitude ( $M$ ). Assuming binomial statistics this predicted a linear relationship between  $V/M$  and  $M$ ,

with the inverse of the slope estimating  $N$ , and the y-axis intersection estimating  $a$  (fig 3.7a). However, in contrast to the model of synaptic dynamics, the variance fitting method produced large differences in the estimates for the parameters  $N$  and  $a$ , typically predicting a large decrease in  $N$  and an increase in  $a$  in adenosine (fig 3.7c and d). The variability in transmission observed in adenosine was generally higher than would be predicted from a simple reduction in the probability of release – predicted from the model of short-term synaptic dynamics. While the model of synaptic dynamics estimated no significant change in  $aN$  (the maximal synaptic strength) the binomial analysis of variance predicted a large decrease. Similar changes in  $a$  and  $N$  were estimated using an analysis of failure rates to predict binomial parameters. These counterintuitive results may indicate a deviation from binomial statistics, however it is also possible that they have arisen due to problems with the mean variance analysis technique. In particular if there are changes in quantal amplitude (even if they are minor) within the EPSP trains the results may be skewed towards higher  $N$  and lower  $a$ , and it is possible that the extent to which  $q$  changes within a train is different in adenosine and control/8-CPT. Thus I decided to modify the approach and investigate these hypotheses further.

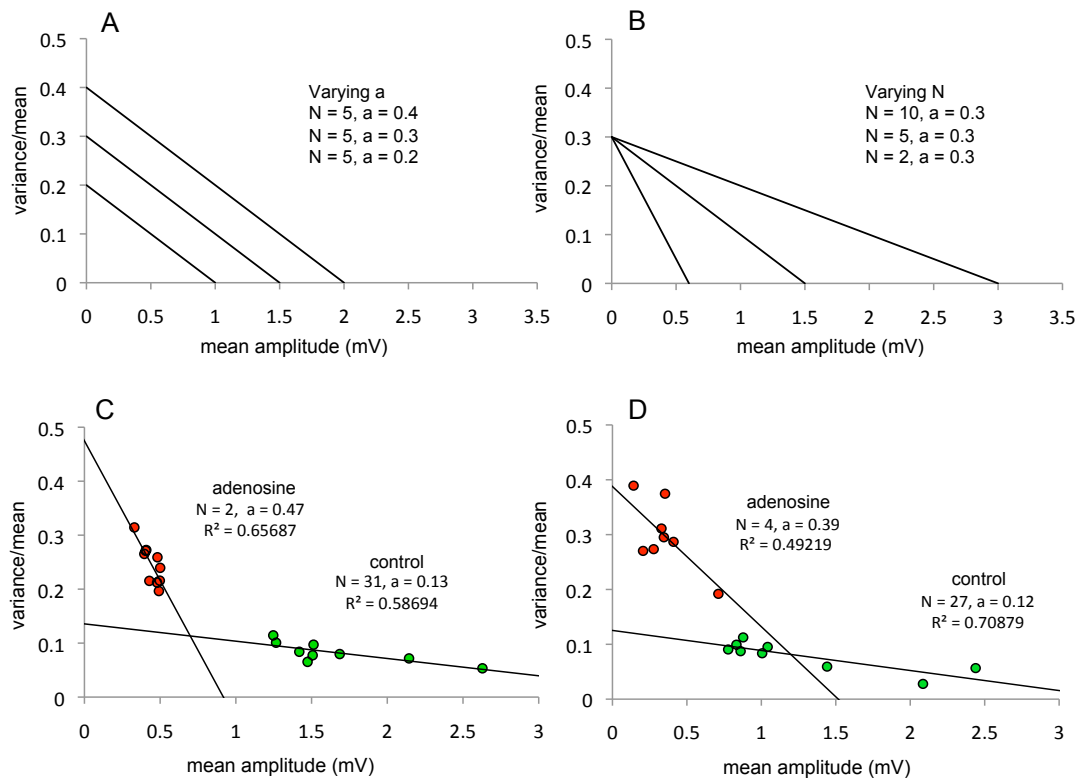


**Fig 3.7** Mean-variance analyses provide conflicting estimates of parameters between control and adenosine. (A and B) V/M against mean (M) amplitude plots across spectrum of probability of release (0-1) predict a linear trend. (A) Illustrating the effect of varying  $a$ . (B) Illustrating the effect of varying  $N$ . (C and D) Mean-variance analysis used to predict  $a$  and  $N$  for 2 typical connections in control and adenosine. In adenosine,  $a$  is increased and  $N$  shows a large decrease.

The changes in  $a$  and  $N$  were predicted because the increase in variability in adenosine was significantly higher than would be expected based on a simple drop in the probability of vesicle release. I wanted to investigate this phenomena further thus I decided to isolate a binomial parameter experimentally to determine the extent to which it was modulated by adenosine. This experimental determination of a binomial parameter would also enable further inferences to be drawn regarding the release statistics. To do this I included strontium chloride in the aCSF (full details – chapter 2.3.4). Strontium is known to prolong the asynchronous phase of vesicle release (Miledi, 1966), thus by using a combination of 4 mM  $\text{SrCl}_2$  and 1 mM



CaCl<sub>2</sub> in the extracellular medium I was able to detect asynchronous EPSPs (aEPSPs) in the post-synaptic neuron following synchronous EPSPs evoked by pre-synaptic action potentials (fig 3.8a).

In these experiments, following detection of a strong mono-synaptic connection (>1 mV) I first recorded the post-synaptic response to trains of action potentials at 30 Hz. Following this I switched from aCSF to aCSF containing SrCl<sub>2</sub> and recorded up to 100 sweeps of the post-synaptic response to several action potentials, I then bath applied 100 µM adenosine and repeated the protocol, before switching back to the standard 2 mM CaCl<sub>2</sub> aCSF and recording the 30 Hz stimulation protocol in 100 µM adenosine. At the end of the experiment adenosine was washed off and 2 µM 8-CPT bath applied to characterise the tonic effect of endogenous activation of A<sub>1</sub> receptors in the slice. Thus these experiments allowed me to collect the typical EPSP train data as well as a series of aEPSPs in both control conditions and in adenosine. Upon application of adenosine there was a marked reduction in the frequency of aEPSPs and this meant that in some experiments (2 out of 7) there were insufficient aEPSPs for further detailed analysis.

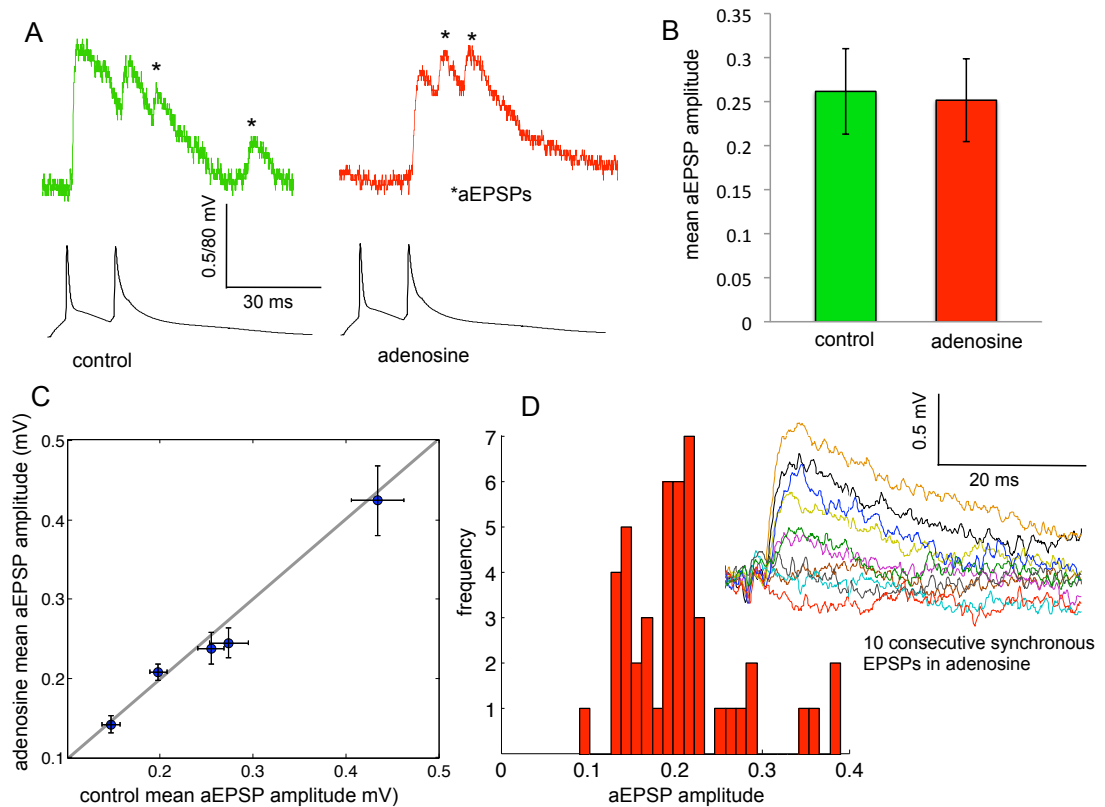


**Fig 3.8** Adenosine had no significant impact on the amplitude of asynchronous EPSPs (aEPSPs) measured in strontium. (A) Example individual traces illustrating aEPSPs recorded in strontium in control and in adenosine. (B and C) Adenosine had no significant impact on the amplitude of aEPSPs. (D) An example distribution of aEPSPs recorded from a single connection in adenosine. Inset illustrates 10 consecutive initial EPSPs recorded in normal aCSF in adenosine. There were 4 transmission failures and 4 EPSPs larger than the maximum amplitude of the aEPSPs (>0.4 mV).

Examining aEPSPs rather than action potential independent minis (mEPSPs) gives the advantage of knowing the pre-synaptic origin of the quantal events. Although some foreign spontaneous EPSPs were observed in the post-synaptic trace, only EPSPs of rise time within 2 standard deviations of the rise time measured from the evoked EPSPs were included in the analysis. I found that there was a 250-500% increase in the probability of measuring EPSPs meeting this criterion in a 100 ms window immediately after the evoked synchronous response compared to a window immediately before stimulation. Thus I could be sure that the majority of aEPSPs included in the analyses originated from the pre-synaptic neuron.

Adenosine was found to have no significant impact on the amplitude of aEPSPs (control =  $0.26 \pm 0.11$  mV, adenosine =  $0.25 \pm 0.11$  mV, paired one-tailed t-test,  $P = 0.10$ ,  $n = 5$ , fig 3.8b-c). Fig 8d illustrates a typical distribution of aEPSP amplitudes for a single connection in adenosine.

The EPSP train amplitudes and variances were then again used to derive the binomial parameters. In control conditions there was a good correlation between the mean aEPSP amplitude measured in strontium and the amplitude of  $a$  predicted from the mean-variance or failure rate fitting procedure (linear regression, gradient = 0.84,  $R^2 = 0.82$ ,  $P = 0.02$ ,  $n = 5$ ). However as was observed previously, the binomial fitting procedures predicted an increase in  $a$  in adenosine, which was not observed in strontium.

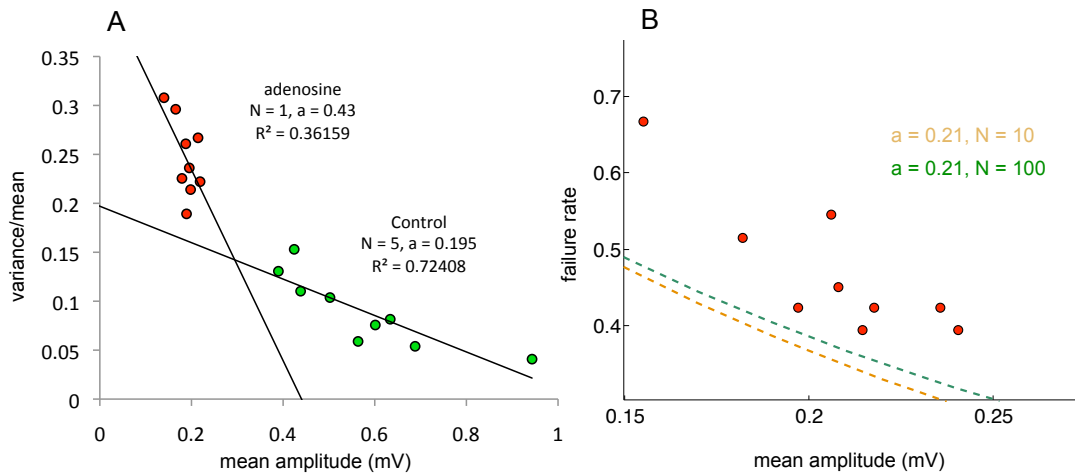


**Fig 3.9** Analysis of strontium experiments indicates deviation from binomial release statistics. (A) Mean-variance analysis of EPSPs in control and in adenosine. The mean amplitude of aEPSPs for this connection was 0.21 mV in both control and adenosine. Mean variance analysis predicts amplitudes of 0.195 in control and 0.43 in adenosine. (B) Failure rate against amplitude of EPSP train data in adenosine. If the binomial parameter  $a$  is constrained to the mean aEPSP amplitude the data cannot be fitted to a binomial model. Dotted lines illustrate binomial fits for  $N = 10$  and  $N = 100$ , which both predict fewer EPSP failures than were observed.

While these results do suggest that upon application of adenosine there may be some deviation away from binomial independent release statistics some care needs to be taken with this interpretation given the assumptions inherent in the analysis technique. Nevertheless further evidence for this was found by analysing the rate of transmission failure in adenosine. I plotted the rate of failures against mean amplitude to again estimate the binomial parameters, this time however I constrained the fitting procedure with the quantal amplitude ( $a$ ) obtained from the aEPSPs measured in strontium. This method resulted in vastly increased predictions for  $N$  in adenosine (fig 3.9b). In several cases the best fit for  $N$  was increased to over 1000, or could not be fit at all. This data suggests that in adenosine release failures do not occur independently and that the transmission can no longer be described using binomial statistics. This result is highlighted by the fact that there was a strong tendency for EPSPs in adenosine to be larger than

the aEPSPs measured in strontium, despite the high rate of transmission failures (fig 3.8d).

It is however important to note that while the data could be well described within a binomial model in control conditions the limitations of the analysis technique (particularly the assumption of no change in quantal amplitude within a train, and the assumption of no inter or intra-site variance in parameters) it remains possible that the parameters identified in control are also subject to errors.

### 3.3 Discussion

These results demonstrate that adenosine can powerfully suppress synaptic transmission between thick-tufted layer 5 pyramidal neurons. Using paired intracellular recordings I have demonstrated that adenosine modulates a number of properties of mono-synaptic transmission, including the variability, reliability and short-term dynamics. By fitting averaged EPSP trains to a model of synaptic dynamics I have demonstrated that the changes can be accurately described by a reduction in the probability of transmitter release. However by measuring aEPSP amplitude using strontium I have also shown that transmission in adenosine cannot be described by binomial statistics, suggesting that failures of release in adenosine do not occur independently and that reliability of transmission decreases by more than would be expected given the decline in probability of transmitter release.

The suppression of transmission was blocked by the A<sub>1</sub> receptor antagonist 8-CPT. The addition of 8-CPT to the bath solution caused EPSP amplitude to increase significantly above control conditions indicating the presence of a

persistent endogenous tone that is investigated in the next chapter.

Although  $A_{2A}$  receptor mRNA has been detected at low levels in the rat cortex (Dixon *et al.*, 1996), I did not find any evidence that the synaptic actions of adenosine included a significant  $A_{2A}$  component. The  $A_1$  to  $A_{2A}$  receptor ratio is known to shift towards increased  $A_{2A}$  activation in the hippocampus of aged (24 months) rats (Rebola *et al.*, 2003), indicating that perhaps the lack of an  $A_{2A}$  component in these results was due to the earlier period of development that was examined.

The increase in EPSP CV (fig 3.6 a, c) indicates that the changes in adenosine were induced pre-synaptically, although a small post-synaptic component was evident in the small decrease in EPSP half-width. However this modulation did not appear to induce a significant reduction in quantal amplitude measured from aEPSPs.

By quantifying the changes in short-term plasticity using a model of synaptic dynamics I have demonstrated that the changes induced by adenosine can be well captured by a change only in the probability of release. While the simple phenomenological model used necessarily neglects some known components of depression and facilitation (Zucker and Regehr, 2002), it was able to capture the dynamics in each pharmacological manipulation. It was also notable that connections with the largest amplitude initial EPSPs were most strongly suppressed by adenosine, meaning that the distribution of synaptic amplitudes underwent a dramatic shift in adenosine. The distribution of amplitudes can be captured by a log-normal distribution (Song *et al.*, 2005) in each manipulation, although in adenosine the skew

towards strong connections is reduced. The functional significance of this shift away from a heavy-tail distribution is unclear but is likely to have a significant impact of network dynamics.

It was also notable that in adenosine connections exhibited highly augmented recovery EPSPs. This augmentation appeared to be masked by depression in control conditions. Augmentation at connections between pyramidal neurons in the pre-frontal cortex has previously been implicated in working memory as it can support persistent activity following a transient input (Hempel *et al.*, 2000). This is perhaps a mechanism through which adenosine can act to facilitate the generation of slow waves in the absence of sensory inputs during sleep (Benington *et al.*, 1995).

While the averaged EPSP train data were well fit to a model of synaptic dynamics the variability in EPSP amplitudes between sweeps presents a more complex picture. Using mean-variance analysis, connections in control conditions were parameterised under an assumption of independent binomial release statistics and the predicted values for quantal amplitude were well matched by the measured amplitudes of aEPSPs in strontium. However in the presence of adenosine my results suggest that EPSP failure rates and variability increased by more than would be predicted under a binomial model of independent vesicle fusion and transmitter release. There could be several reasons for this discrepancy between control and adenosine

One possible explanation is that in adenosine failures of release are compound rather than independent. There is increasing evidence that

multiquantal transmitter release occurs at cortical synapses (Loebel *et al.*, 2009; Huang *et al.*, 2010). Assuming multiple vesicles can fuse and release transmitter at each terminal during an action potential then the disruption of  $\text{Ca}^{2+}$  entry by  $A_1$  receptor activation may influence multiple release events simultaneously. An alternative explanation is that under  $A_1$  receptor activation there is an increased rate of failure of action potential transduction in the axon. If this were to occur multiple pre-synaptic terminals could be simultaneously affected. However it should be noted that, in control conditions, and in agreement with previous research (Loebel *et al.*, 2009) the number of release terminals predicted by mean-variance analysis regularly exceeded the number of synaptic contacts that have been observed using electron microscopy at these connections (Markram *et al.*, 1997), thus favouring the multiquantal release interpretation.

A third possibility is that the method of analysis is itself problematic when applied to EPSP train data. It may be the case that small deviations away from the assumptions in the technique (for example that within a EPSP train amplitude differences can be assumed to be solely due to pre-synaptic mechanisms) are translated to large changes in the parameters that are calculated. There may be slight differences in the deviations away from these assumptions between control and adenosine, resulting in large changes in parameters to be predicted in the binomial fits.

I have demonstrated that the synaptic actions of adenosine are amenable to quantitative descriptions of synaptic dynamics. However more work needs to be done to understand the dramatic increases in the variability and



transmission failures that cannot be described assuming binomial statistics. While adenosine is well known for its suppression of synaptic transmission, these effects are often considered in the context of population averaged EPSPs induced by extracellular stimulation. By examining the statistics of paired recordings my results quantify the reduction in reliability that should be considered one of adenosine's major effects. Consideration of this reduction in the reliability in synaptic transmission will be required for further understanding of the functional implications of adenosine A<sub>1</sub> receptor activation in the neocortex

Extracellular adenosine levels rise in various parts of the brain in response to sleep deprivation and this increase is known to modulate network activity in the neocortex (Schmitt *et al.*, 2012). The precise ways in which complex network dynamics such as the slow oscillations in the neocortex are generated are likely to be understood through the utilisation of quantitative network models as well as experiments. This research demonstrates that aspects of neuromodulation by adenosine can be well captured using simple tractable models, however more research must be conducted before the stochastic aspects of synaptic transmission in individual sweeps can be reduced to simple models.

## **4. Adenosine A<sub>1</sub> receptor activation underlies the developmental shift at layer 5 pyramidal cell synapses and is a key determinant of mature synaptic strength**

### 4.1 Introduction

In the neocortex profound changes occur in the properties of synaptic transmission during early post-natal development (Feldmeyer and Radnikow, 2009). At early stages, excitatory synapses across the neocortex are typically subject to prominent short-term synaptic depression (STSD) at a variety (5-100 Hz) of stimulation frequencies. This depression, which arises due to a combination of high transmitter release probability (Feldmeyer and Radnikow, 2009) and a relatively slower vesicle replenishment process (Thomson and Lamy, 2007), plays a key role in cortical information processing (Abbott and Regehr, 2004).

Much of the structural and functional information about synaptic transmission in the neocortex has been obtained from dual (or multiple) intracellular recordings (Silberberg *et al.*, 2005; Thomson and Lamy, 2007) in brain slices, and much of this data has come from *in vitro* studies on developing rodents (postnatal 2-3 weeks), as this preparation offers maximised probability of success during recordings. An increase in myelination during development causes a reduction in the resolution of the IR-DIC optics commonly used in brain slice experiments. There is also increased difficulty in preventing tissue distortion and maintenance of a clean patch pipette tip required for successful whole-cell patch clamp recordings. The prominent STSD that dominates excitatory synapses across

the neocortex at this stage of development (Feldmeyer and Radnikow, 2009) has therefore been reflected upon more frequently in the literature.

However during maturation this depression becomes weaker and at some synapses develops into weak short-term facilitation over a range of stimulation frequencies. This change is associated with a decrease in reliability and efficacy (Reyes and Sakmann, 1999; Williams and Atkinson, 2007), and has been observed at a number of synaptic pathways across the neocortex (Cheetham and Fox, 2010) and other parts of the brain (Iwasaki and Takahashi, 2001). It has been described as particularly prominent in connections between thick-tufted pyramidal neurons in layer 5 of the neocortex (Reyes and Sakmann, 1999).

Most evidence suggests that the changes in dynamics that are observed with development are mediated by a decrease in the pre-synaptic probability of transmitter release (Choi and Lovinger, 1997; Li and Burke, 2002), although a decrease in vesicle recovery time constants has also been suggested to play a role (Thomson and Lamy, 2007).

A large number of factors contribute to the variation in the probability of transmitter release observed across synapses, and indeed individual synapses are highly dynamic with respect to efficacy and reliability.

Transmitter release probability can be modulated by changes in calcium channel expression (Iwasaki *et al.*, 2000), the history of previous activity at the synapse (Abbott *et al.*, 1997) and by a variety of neuromodulators (Wu and Saggau, 1997).

One such neuromodulator that is known to affect probability of release across the brain is adenosine. Adenosine is known to play important roles in the modulation of sleep, locomotion and respiration (Dunwiddie and Masino, 2001); and is released during pathological seizures and ischemia, helping minimise excitotoxic damage (Dale and Frenguelli, 2009), but also during normal physiological activity (Fredholm, 1996). Activation of pre-synaptic A<sub>1</sub> receptors has been shown to decrease the probability of transmitter release at a range of synapses and thus transform strong depressing synapses into weaker facilitating ones (Dunwiddie and Haas, 1985; Varela *et al.*, 1997).

Adenosine has been detected at low but pharmacologically significant concentrations in brain tissue both *in vitro* (Dunwiddie and Diao, 1994) and *in vivo* (Porkka-Heiskanen *et al.*, 2000), and the tonic activation of A<sub>1</sub> receptors in hippocampal brain slices increases during development (Sebastiao *et al.*, 2000). Thus I hypothesised that adenosine may play a role in this developmental switch in the properties of synaptic transmission.

In this chapter I examine the extent to which the tonic activation of A<sub>1</sub> receptors is responsible for the developmental changes associated with this switch in dynamics at synapses between thick-tufted layer 5 pyramidal neurons of the somatosensory cortex, demonstrating that increased and heterogeneous activation of A<sub>1</sub> receptors drives many of the developmental changes. I provide evidence that the increased endogenous activation is driven by an increased but highly local adenosine tone.

## 4.2 Results

### 4.2.1 Characteristics of connections across development

Using paired whole cell current-clamp recordings of thick-tufted layer 5 pyramidal neurons in rat somatosensory cortex I first examined the characteristics of transmission at synaptic connections at three developmental stages. These stages I will hereby refer to as immature (post-natal 11-14 days), juvenile (P18-22, around time of weaning) and mature (P27-32, equivalent to young adult), based on previously established terminology. These stages were chosen to cover the period of transition from prominent synaptic depression to weak facilitation, as previously reported (Reyes and Sakmann, 1999).

The mean ( $\pm$  std dev) amplitude of isolated EPSPs at each age was  $1.54 \pm 0.96$  mV for immature,  $1.33 \pm 0.95$  mV for juvenile, and  $0.51 \pm 0.43$  mV for mature connections. Connections from the mature cortex were significantly weaker than those from either juvenile (2-tailed Mann Whitney-U test,  $P = 0.004$ ,  $n = 38$  and  $23$ ) or immature cortex (2-tailed Mann Whitney-U test,  $P = 0.01$ ,  $n = 8$  and  $23$ ). However there was no significant difference in the mean EPSP amplitudes recorded from immature and juvenile connections (2-tailed Mann Whitney-U test,  $P = 0.52$ ,  $n = 8$  and  $38$ ).

The rise times (10 – 90%) of EPSPs did not significantly change (immature/juvenile, one-tailed unpaired t-test,  $P = 0.14$ ; juvenile/mature, one-tailed unpaired t-test,  $P = 0.5$ ) during development (immature,  $3.3 \pm 1.4$  ms; mature,  $2.6 \pm 0.8$  ms). However the half-width of EPSPs was

significantly longer (immature/juvenile, one-tailed unpaired t-test,  $P = 0.51$ ; juvenile/mature, one-tailed unpaired t-test,  $P = 0.01$ ; immature/mature, one-tailed unpaired t-test,  $P = 0.02$ ) at the youngest developmental stages ( $22.5 \pm 5$  ms at immature;  $21.4 \pm 3.7$  ms at juvenile), and shortest at the mature period ( $17 \pm 7$  ms).

When trains of EPSPs were evoked at 30 Hz, the paired pulse ratio (second EPSP amplitude/first EPSP amplitude) significantly increased at each stage of development. EPSP variability (measured from the CV of the initial EPSP amplitude) increased significantly at mature connections (section 4.2.4), but showed no significant change between immature and juvenile connections. Full details of the EPSP characteristics are outlined in figure 4.1.

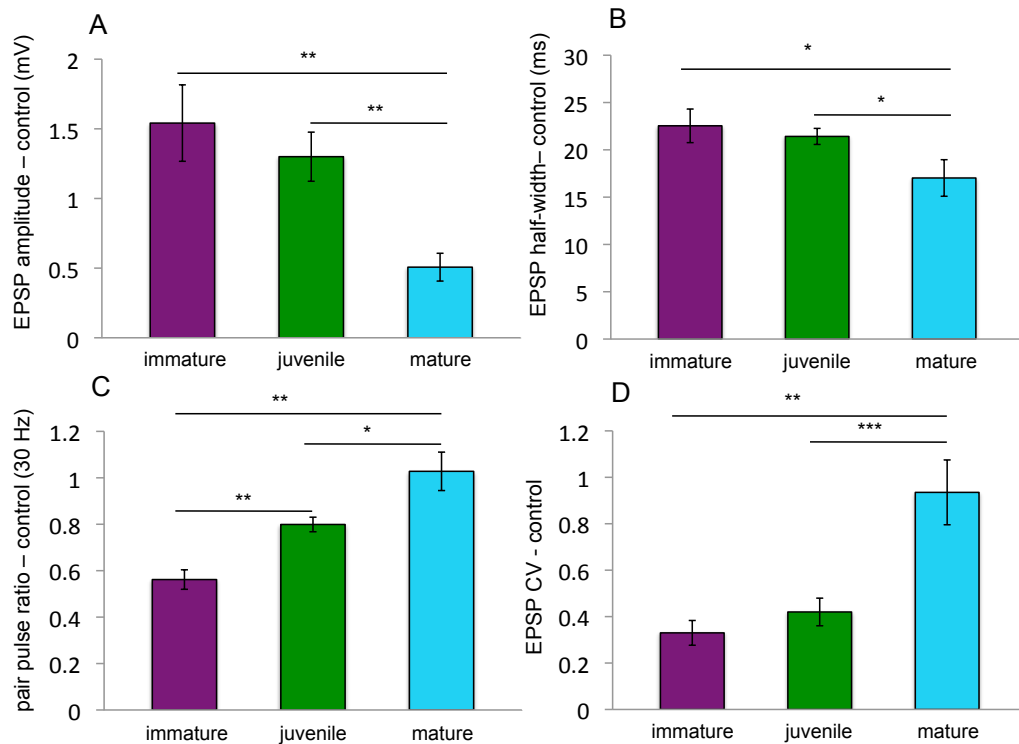


**Fig 4.1** The characteristics of synaptic transmission at three stages of post-natal development. Connections were recorded from neocortical slices taken at postnatal days (P) 11-14 (immature,  $n = 8$ ), 18-22 (juvenile,  $n = 38$ ), and 28-32 (mature,  $n = 23$ ). (A) Mean EPSP amplitude declined significantly between the juvenile and mature stage, but showed no significant change between immature and juvenile. (B) EPSP half-width declined slightly at each stage of development. (C) Paired pulse ratio (EPSP2/EPSP1 at 30Hz) increased significantly at each stage. (D) EPSP variability (CV) increased significantly between the juvenile and mature stage, but not between immature and juvenile stages.

#### 4.2.2 Suppression of EPSPs by adenosine and detection of tone by 8-CPT

The synaptic connections recorded in control conditions will be measured in the presence of any endogenous extracellular adenosine in the tissue. In order to characterise the activation of adenosine receptors in these conditions, I bath applied a high concentration of adenosine (100  $\mu$ M) to maximally activate the adenosine receptors (see chapter 3), before applying the A<sub>1</sub> receptor antagonist 8-CPT to fully block the receptors (and therefore remove any effects of endogenous adenosine). My previous experiments demonstrated the equivalence, at this synapse, of applications of 100  $\mu$ M adenosine and applications of a high concentration (5  $\mu$ M) of the A<sub>1</sub>R

specific agonist CPA, indicating that the synaptic effects mediated by adenosine occurred through the A<sub>1</sub> receptor. Adenosine was used for the majority of experiments, rather than CPA, because it could be easily washed from the slice, ensuring that 8-CPT could fully block the A<sub>1</sub> receptors.

Thus the experiments provided data on the properties of synaptic transmission in the presence of endogenous adenosine (control conditions, green in fig 4.2), with maximal A<sub>1</sub>R activation (addition of 100 μM adenosine, red) and with A<sub>1</sub>Rs blocked (blue, 2 μM 8-CPT, A<sub>1</sub>R antagonist)

The application of adenosine most strongly depressed EPSP amplitude in connections from the two earliest developmental periods (from  $1.54 \pm 0.96$  mV to  $0.31 \pm 0.33$  mV, immature; and from  $1.33 \pm 0.95$  mV to  $0.28 \pm 0.25$  mV, juvenile connections), a depression of ~80% and ~79% respectively. At the mature connections EPSP depression (~61%) was significantly reduced compared to both the immature (2-tailed Mann Whitney-U test,  $P = 0.01$ ) and the juvenile connections (2-tailed Mann Whitney-U test,  $P = 0.002$ ). At mature connections EPSP amplitude was reduced from  $0.51 \pm 0.43$  mV to  $0.20 \pm 0.18$  mV.

The mean EPSP half-width was significantly reduced by adenosine at immature (from  $22.5 \pm 5$  to  $15.4 \pm 2.9$  ms, paired 2-tailed t-test,  $P = 0.003$ ,  $n = 8$ ) and juvenile connections (from  $21.4 \pm 3.7$  to  $16.6 \pm 2.4$  ms, paired 2-tailed t-test,  $P < 0.001$ ,  $n = 32$ ), but not at mature connections (from  $17.0 \pm 7.2$  to  $14.9 \pm 5$  ms, paired 2-tailed t-test,  $P = 0.13$ ,  $n = 19$ ).



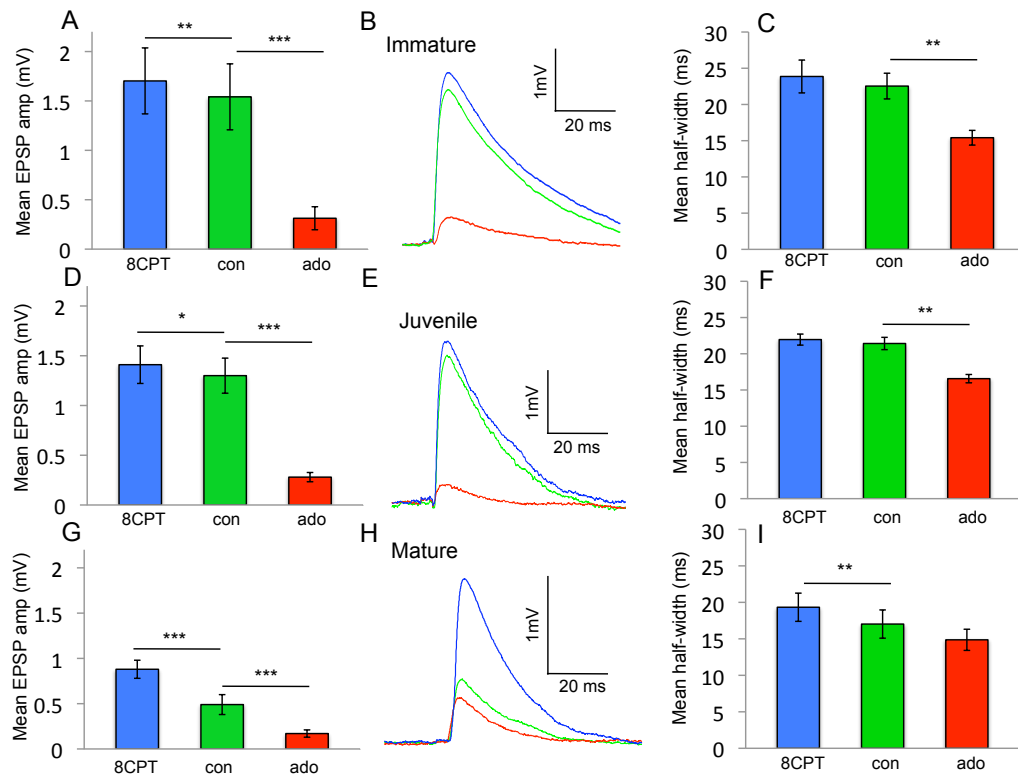


**Fig 4.2** Effect of applied and endogenous adenosine on synaptic transmission at each stage of development (A-C: immature, D-F: juvenile, G-I: mature). Connections were powerfully suppressed by adenosine at each period of development (A, D and G). The EPSP amplitude ratio between 8-CPT and adenosine did not change significantly during development, however the endogenous activation of A<sub>1</sub>Rs increased at mature connections (relative height of green column in A, D and G). (B, E and H) Representative sweep-averaged EPSP traces illustrate increased endogenous activation of A<sub>1</sub>Rs at mature connections (H). Adenosine A<sub>1</sub>R activation produced a small decrease in EPSP half-width at each stage of development (C, F and I).

Application of 8-CPT (2 μM) following adenosine wash blocked the effects of any endogenous adenosine at the A<sub>1</sub> receptor, and therefore in conjunction with the EPSP characteristics in adenosine and control could be used to determine the relative baseline activation of A<sub>1</sub> receptors in control conditions. Application of 8-CPT to immature and juvenile slices returned EPSPs to amplitudes slightly, but significantly increased from control conditions (immature, control = 1.54 ± 0.96 mV, 8-CPT = 1.7 ± 0.95 mV, one-

tailed Mann Whitney-U test,  $P = 0.006$ ,  $n = 8$ ; juvenile control =  $1.33 \pm 0.95$  mV, 8-CPT =  $1.46 \pm 1$  mV, one-tailed Mann Whitney-U test,  $P = 0.01$ ,  $n = 38$ ). However in mature cortex the application of 8-CPT resulted in a large increase in mean EPSP amplitude compared to control conditions (fig 4.2g, control =  $0.51 \pm 0.43$  mV, 8-CPT =  $0.99 \pm 0.67$  mV, one-tailed Mann Whitney-U test,  $P = 0.001$ ,  $n = 21$ ). The ratios of mean EPSP amplitude in control compared to amplitude in 8-CPT were 91, 92 and 51% for immature, juvenile and mature connections respectively. This implies that there is an increased baseline activation of A<sub>1</sub> receptors by endogenous adenosine in the mature cortex.

Strikingly, the ratios of mean EPSP amplitude in adenosine compared to 8-CPT showed no significant difference (two-tailed Mann Whitney U tests, immature/juvenile,  $P = 0.3$ ; immature/mature,  $P = 0.41$ ; juvenile/mature,  $P = 0.24$ ) across any of the developmental stages ( $0.18 \pm 0.11$ ,  $0.19 \pm 0.15$  and  $0.2 \pm 0.1$  for immature, juvenile and mature respectively), suggesting that the relative effect of A<sub>1</sub>R activation shows little change across development. Thus the fall in EPSP amplitudes recorded in control conditions across development is likely due, at least in part, to increased activation of A<sub>1</sub> receptors by endogenous adenosine. However since blocking A<sub>1</sub>Rs at mature connections does not increase EPSP amplitude back to levels observed at immature/juvenile connections there must also be an adenosine independent mechanism involved.

#### 4.2.3 Adenosine controls the synaptic dynamics observed at these connections

I next examined how adenosine affects short-term synaptic dynamics at the three stages of development, examining the post-synaptic response to trains of pre-synaptic action potentials under the three pharmacological manipulations (control, adenosine, 8-CPT). In control conditions connections from the youngest two age groups typically exhibited prominent short-term depression. For immature connections the mean PPR at 30 Hz was  $0.56 \pm 0.11$  (range 0.44 – 0.73,  $n = 9$ ) and for juvenile connections was  $0.80 \pm 0.31$  (range 0.58 - 1.04,  $n = 14$ ). No immature connections ( $n = 8$ ) and only 2 out of 14 juvenile connections exhibited paired-pulse facilitation at 30 Hz. However connections in mature cortex were much more likely to exhibit paired-pulse facilitation. The mean PPR (30 Hz) at the mature connections was  $1.08 \pm 0.24$  (range 0.66 – 1.54,  $n = 15$ ), with 9 out of 15 connections showing paired-pulse facilitation. The mean PPRs significantly increased at each stage of development (immature/juvenile, two-tailed Mann Whitney-U test,  $P < 0.001$ ,  $n = 8$  and 14; juvenile/mature, two-tailed Mann Whitney-U test,  $P = 0.03$ ,  $n = 14$  and 15).

Upon application of 100  $\mu\text{M}$  adenosine, the mean PPR increased in connections at each of the developmental stages (to  $0.97 \pm 1.7$  in the immature group, to  $1.24 \pm 0.78$  in the juvenile group and  $1.4 \pm 0.62$  in the mature group). Notably, the mean PPR in adenosine increased during development, however this increase was significant only between immature and mature connections (immature/juvenile, two-tailed Mann Whitney-U

test,  $P = 0.4$ ; juvenile/mature, two-tailed Mann Whitney U test,  $P = 0.13$ ; immature/mature, two-tailed Mann Whitney U test,  $P = 0.041$ ), although it is notable that the  $P$ -value loses significance at 95% confidence if accounting for the multiple statistical comparisons.

Blockade of  $A_1$  receptors with 8-CPT ( $2 \mu\text{M}$ ) returned the immature and juvenile connections to the paired-pulse depression observed in control conditions and also converted the mature connections from weakly facilitating to depressing. The mean 30 Hz PPRs in 8-CPT were  $0.42 \pm 0.05$ ,  $0.56 \pm 0.1$ , and  $0.77 \pm 0.21$  for immature ( $n = 8$ ), juvenile ( $n = 15$ ), and mature ( $n = 16$ ) respectively. All but two of the mature connections exhibited paired-pulse depression in 8-CPT (21 out of 23 connections).

In order to further quantify the changes in synaptic dynamics, I fitted the data from the mature connections to a simple model of short-term synaptic dynamics, using the same methods discussed in the previous chapter. This allowed a comparison of release parameters across all of the three ages. The simultaneous changes in amplitude and synaptic dynamics produced by the pharmacological manipulations were again well captured by a change only in the probability of release. All connections were selected for model fitting based on the same minimum signal to noise criteria as outlined in chapter 3.

At each developmental stage adenosine was found to reduce the probability of release without significantly changing  $aN$  (maximal efficacy). In control conditions, the mean probability of release ( $p$ ) was measured as  $0.51 \pm 0.07$ ,  $0.42 \pm 0.08$ , and  $0.28 \pm 0.13$  for immature, juvenile, and mature connections respectively. Comparing across the developmental stages,  $p$  was

significantly reduced at the mature connections compared to both immature and juvenile connections (mature/juvenile, one-tailed unpaired t-test,  $P = 0.001$ ,  $n = 12$  and  $24$ ; mature/immature, one-tailed unpaired t-test,  $P = 0.001$ ,  $n = 12$  and  $6$ ), with no difference between the earliest developmental stages (immature/juvenile, one-tailed unpaired t-test,  $P = 0.13$ ,  $n = 6$  and  $24$ ).

When adenosine was applied to these connections  $p$  dropped significantly to  $0.09 \pm 0.1$  (one-tailed paired t-test,  $P < 0.001$ ,  $n = 6$ ),  $0.1 \pm 0.1$  (one-tailed paired t-test,  $P < 0.001$ ,  $n = 24$ ), and  $0.13 \pm 0.12$  (one-tailed paired t-test,  $P < 0.001$ ,  $n = 12$ ) at immature, juvenile and mature connections respectively.

The full activation of adenosine receptors abolished the developmental change in  $p$ , as no significant difference was seen between any of these values across development (immature/juvenile, two-tailed unpaired t-test,  $P = 0.47$ , immature/mature, two-tailed unpaired t-test,  $P = 0.32$ , juvenile/mature, two-tailed unpaired t-test,  $P = 0.26$ ).

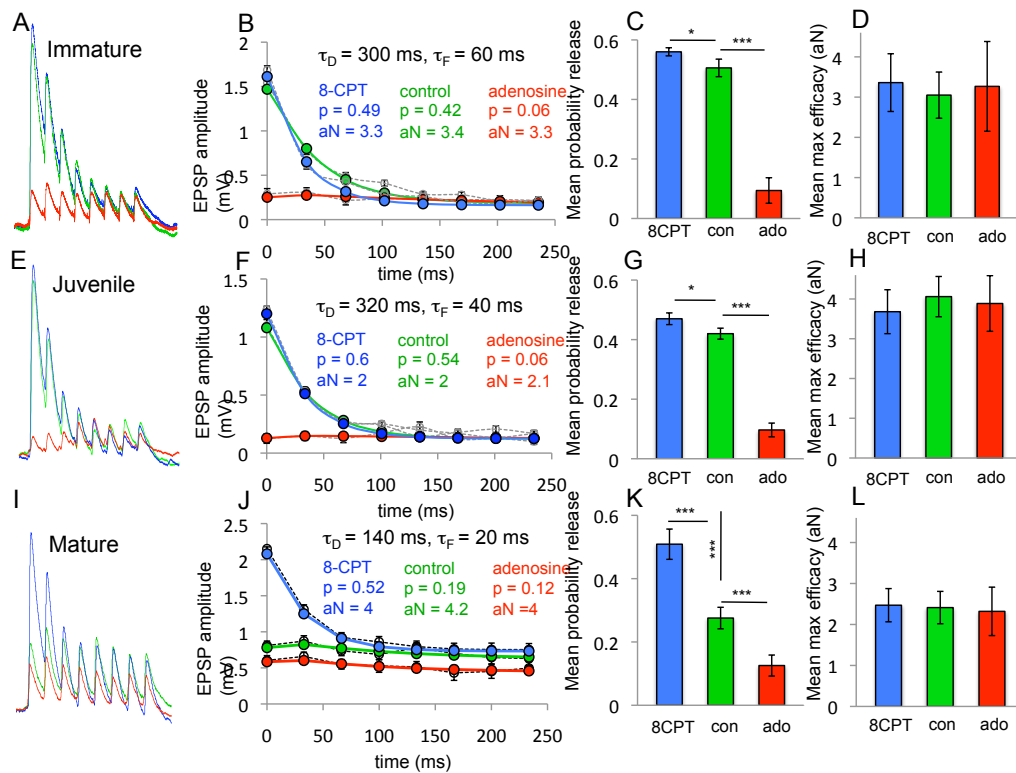


**Fig 4.3** Increased A<sub>1</sub>R activation underlies the developmental shift from depression to facilitation at synapses between thick-tufted layer 5 pyramidal neurons. (A, E and I) Typical sweep-averaged EPSP trains at each stage of development. In control conditions EPSPs at mature connections exhibit weak facilitation, however blocking A<sub>1</sub>Rs with 8-CPT results in a return to depression. In 8-CPT, EPSPs exhibited prominent depression at each stage of development. (B, F and J) Fitting EPSP trains to a model of short-term synaptic dynamics suggests the effects of adenosine are governed by a decrease in the probability of release. No significant change in maximum synaptic efficacy (aN) was detected in adenosine. (C, G and K) In control conditions, across development there was a significant decrease in probability of release. However when A<sub>1</sub> receptors were blocked this effect was abolished indicating that the decline in probability of release observed in control conditions was solely due to increase activation of A<sub>1</sub>Rs by endogenous adenosine. (D, H and L) Maximum synaptic efficacy (aN) showed no change in adenosine or 8-CPT, however was significantly reduced at mature synapses compared to immature and juvenile.

At each developmental stage, upon application of 8-CPT, the probability of release significantly increased compared to control (immature =  $0.56 \pm 0.06$ , one-tailed paired t-test,  $P = 0.02$ ,  $n = 6$ ; juvenile =  $0.47 \pm 0.09$ , one-tailed paired t-test,  $P = 0.012$ ,  $n = 24$ ; mature =  $0.51 \pm 0.18$ , one-tailed paired t-test,  $P < 0.001$ ,  $n = 12$ ). Strikingly, across the developmental stages, there was no significant difference between the mean probabilities of release in 8-CPT (immature/juvenile, two-tailed unpaired t-test,  $P = 0.12$ ; immature/mature,

two-tailed unpaired t-test,  $P = 0.47$ ; juvenile/mature, two-tailed unpaired t-test,  $P = 0.48$ ). This provides further evidence that the fall in EPSP amplitude during development is due to pre-synaptic A<sub>1</sub> receptor activation by endogenous adenosine.

Notably, the recovery time constant for depression decreased significantly (immature/juvenile, one-tailed Mann-Whitney U test,  $P = 0.003$ ; juvenile/mature, one-tailed Mann-Whitney U test,  $P = 0.004$ ) during development (mean  $\pm$  std dev, immature =  $340 \pm 124$  ms,  $n = 6$ ; juvenile =  $179 \pm 51$  ms,  $n = 24$ ; mature =  $122 \pm 73$  ms,  $n = 12$ ). This reduction contributed to the PPR (at 30 Hz) remaining significantly reduced in 8-CPT at mature connections compared to juvenile and immature connections (immature/mature, one-tailed Mann-Whitney U test,  $P < 0.001$ ; juvenile/mature, one-tailed Mann-Whitney U test,  $P < 0.001$ ).

#### 4.2.4 Effects of A<sub>1</sub>R activation on EPSP variability and reliability

To further examine the effects of tonic A<sub>1</sub> receptor activation I calculated the coefficient of variation (CV, standard deviation/mean) of EPSP amplitudes for each pharmacological manipulation at each stage of development. Changes in the CV give an indication of pre-synaptic changes in synaptic transmission, as the CV is largely independent of quantal amplitude (Faber and Korn, 1991).

In control conditions the mean CVs across connections at each stage of development were  $0.33 \pm 0.15$  ( $n = 8$ ),  $0.42 \pm 0.28$  ( $n = 38$ ), and  $0.94 \pm 0.61$  ( $n = 23$ ) for immature, juvenile and mature respectively. The mean CV at

mature connections was significantly higher than the CV at both immature and juvenile connections (immature/mature, unpaired one-tailed Mann-Whitney U test,  $P = 0.006$ ; juvenile/mature, unpaired one-tailed Mann-Whitney U test,  $P < 0.001$ ), but there was no significant difference between the mean CVs at immature and juvenile connections (unpaired one-tailed Mann-Whitney U test,  $P = 0.16$ ). Upon application of adenosine ( $100 \mu\text{M}$ ) the CV significantly increased at each developmental stage, to  $1.32 \pm 0.49$ ,  $1.52 \pm 1.03$ , and  $1.48 \pm 0.6$  for immature (one-tailed Wilcoxon matched pairs test,  $P < 0.001$ ), juvenile (one-tailed Wilcoxon matched pairs test,  $P < 0.001$ ) and mature connections (one-tailed Wilcoxon matched pairs test,  $P < 0.001$ ) respectively. Notably, with maximal  $A_1R$  activation, there was no significant difference in the CV between the developmental stages (immature/juvenile, unpaired two-tailed Mann-Whitney U test,  $P = 0.64$ ; immature/mature, unpaired two-tailed Mann-Whitney U test,  $P = 0.54$ ; juvenile/mature, unpaired two-tailed Mann-Whitney U test,  $P = 0.27$ ).

When  $A_1$  receptors were fully blocked with 8-CPT ( $2 \mu\text{M}$ ), at each developmental stage the mean CV declined to lower than control conditions (CV =  $0.28 \pm 0.1$ ,  $0.41 \pm 0.24$ , and  $0.42 \pm 0.25$  for immature, juvenile and mature connections respectively). However the difference in CV between control and 8-CPT was only significant at mature connections (immature – one-tailed Wilcoxon matched pairs test,  $P = 0.07$ ; juvenile – one-tailed Wilcoxon matched pairs test,  $P = 0.19$ ; mature – one-tailed Wilcoxon matched pairs,  $P < 0.001$ ). There was no significant difference between the mean CVs in 8-CPT across developmental stages (immature/juvenile,



unpaired two-tailed Mann Whitney U test,  $P = 0.28$ ; immature/mature, unpaired two-tailed Mann Whitney U test,  $P = 0.09$ ; juvenile/mature, unpaired two-tailed Mann Whitney U test,  $P = 0.82$ ).

Plotting the CV against EPSP amplitude demonstrates that the connections fall upon the same power law curve for each of the pharmacological manipulations. A similar curve described the data at each developmental stage, however the clustering of data for each pharmacological manipulation was quite different. A bivariate Gaussian was used to give an indication of the distributions for each manipulation (fig 4.4c, f and j). For the immature and juvenile connections the control and 8-CPT conditions were nearly coincident, with little overlap with the adenosine distribution. For the mature connections the control distribution overlapped with the distributions for both 8-CPT and adenosine, thus suggesting that there is a much wider degree of A<sub>1</sub>R activation by endogenous extracellular adenosine at mature synapses.

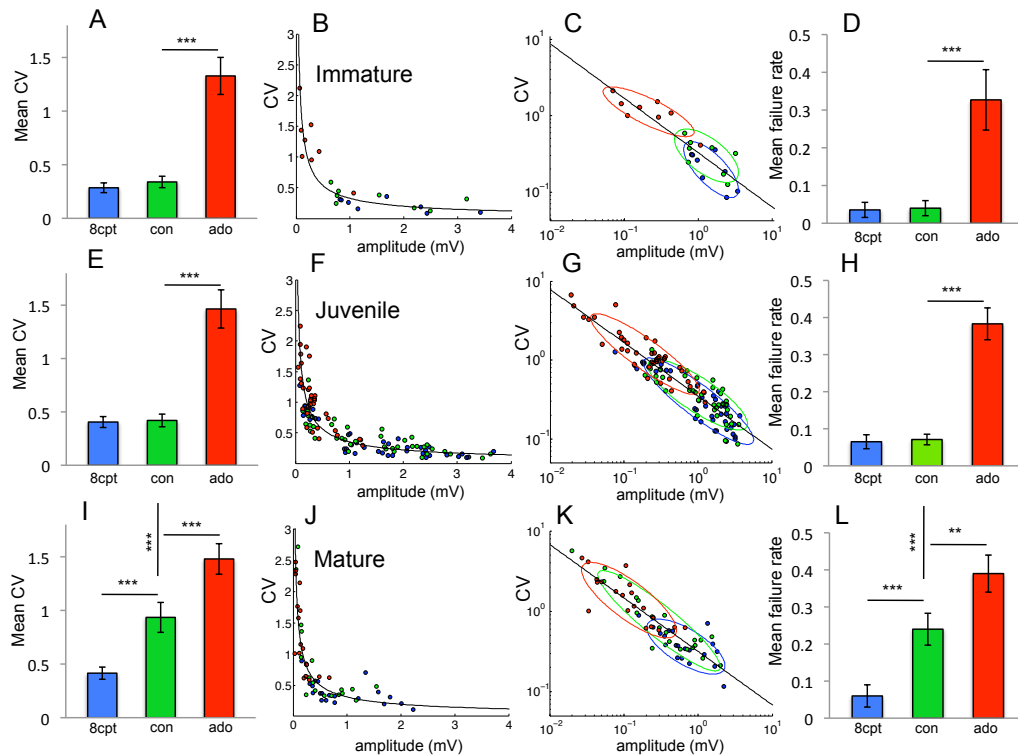


**Fig 4.4**  $A_1$  receptor activation determines variability and reliability at mature layer 5 pyramidal synapses. A-D: Immature, E-H: Juvenile, I-L: Mature. (A, E and I) The mean CV in each pharmacological manipulation. Adenosine significantly increased the CV at each stage of development. The mean CV increased significantly in control conditions at mature connections. However upon application of 8-CPT this developmental effect was abolished. Scatter plots of CV against EPSP amplitude (B, E and I), and in log-log form (C, F and J) show that connections in each pharmacological manipulation follow the same empirical power-law, and illustrate the spread of the data in each condition. Bivariate-Gaussian fits (ellipses) quantify this spread and demonstrate that, in control conditions, mature connections are scattered across the whole spectrum of  $A_1$ R activation, whereas immature and juvenile connections are distributed similarly to the connections in 8-CPT. (D, G and K) Mean failure rate of isolated EPSPs show the same pattern as CVs.

The similarities in CV across the developmental stages in  $100 \mu\text{M}$  adenosine and again in  $2 \mu\text{M}$  8-CPT suggest that pre-synaptic activation of  $A_1$  receptors is responsible for the developmental shift observed in control conditions.

To further test this hypothesis I measured the EPSP failure rate (for the first EPSP) for each manipulation. Mean failure rates across connections showed the same pattern as the CV (fig 4.4d, h and l). In control conditions, the failure rate was significantly higher (immature/mature, one-tailed Mann-Whitney U test,  $P = 0.011$ ; juvenile/mature, one-tailed Mann-Whitney U test,

$P = 0.02$ ) at mature connections ( $0.28 \pm 0.08$ ) compared to both immature ( $0.04 \pm 0.02$ ) and juvenile ( $0.07 \pm 0.02$ ) connections. Failure rates increased significantly upon application of adenosine at all three ages. Upon application of 8-CPT, only at mature connections did the failure rate decline significantly compared to control (to  $0.06 \pm 0.04$ , one-tailed Wilcoxon matched pairs test,  $P = 0.03$ ). Similar to the CV data, there was no significant difference in EPSP failure rate across any of the developmental stages when  $A_1$ Rs were fully activated (adenosine) or blocked (8-CPT).

In summary the changes in EPSP reliability are broadly consistent with the mean EPSP amplitude data, demonstrating increased  $A_1$ R activation in control conditions at mature connections. However this data suggests that the variation observed in mean CV and failure rates in control conditions across development can be fully explained by activation of  $A_1$  receptors by endogenous adenosine, as when  $A_1$  receptors were fully activated or blocked there was no difference in the CV across the developmental stages.

The adenosine independent component observed in the reduction in mean EPSP amplitude during development is not present in the CV and failure data, which can be fully accounted for by increased  $A_1$ R activation in control conditions. This suggests that the quantal amplitude has been reduced over this developmental period as this change could reduce the overall mean amplitude of the initial EPSP without changing the CV or failure rate.

Given that the CV is independent of quantal amplitude these changes again suggest a pre-synaptic effect for adenosine in reducing the probability of transmitter release.

#### 4.2.5 Estimating A<sub>1</sub>R activation by endogenous adenosine

When taken together these results provide strong evidence that the loss of prominent short-term synaptic depression during the first month of post-natal development is governed to a significant extent by an increase in baseline A<sub>1</sub> receptor activation.

The results so far, however, cannot distinguish whether this change arises due to a change in A<sub>1</sub> receptor properties (for example their agonist affinity or pre-synaptic location), or whether an increase in the concentration of adenosine at the synapse drives the change, or a combination of the two. Nevertheless, that the relative effects (i.e. the ratios of EPSP amplitude and CV in adenosine and 8-CPT) of adenosine are similar across each developmental stage, suggests that the change arises from an increase in extracellular adenosine concentration at the synapse.

In order to distinguish more fully between these scenarios I first conducted concentration response experiments on a number of synaptic connections. Given the similarities in baseline activation between the immature and juvenile connections I restricted these experiments to only juvenile and mature connections. A method was used that accounts for the activation of receptors by endogenous extracellular adenosine (see chapter 2.3). The relative amplitude  $(E - E_{CPA}) / (E_{8-CPT} - E_{CPA})$  was measured for unitary EPSPs of amplitude E measured in 2 μM 8-CPT, control conditions, 10, 30 and 100 μM adenosine, and 5 μM CPA (non-hydrolysable A<sub>1</sub>R agonist). The IC<sub>50</sub> was 15 μM at both juvenile ( $n = 6$ ) and mature ( $n = 4$ ) synapses, with SEM ranges of 9-23 μM and 6-40 μM respectively. In three out of six of the juvenile

connections no endogenous adenosine was measurable, and the average EPSP amplitude in control was 87% of that in 8-CPT (when the A<sub>1</sub> receptors are blocked). The mean concentration of adenosine in the tissue was calculated as 2 (0.4 – 8) μM. In contrast, at all the mature synapses examined there was a measurable endogenous adenosine concentration. The mean of concentration of adenosine was calculated as 23 (10 – 50) μM, with the control EPSP amplitude only 40% of the amplitude recorded in 8-CPT. It should be emphasised that these concentrations, like those quoted in published literature, are bath applied equivalents. Adenosine is rapidly removed from the extracellular space by a number of mechanisms (Haas and Selbach, 2000; Dunwiddie and Masino, 2001) and so the concentration at the synapse is much less (by a factor of ~20) than that present in the bath (Sebastiao *et al.*, 2000).

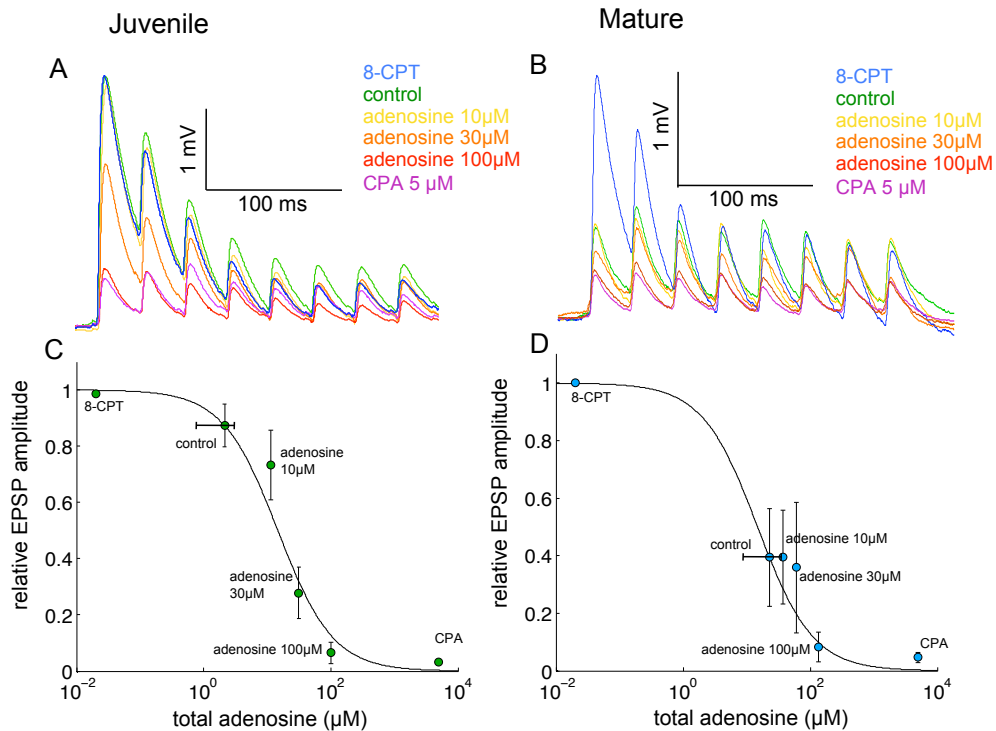


**Fig 4.5** Endogenous adenosine concentration at synapses increases during development. (A and B) Averaged EPSP trains in control conditions, increasing concentrations of bath-applied adenosine, and in 8-CPT ( $A_1R$  blocked) and CPA ( $A_1R$  fully activated), for a representative juvenile connection (A) and a representative mature connection (B). CPA/8-CPT EPSP amplitude ratio remains similar across development, however in control conditions EPSPs are much closer to 8-CPT amplitudes at juvenile connections, and CPA amplitudes at mature connections. (C and D) Average adenosine concentration response curves with relative EPSP amplitude  $(E - E_{CPA}) / (E_{8CPT} - E_{CPA})$  versus total adenosine concentration (sum of bath-applied and estimated bath-applied-equivalent endogenous adenosine) for juvenile ( $n = 6$ ) and mature ( $n = 4$ ) connections. Amplitudes in the  $A_1R$  antagonist 8-CPT and  $A_1R$  agonist CPA were plotted at  $0.05 \mu\text{M}$  and  $500 \mu\text{M}$  for comparison.

The concentration response profiles provide an indirect indication of adenosine concentration. I therefore decided to directly measure the adenosine concentration in the slices using enzymatic microelectrode biosensors (Llaudet *et al.*, 2003). The biosensors employ a sequential enzymatic conversion to produce an electrochemical signal that is proportional to the concentration of the specific analytes detected. Full details of the methods are documented in chapter 2.1.3. Briefly, an adenosine (ADO), inosine (INO) and null biosensor were carefully inserted into layer 5 of the somatosensory cortex. The sensors were left in the tissue

for ~30 minutes and then removed. The drop in the biosensor current upon removal from the slice is used to measure the adenosine concentration in the extracellular space. The experiment is done this way round (rather than looking at the rise in signal upon insertion) as insertion damages the slice and releases purines. The ADO sensor responds to adenosine and its metabolites inosine and hypoxanthine, while the INO sensor only responds to inosine and hypoxanthine. The null sensor will respond to any electrointerferents that pass through the biosensor screening layer and acts as a control. At the end of each experiment the sensors were calibrated using 10  $\mu\text{M}$  adenosine or inosine solution. Thus subtracting the null and then the calibrated INO signal from the calibrated adenosine response isolates the adenosine signal (assuming that the tissue is homogeneous and there are the same concentrations of purines measured by each sensor, see Wall *et al.*, 2007).

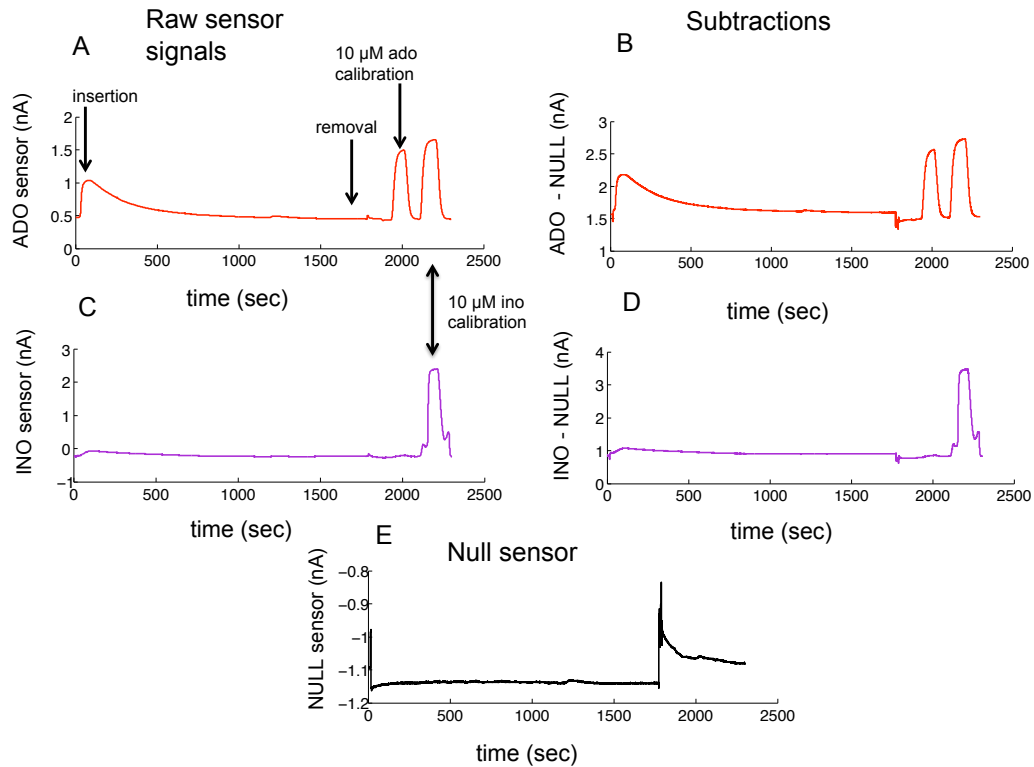


**Fig 4.6** Use of enzymatic biosensors to detect endogenous adenosine. 3 sensors (ADO, INO and NULL) were inserted into the slice (A, C and E) and allowed to stabilise. Upon removal from the slice there is a drop in signal in the ADO and INO sensors that can be seen once the NULL signal (E) is subtracted (B and D at ~1800 seconds). Following removal from the slice the sensors are calibrated using their responses to 10  $\mu$ M adenosine and inosine. It can be seen from fig A that the ADO sensor responds to both adenosine and inosine, resulting in a total purine signal.

There was no significant difference detected in the total (adenosine plus inosine) purine tone between juvenile and mature slices (juvenile =  $1.1 \pm 0.4$   $\mu$ M, mature =  $0.8 \pm 0.6$   $\mu$ M, two-tailed unpaired t-test,  $P = 0.33$ ,  $n = 8$ ). The isolated extracellular adenosine tone was also not significantly different (juvenile =  $0.5 \pm 0.4$   $\mu$ M, mature =  $0.3 \pm 0.3$   $\mu$ M, two-tailed unpaired t-test,  $P = 0.17$ ,  $n = 8$ ) between juvenile and mature slices.



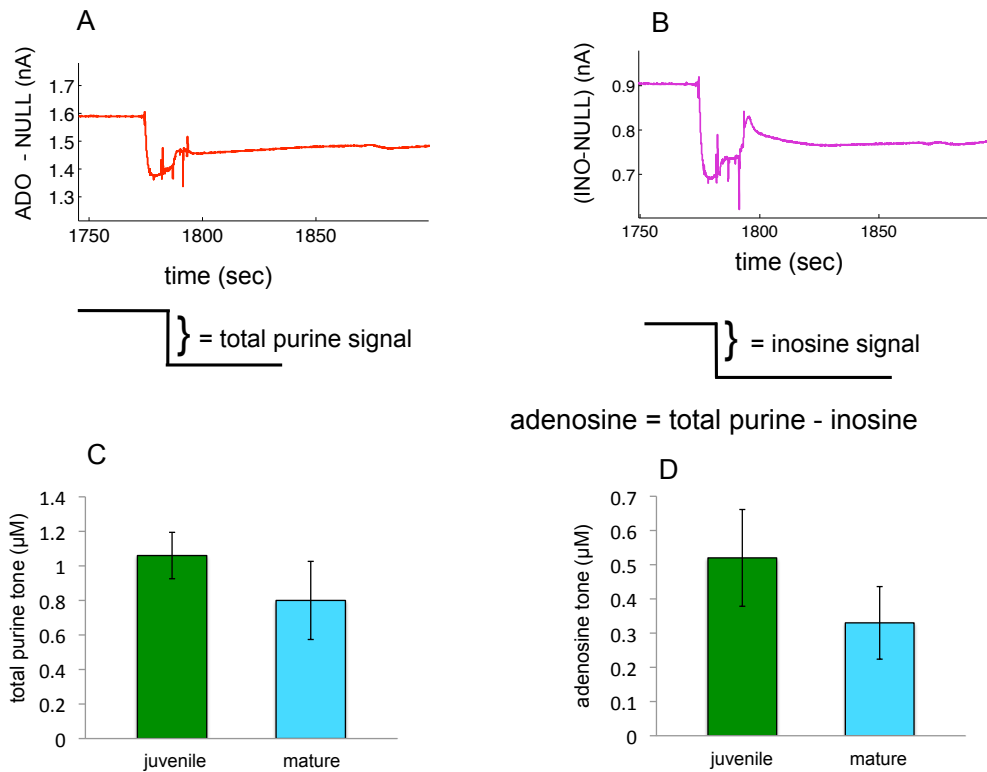


**Fig 4.7** No significant difference was detected in the concentration of adenosine between juvenile and mature slices. (A and B) Following subtraction of the null signal, removal of the ADO (A) and INO (B) sensors from the slice results in a drop in signal corresponding to the slice tone. These signals were calibrated and an adenosine tone was calculated by subtracting the inosine tone from the total purine tone. (C and D) No significant difference was detected in the average purine (C) or adenosine (D) tone between juvenile and mature slices.

The biosensors effectively measure a weighted mean concentration of adenosine within the extracellular space, which will include synaptic, perisynaptic and extrasynaptic compartments. The lack of difference across the developmental stages suggests there is no global increase in extracellular adenosine concentration. However localised changes that only occur in the synaptic compartment will probably not be detected by the biosensors.

#### 4.2.6 Variability in baseline A<sub>1</sub>R activation

Given that the EPSP characteristics were not significantly different in 100  $\mu$ M adenosine compared to when A<sub>1</sub> receptors were maximally activated in CPA I can estimate the fractional activation of A<sub>1</sub>R receptors by endogenous adenosine in control conditions in all connections that were recorded in control, adenosine and 8-CPT. Figure 4.8a plots the percentage A<sub>1</sub>R activation  $(E_{8-CPT} - E_{con}) / (E_{8-CPT} - E_{ado})$  versus control amplitude ( $E_{con}$ ) for juvenile and mature connections. The average A<sub>1</sub>R activation in control was significantly lower (one-tailed unpaired t-test,  $P < 0.001$ ,  $n = 18$  and  $33$ ) for the juvenile (14%) compared to the mature connections (64%). Given that there is a significant trend (exponential,  $R^2 = 0.412$ ,  $P < 0.001$ ) of stronger synapses (in control) having lower baseline A<sub>1</sub>R activation I can say that endogenous adenosine concentrations, to a significant degree, determine the amplitude of EPSPs at mature synapses.

It is also noticeable (fig 4.8a) that there is considerable variability in A<sub>1</sub>R activation between synapses at the same stage of development. In many experiments mono-synaptic connections were detected in both directions between a pair of neurons (i.e. reciprocal connections). In figure 4.8a dotted lines indicate synapses that were connected reciprocally (10 out of 14 connections), or were recorded from different slices from the same individual (4 out of 14 connections). It is clear from the figure that there was considerable variability in A<sub>1</sub>R activation even between these reciprocal connections and connections from the same individual. To quantify this variability, the spread in A<sub>1</sub>R activation (equating to the mean vertical

height of the dotted lines in figure 4.8a) in synapses from the same neocortex (comprised of 10 pairs of reciprocal connections and 4 other pairs of connections in slices from the same individual) was compared to the average spread across all the data within each developmental stage.

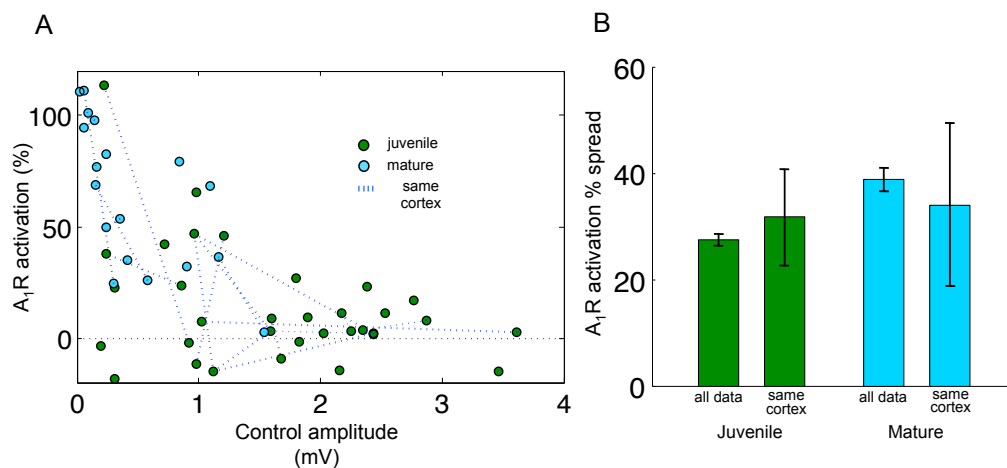


**Fig 4.8** Basal A<sub>1</sub> receptor activation varies significantly between synapses within same individual and within the same slice. (A) Relative A<sub>1</sub>R activation  $(E_{8CPT} - E_{Con}) / (E_{8CPT} - E_{Ado})$  versus control amplitude for juvenile and mature connections, dotted lines joining connections indicate connections from the same individual (reciprocal connections ( $n = 10$ ) or from different slices ( $n = 4$ )). (B) Comparison of spread across all data and spread in connections from same neocortex. Lack of significant difference for both juvenile and mature connections provides evidence for marked heterogeneity in endogenous A<sub>1</sub>R activation between synapses in the same individual.

Strikingly, there was no significant difference in the mean A<sub>1</sub>R activation

spread between connections from the same neocortex versus all the data.

For example the mean spread between juvenile connections from the same neocortex (the mean height of the dotted lines = 32%,  $n = 8$ ) compared to an average spread of 26% across all the juvenile data. There was a similar lack of difference for the mature data ( $n = 6$ ). These results provide some evidence (which could be strengthened with more data) that the heterogeneity in A<sub>1</sub>R activation is not due to variability in a globally uniform

extracellular adenosine concentration in the neocortex of individuals. Instead, the extracellular adenosine concentration is a local variable that varies significantly from synapse to synapse within the neocortex, and this increases with development. This is supported by the biosensor data, which detected no significant difference in the global concentration of adenosine across the developmental stages.

### 4.3 Discussion

In this chapter I provide strong evidence that increased pre-synaptic activation of A<sub>1</sub> receptors is at least partly responsible for the developmental increase in variability, reduction in reliability and the change in synaptic dynamics observed at synapses between thick-tufted layer 5 pyramidal neurons (Reyes and Sakmann, 1999). The increase in A<sub>1</sub> receptor activation is also partially responsible for the decrease in mean EPSP amplitude observed over the same period of development. That the mean EPSP amplitude but not CV or failure rate declines independently of A<sub>1</sub>R activation during this period of development suggests that a post-synaptic component may be responsible.

The developmental decrease in release probability has been previously reported at a number of synapses across the CNS (Feldmeyer and Radkinow, 2009), thus the A<sub>1</sub>R-dependent mechanism identified here could occur at synapses in other brain regions.

The change in synaptic dynamics at neocortical synapses co-occurs with the changes in the intrinsic membrane properties of layer 5 pyramidal neurons

(Etherington and Williams, 2011) that may tune the network to respond preferentially to higher frequency input patterns. A reduction in input resistance and membrane time constant sharpens EPSPs and the reduction in short-term depression allows connections to faithfully transmit action potential trains at higher frequencies. The increase in A<sub>1</sub>R activation may contribute to these changes in intrinsic membrane properties, and this is examined in the following chapter.

Previous research using double-exponential fits to a use-dependent blockade of NMDA receptors (Gonzalez-Burgos *et al.*, 2008) has provided evidence for two populations of synapses with high and low release properties, with the immature high release synapses diminishing during development. My results suggest however that there is no distinct removal of synapses with high probability of release, instead a spreading out from a tightly distributed population of synapses with little endogenous A<sub>1</sub>R activation to a more heterogeneous population of mature synapses with all degrees of endogenous A<sub>1</sub>R activation represented.

A number of mechanisms may contribute to the increase in A<sub>1</sub>R activation during development. An increase in the expression of, or affinity at A<sub>1</sub> receptors, or an alteration of the G-protein transduction pathway that links them to the suppression of transmitter release could occur during development. A<sub>1</sub> receptor expression is known to decline at the calyx of Held during development, and this occurs in conjunction with a reduced pre-synaptic response to adenosine (Kimura *et al.*, 2003). My results however provide little support for this hypothesis. The overall response to

adenosine (ratio of 8-CPT to 100  $\mu$ M adenosine or CPA) of various EPSP characteristics shows little change with development. There is also little difference in the  $IC_{50}$  calculated from the concentration response curves between juvenile and mature synapses. These findings suggest that there is little change in receptor expression, affinity or intracellular signal transduction.

More likely, is that the concentration of endogenous extracellular adenosine increases with development. Previous research has demonstrated an increased adenosine tone in the aged nervous system (Sebastiao *et al.*, 2000; Rex *et al.*, 2005). Upon release or generation (via ATP) in the extracellular space adenosine is rapidly broken down or otherwise removed by uptake into cells (Dunwiddie & Masino, 2001), meaning that its concentration in tissue is likely to be heterogeneous and highly dependent on the local distribution of sources and mechanisms for removal.

Although the biosensor experiments did not identify a significant change in concentration with development, these biosensors provide a weighted mean of purine concentration over relatively large volumes of tissue as the signal produced is proportional to the surface area of the sensor (Dale *et al.*, 2005). Thus very local increases in adenosine concentration will not be detected by biosensors. My data shows that there is little correlation in endogenous  $A_1R$  activation even between reciprocal connections indicating that heterogeneity in  $A_1R$  activation can persist locally from synapse to synapse, and this may govern the increase in mean activation, rather than an increase in adenosine tone over larger spatial volumes.

Given the highly heterogeneous nature of endogenous A<sub>1</sub>R activation, its apparent stability over the time course of the control recordings, and its highly significant contribution to EPSP amplitudes and short-term dynamics in mature tissue, emplacement of adenosine sources and sinks near synapses with functional A<sub>1</sub> receptors could potentially serve as a novel form of long-term plasticity in the adult neocortex.

My experiments were conducted using isolated slices of neocortical tissue and thus how this data translates to the *in vivo* situation remains an open question. Recent *in vitro* electrophysiological experiments have shown that diurnal variations in extracellular adenosine that occur *in vivo* are preserved in *in vitro* slices (Schmitt *et al.*, 2012). This indicates that while network activity is largely silenced *in vitro* due to a loss of synaptic inputs and potentially due to changes in the ionic make-up of the aCSF vs CSF, the adenosine levels recorded in slices may be reduced, but do provide some reflection of the *in vivo* state of the neocortex before death. Although adenosine is rapidly broken down in the extracellular space, the persistent tone seen in slices must be produced and maintained in dynamic equilibrium *in vitro*. Extracellular adenosine concentration is predominantly regulated by the enzyme adenosine kinase (Diogenes *et al.*, 2012), and manipulation of this enzyme alters sleep homeostasis in rats (Palchykova *et al.*, 2010). Notably, development of the highly heterogeneous A<sub>1</sub>R activation seen in these experiments coincides with the development of the diurnal sleep-wake cycle in juvenile rats (Gvilia *et al.*, 2011). Thus an

alteration in adenosine kinase expression presents a candidate mechanism for further research into this developmental shift.



## **5. Characterisation of the post-synaptic suppression of thick-tufted layer 5 pyramidal neurons by adenosine using naturalistic current injection and dynamic I-V curves**

### 5.1 Introduction

Neuromodulators that control pre-synaptic transmitter release can also modulate neuronal membrane excitability. GPCRs such as the  $M_1$ ,  $GABA_B$ ,  $A_1$  and 5HT-1 receptors, which couple to the  $G_{\alpha i/o}$  subunit, typically activate G-protein coupled inwardly rectifying potassium (GIRK) channels as well as lowering cellular cAMP levels by the inhibition of adenylyl cyclase. These effects are normally characterised as post-synaptic because they modulate synaptic inputs as they are integrated in the dendrites and soma. The activation of GIRK channels reduces membrane excitability by causing a hyperpolarisation and a decrease in input resistance thereby increasing the distance between resting potential and action potential threshold and shunting post-synaptic potentials. In some cases the inhibition of adenylyl cyclase can also induce intracellular modulatory effects.

The hyperpolarisation and concomitant decrease in input resistance driven by the  $A_1$  receptor mediated activation of GIRK channels has been observed in a number brain areas and neuron types. Activation of  $A_1$  receptors typically results in a hyperpolarisation of  $\sim 8$  mV in responsive neurons (e.g. in hippocampal pyramidal neurons, Greene and Haas, 1985; Arrigoni *et al.*, 2006). In some neurons  $A_1$  receptor activation induces a hyperpolarisation mediated by the inhibition of HCN channels (Li *et al.*, 2011) or activation of SK-channels (Clark *et al.*, 2009). To date the effects of adenosine on pyramidal neurons in layer 5 of the neocortex have not been studied. While

a hyperpolarisation and reduction of input resistance will decrease the overall excitability of neurons it remains unclear precisely how these effects will interact with other electrophysiological processes to modulate neuronal firing outputs and retrograde signals in the dendrites.

The distinctive dendritic arborisations of pyramidal neurons are perhaps most strikingly exemplified by the large thick-tufted pyramidal neurons found in layer 5 of the neocortex, where an apical dendrite that can reach nearly ~1 mm in length branches extensively once it reaches layer 1. This creates two spatially separate regions that receive synaptic inputs from distinct neurons and brain areas. Pyramidal neurons in layer 5 tend to receive local inputs from other layer 5 neurons onto their basal dendrites and inputs from parvalbumin positive interneurons onto their soma (Markram *et al.*, 2004). Inputs to the apical tuft come from a range of sources including the thalamus (Rubio-Garrido *et al.*, 2009), other cortical regions, as well as GABAergic inputs from somatostatin positive interneurons that may be found in layer 5 (Wang *et al.*, 2004). As well as receiving distinct inputs there is evidence for the differential expression of various ion channels (Takigawa and Alzheimer, 1999; Berger *et al.*, 2001) on different regions of the soma and dendrites. This separation of input pathways gives the neuron the potential capacity to target specific inputs for modulation, however it remains unclear to what extent this actually occurs.

Sodium action potentials in neocortical pyramidal neurons are initiated in the axon (at the initial segment) and propagate both down the axon and back along the dendritic tree. Action potential back-propagation in the

dendrites can occur actively via the activation of voltage gated  $\text{Na}^{2+}$  and  $\text{Ca}^{2+}$  channels (Stuart *et al.*, 1997). These back-propagations can act as a retrograde signal to the dendritic tree communicating the level of neuronal output. The amplitude of single back-propagating action potentials can rapidly attenuate as they travel down the dendrite (Callaway and Ross, 1995). However action potentials evoked in high frequency bursts during physiological spike trains are able to back-propagate more effectively and evoke dendritic electrogenesis (Williams and Stuart, 2000). The process of bursting itself is facilitated by apical dendrite depolarisation (Williams and Stuart, 1999). The extent to which action potentials back propagate can control the sign of long-term plasticity processes in the dendrites (Sjostrom and Hausser, 2006).

The manner in which these processes are modulated by the activation of post-synaptic GPCRs and what impacts this will have on the output behaviour of neurons remains an open question. It is also unclear the extent to which neuromodulation can differentially target specific regions and inputs to the same neuron.

In this chapter I wished to address how post-synaptic modulation by adenosine affects the action potential outputs of thick-tufted layer 5 pyramidal neurons. In particular I was interested in the extent to which the temporal distribution of action potentials may be affected (i.e. bursting), to what extent the modulation depends on the location of the input, and how the back-propagation of action potentials into the apical dendrite is modulated.

To investigate these questions I have used a method that measures the neuronal I-V relationship during ongoing activity generated by the injection of a naturalistic noisy current trace (Badel *et al.*, 2008). I have used this method to generate a reduced neuronal model (rEIF) that has been used previously to accurately predict sub-threshold voltages and spike times. This allows a range of electrophysiological parameters to be extracted.

Using somatic and dendritic current injections I demonstrate that the dynamic I-V approach can be used to parameterise an rEIF model that predicts spike times accurately in control conditions as well as in adenosine and 8-CPT. Despite a relatively small hyperpolarisation and reduction in input resistance both at the soma and dendrite, adenosine produces a powerful suppression of firing, which is significantly increased when current is injected in the apical dendrite. As with synaptic transmission I demonstrate that the activation of A<sub>1</sub> receptors by endogenous adenosine increases during development. Finally, I find that adenosine produces a loss of action potential bursting in some neurons and a selective shunting of back-propagating bursts in the apical dendrite.

## 5.2 Results

### 5.2.1 Calculation of Dynamic I-V curve and rEIF parameters

Whole-cell patch clamp recordings were made from large thick-tufted pyramidal neurons in layer 5 of the somatosensory cortex, identified using IR-DIC optics, in slices taken from young rats (P17-32). Neuronal identity was confirmed *post-hoc* using the avidin-biotin staining technique (see

chapter 2.2). Several different naturalistic noisy currents (40 seconds long, computed previously and recorded as test files) were injected into neurons at 2-minute (start-to-start) intervals following the injection of typical step current protocols (to generate standard current-voltage relationships). In some cases dual recordings were made from the soma of the same neuron so that current could be injected from one pipette and the voltage read simultaneously from both. This allowed assessment of the accuracy of the de-filtering process (chapter 2.3.7) that was used to remove artefacts introduced by the pipette resistance and capacitance.

The resulting voltage traces, along with the injected currents, were used to generate dynamic I-V curves using methods detailed previously (see Badel *et al.*, 2008 & chapter 2.3.6 for full details). This method allows rapid and accurate characterisation of neuronal properties and can be used to fit simple models that accurately predict sub threshold and spiking behaviour. In brief, the relationship between the injected current trace and voltage response is used to calculate the transmembrane current at each time point (fig 5.1.b). This transmembrane current is used to build a scatter plot against the membrane potential (fig 5.1.c), the average of this plot yields the dynamic I-V curve, which entails a linear sub-threshold response and exponential spike upswing (fig 5.1.d). This dynamic I-V curve is then used to parameterise an exponential integrate and fire model (EIF). The pyramidal neurons' refractory properties are captured by treating post-spike time slices separately (fig 5.2.a), yielding separate EIF parameters that exponentially relax back to the pre-spike parameters (fig 5.2.b). Finally the

response of the rEIF (refractory exponential integrate-and-fire) parameters to the second current trace are calculated and tested against the voltage response to this current to test the accuracy of the subthreshold (fig 5.2.c) and action potential firing predictions (fig 5.2.d). This process is typically able to predict 75-90% of action potentials within a 2ms window of precision. The resting potential calculated from the dynamic I-V curve and rEIF model did not differ significantly from that observed prior to or following the current injection protocols (measured =  $-65.3 \pm 3.7$  mV, calculated =  $-65.5 \pm 4.1$  mV, paired two-tailed t-test,  $P = 0.69$ ,  $n = 27$ ). Figure 5.1 illustrates the processes used to generate the dynamic I-V curve.

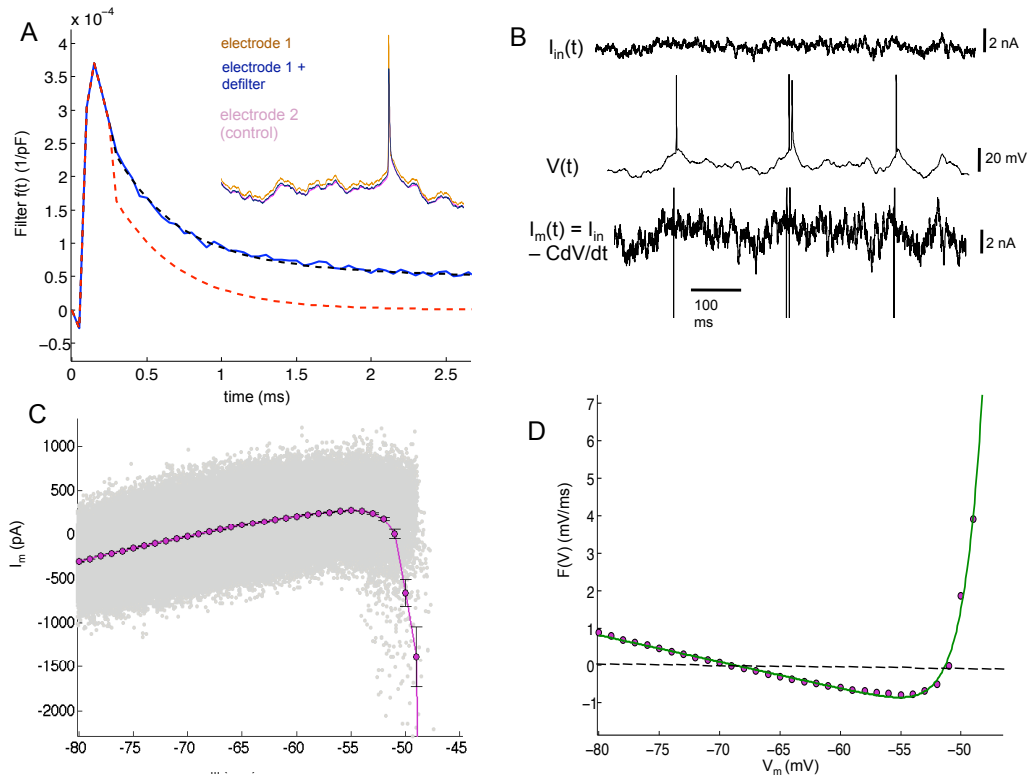


**Fig 5.1** Protocol for the generation of the dynamic I-V curve. (A) The optimal linear filter for combined electrode and neuron (blue), sum of two exponentials fit to tail of combined filter (black), slower exponential subtraction (pure electrode filter, red). Inset: second recording electrode (pink) used to test accuracy of de-filtering (blue). See methods for further details. (B) Fluctuating current injected into neuron ( $I_{in}(t)$ , top), de-filtered voltage recording ( $V(t)$ , middle), rate of change of voltage multiplied by capacitance and subtracted from injected current gives the transmembrane current ( $I_m(t)$ , bottom). (C) Scatter plot of transmembrane current  $I_m(t)$  against  $V(t)$ , excluding points within 200 ms post-spike. The average transmembrane current gives the dynamic I-V curve (pink). (D) An inverted (to give  $F(V)$ ) dynamic I-V curve, fit to rEIF model (green).

The dynamic I-V curve offers an experimental measurement that can be used to parameterise one-variable Integrate-and-Fire models of neurons. The process has been used previously (Badel *et al*, 2008) to demonstrate that forms of Exponential Integrate-and-Fire models (EIF) can be used to accurately predict spike times and sub-threshold voltages produced by the injection of novel current traces. Thus the voltage and current traces were used to create dynamic I-V curves for each of the experimental manipulations (control, adenosine, 8-CPT), characterising both the pre (fig 1) and post spike response properties (fig 2). These were then used to

parameterise a refractory Exponential Integrate and Fire model (rEIF) to examine the changes produced by adenosine.

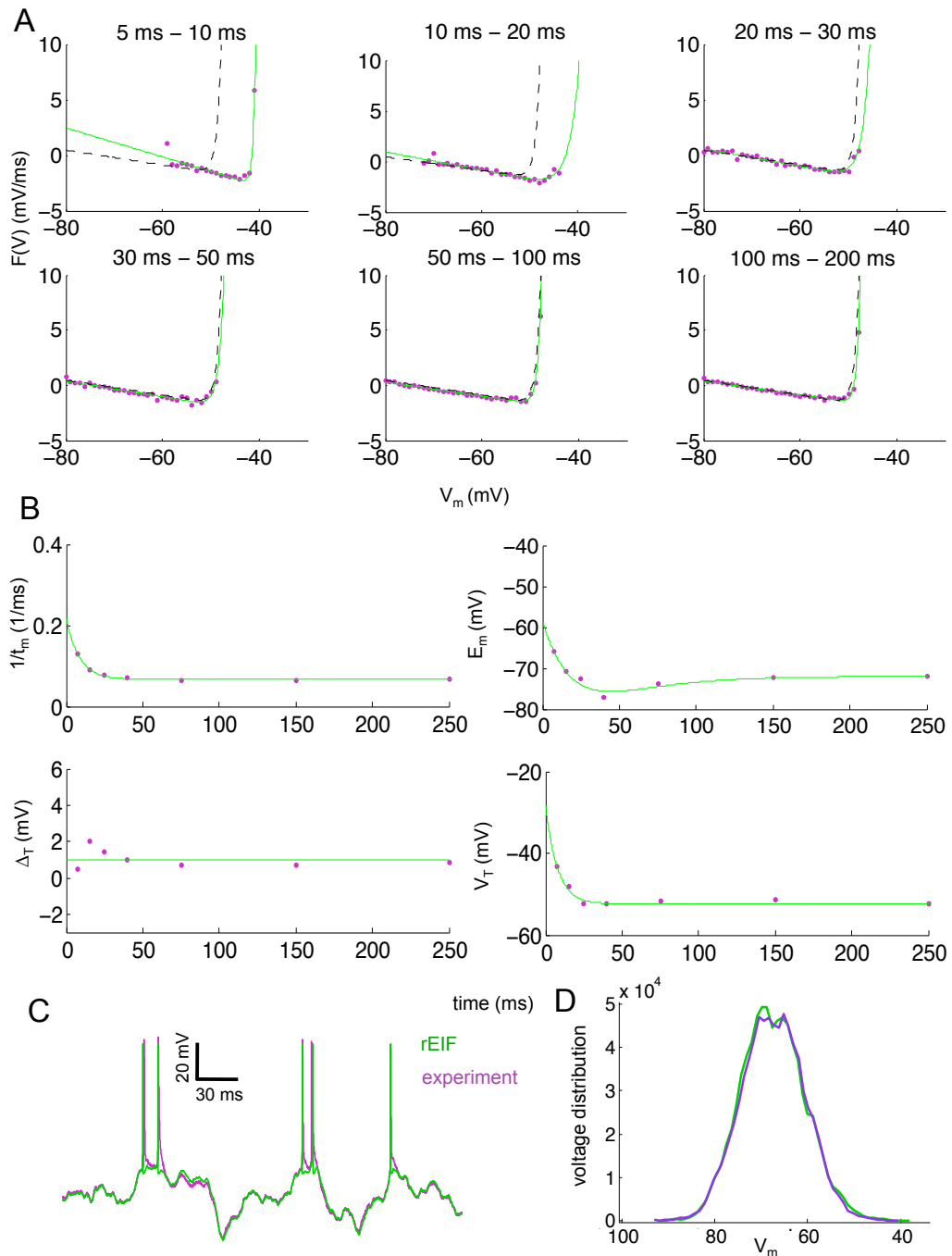


**Fig 5.2** Measurement of post-spike refractory properties in control conditions. (A) I-V curves measured at different post-spike windows showing relaxation of refractory properties. (B) Relaxation of EIF parameters post-spike. Symbols show parameters taken from EIF model fits in A, green lines show exponential relaxation of parameters  $1/\tau_m$  and  $V_T$ .  $E_m$  fitted with double exponential,  $\Delta_t$  showed no consistent post-spike changes. (C and D) Verification of rEIF model fit against a second current injection and comparison between model and experiment sub-threshold voltage distributions.



### 5.2.2 Effects of Adenosine on sub-threshold neuronal properties

The application of adenosine (100  $\mu\text{M}$ ) resulted in a hyperpolarisation of the membrane potential in the pyramidal neurons ranging from 0.5 to 5.1 mV (mean  $\pm$  std dev =  $2.20 \pm 1.94$  mV). After allowing the effects of adenosine to reach steady state, noisy current traces were re-injected into the neuron and the resulting voltage traces used to generate dynamic I-V curves and quantify the sub-threshold parameters. When calculated from the dynamic I-V curve and rEIF model, the hyperpolarisation produced by adenosine (100  $\mu\text{M}$ ) was virtually identical to ( $2.19 \pm 2.13$  mV,  $n = 27$ ) and highly correlated with (linear regression, gradient = 1.07,  $R^2 = 0.78$ ,  $P < 0.001$ ) that observed in the quiescent recordings (no current injection). The hyperpolarisation resulted in a significant decrease of the mean resting potential ( $E_M$ ) to -68.5 mV (from -66.31 mV in control, paired one-tailed t-test,  $P < 0.001$ ,  $n = 27$ , fig 5.3b). As well as the hyperpolarisation, adenosine also produced an increase in the action potential threshold ( $V_T$ ) of  $1.32 \pm 1.98$  mV ( $n = 27$ ). Thus the distance from the resting potential to action potential threshold ( $V_T - E_M$ ) was significantly increased in adenosine (increase  $\sim 25\%$ , from  $14.9 \pm 3.6$  mV in control to  $18.6 \pm 3.4$  mV in adenosine, paired one-tailed t-test,  $P < 0.001$ ,  $n = 27$ , fig 5.3c).

The addition of adenosine to the bath solution produced a significant decrease in the membrane time constant ( $\tau_m$ ) from  $14.7 \pm 3.6$  ms to  $11.5 \pm 2.4$  ms (paired one-tailed t-test  $P = 0.002$ ,  $n = 27$ ) and a significant drop in input resistance (calculated from  $\tau_m/C$ ) of  $6.9$  M $\Omega$  (falling from a mean of

38.5 ± 8.8 MΩ in control to 31.6 ± 8.6 MΩ in adenosine, paired one-tailed t-test,  $P < 0.001$ ,  $n = 27$ ). Each of these parameters returned to values above control upon application of 8-CPT to the bath, which in these experiments was applied following adenosine wash. The dynamic I-V curves in measured from each pharmacological manipulation tended to cross at ~80 mV, suggesting a reversal of the currents that produced the changes occurs at this voltage (fig 5.3a).

Although the effects of removing tonic A<sub>1</sub> activation were relatively minor,  $V_T - E_M$  decreased significantly by 1.31 ± 2.1 mV relative to control (paired one-tailed t-test,  $P = 0.03$ ,  $n = 27$ ), while input resistance and  $\tau_m$  increased (by 1.5 ± 3 MΩ and 0.8 ± 2 ms respectively), these changes were also significant (resistance 8-CPT/control, paired one-tailed t-test,  $P = 0.015$ ,  $n = 27$ ,  $\tau_m$  8-CPT/control, paired one-tailed t-test,  $P = 0.03$ ,  $n = 27$ ). However no significant changes were observed in the neuronal capacitance (control = 405 ± 107 pF, adenosine = 390 ± 122 pF, 8-CPT = 404.3 ± 118, control/adenosine, paired one-tailed t-test,  $P = 0.10$ ,  $n = 27$ ) or in the  $\Delta_T$  parameter (corresponding to the sharpness of action potentials, control = 1.03 ± 0.23 ms, adenosine 1.14 ± 0.43 ms, 8-CPT = 1.22 ± 0.4, control/adenosine, paired two-tailed t-test,  $P = 0.48$ ,  $n = 27$ ).

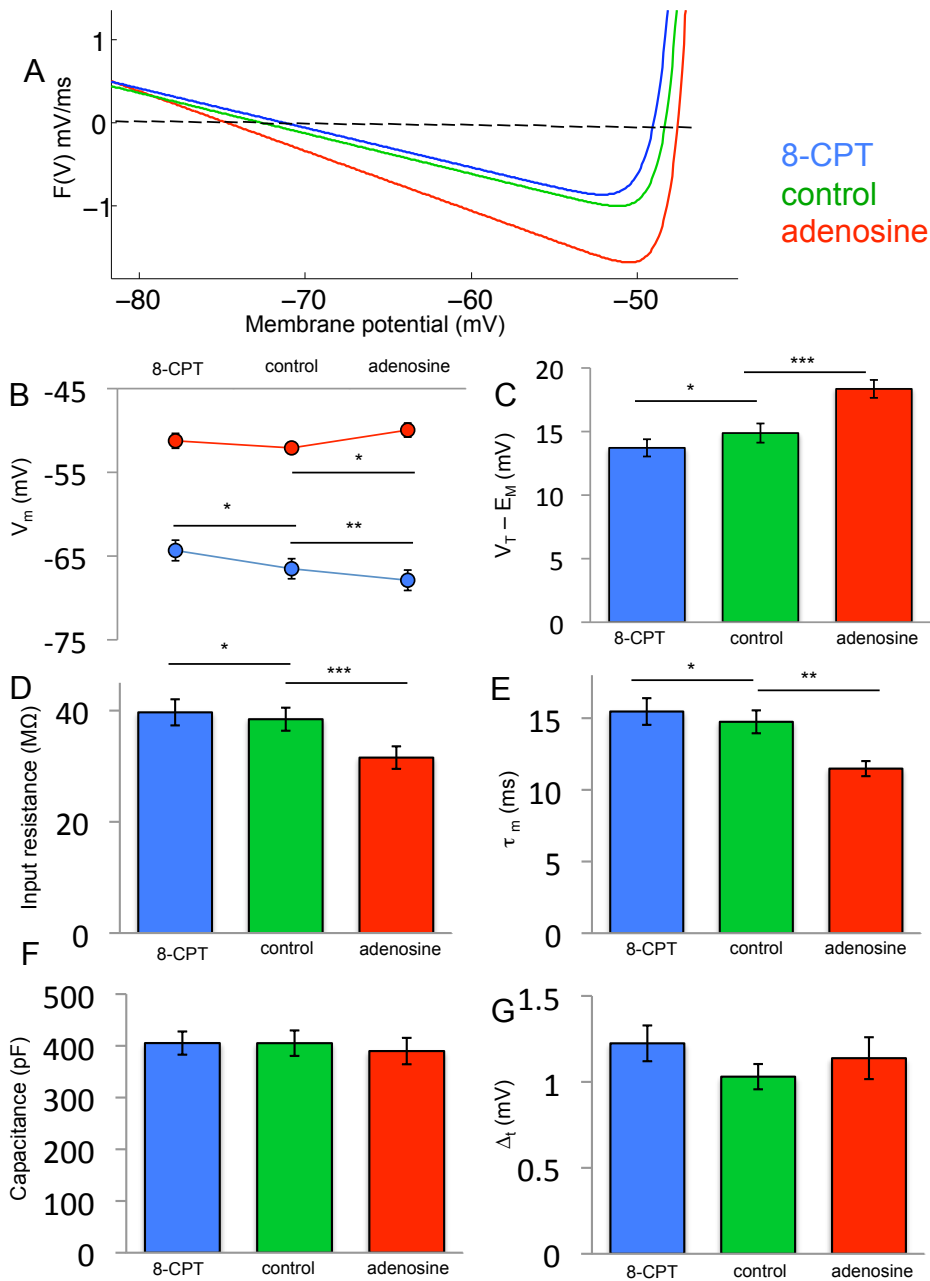


**Fig 5.3** Summary of parameter changes in adenosine and 8-CPT in the rEIF model. (A) Inverted dynamic I-V curve for each pharmacological manipulation, demonstrating increased  $V_T$ , reduced  $E_M$ , and increased slope (reduced input resistance) in adenosine. (B) Adenosine produced a significant hyperpolarisation (blue) and an increase in action potential threshold (red). (C) Distance to action potential threshold ( $V_T - E_M$ ) increased by 3.5 mV in adenosine. (D and E) Adenosine significantly reduced input resistance and the membrane time constant. (C-E) Upon adenosine wash and application of 8-CPT each of these parameter changes reversed to levels significantly different from control, indicating significant basal activation of  $A_1$  receptors. (F and G) No significant changes in capacitance or spike sharpness were detected.

During most experiments standard step currents were injected into the neuron to provide an alternative method to characterise the neurons' I-V response properties. Input resistance was measured from these step responses by taking the gradient of the I-V curve around the resting potential. Across the population the input resistance calculated from the rEIF model was virtually identical to that calculated before the  $I_h$  sag rebound (fig 5.4c, rEIF resistance =  $36.9 \pm 13.3 \text{ M}\Omega$ , pre-rebound resistance =  $36.3 \pm 12.7 \text{ M}\Omega$ , post-rebound =  $29.5 \pm 11.3 \text{ M}\Omega$ , paired two-tailed t-tests, rEIF/pre-rebound,  $P = 0.79$ , rEIF/post-rebound,  $P = 0.02$ ,  $n = 16$ ). This relationship persisted in adenosine (rEIF resistance =  $31.6 \pm 10.9 \text{ M}\Omega$ , pre-rebound resistance =  $31.9 \pm 11.8 \text{ M}\Omega$ , post-rebound =  $26.6 \pm 9.5 \text{ M}\Omega$ , paired two-tailed t-tests, rEIF/pre-rebound,  $P = 0.86$ , rEIF/post-rebound,  $P < 0.001$ ,  $n = 16$ ). Notably, the drop in input resistance in adenosine was reduced following  $I_h$  activation (fig 5.4c, see also section 5.3.8). These results suggest that the dynamic I-V curve measured pre-spike reflects low activation of time-dependent channels such as the HCN channel.

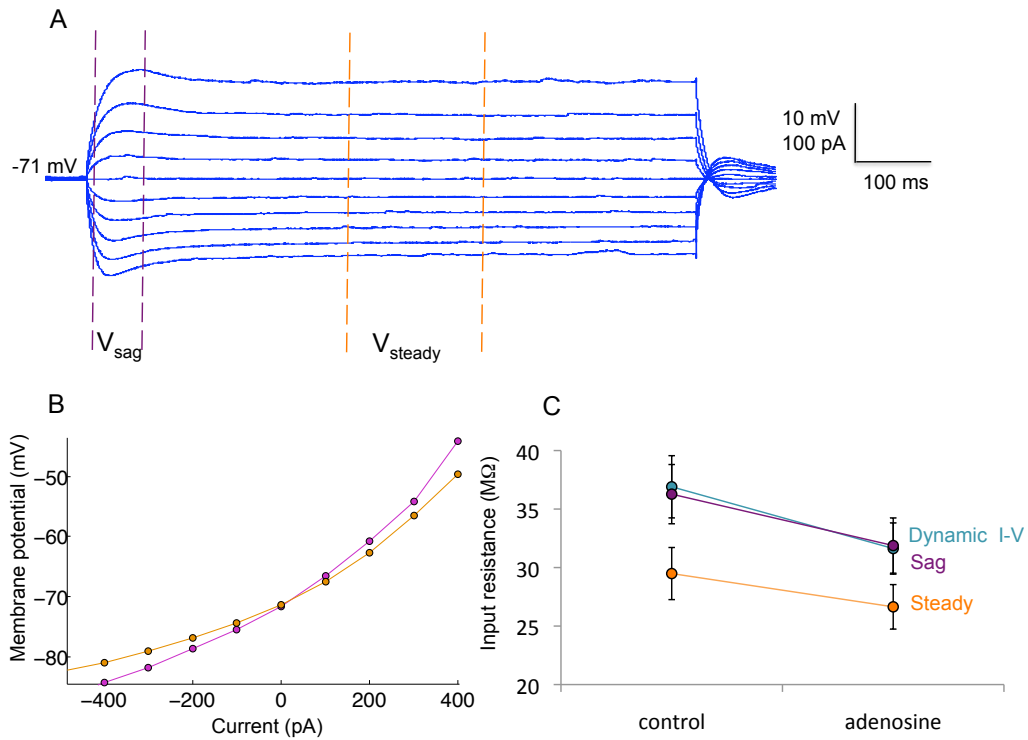


**Fig 5.4** Calculation of input resistance. (A) The I-V curve was calculated from step currents by measuring the maximum voltage change during the initial sag ( $V_{\text{sag}}$ ) or during steady state ( $V_{\text{steady}}$ ). (B) Input resistance was calculated from the I-V curve by measuring the gradient at 0 pA current. (C) The input resistance calculated from the rEIF model corresponds closely to the input resistance calculated from the initial sag that precedes  $I_h$  activation in both control and adenosine.

At the end of each experiment the adenosine was washed off and replaced with 8-CPT to reveal the extent of tonic  $A_1$  receptor activation. In experiments where adenosine was added to the bath solution following the addition of 8-CPT there was no further change in the neuronal membrane potential indicating that the post-synaptic effects of adenosine were also mediated by activation of  $A_1$  receptors (see chapter 3.2.2). Similar to the synaptic experiments the addition of 8-CPT revealed significant variation in baseline  $A_1$  receptor activation between experiments and again there was an increase in baseline activation with age. Fig 5.7b illustrates baseline activation measured from changes in the input resistance  $((R_{\text{CPT}} - R_{\text{con}}) / (R_{\text{CPT}} -$

$R_{\text{ado}}$ ) plotted against age of cortex and illustrates the increasing and more heterogeneous activation with age (section 5.2.6).

Following action potential firing there are transient changes in the response properties of neurons, typically reducing excitability and resulting in a refractory period of 10s-100s milliseconds. I separated the post-spike recovery period into time slices from which the dynamic I-V curve was again calculated for each. The relaxation of changes in  $V_T$  and  $1/\tau_m$  were again well captured by a single exponential and the change in  $E_M$  by a double exponential, however no significant change in these relaxation parameters was detected between control and adenosine.

### 5.2.3 Effects of adenosine on firing and action potentials

Upon bath application of adenosine, the frequency of action potential firing evoked by the injected noisy current was reduced in all neurons, from a mean frequency of  $5.8 \pm 3.9$  Hz in control conditions to  $3.3 \pm 3.7$  Hz. This reduction was highly significant (paired one-tailed t-test,  $P < 0.001$ ,  $n = 27$ ). Following application of the  $A_1$  receptor antagonist 8-CPT, the mean firing frequency increased significantly to  $6.6 \pm 4.0$  Hz (paired one-tailed t-test,  $P < 0.001$ ,  $n = 27$ ), again demonstrating tonic activation of  $A_1$  receptors by endogenous adenosine in control conditions.

Given the heterogeneity in the endogenous activation of  $A_1$  receptors across the population, I will use the changes observed between adenosine (100  $\mu\text{M}$ ) and 8-CPT (2  $\mu\text{M}$ ) as a measure of the total effect of adenosine on the

neuron for the subsequent analyses examining the capacity for adenosine to reduce firing.

Neurons that were driven to fire at the highest frequencies in 8-CPT exhibited the largest absolute loss of firing in adenosine (Figs 5.5a and e). The  $\text{LOG}_{10}$  of the firing frequencies were used in this analysis in order to preserve normal distributions (due to a skewed tail in the data at high frequencies).

The linear trend was weak (linear regression  $R^2 = 0.42$   $P = 0.017$ ) however and a second order polynomial provided a significantly (linear vs second order,  $P = 0.0085$ ) improved fit ( $R^2 = 0.57$ ,  $P < 0.001$ ), capturing the saturation in firing reduction above 8 Hz. The fact that the polynomial curve provided a significantly improved fit compared to the linear trend suggests that the saturation in adenosine mediated loss of firing at high frequencies was a significant effect, indicating that the activation of  $A_1$  receptors had an increasingly limited capacity to reduce firing evoked by high stimulations. However more data would be necessary to identify the exact nature of this saturation.

When the neurons driven to fire at the highest frequencies were removed from the analysis the strength of the trend increased (linear regression  $R^2 = 0.74$ ,  $P < 0.001$ ). These trends persisted when the effects of bursts of action potentials were removed from the analysis (bursts were considered a single spike; fig 5.5 b, d, f).

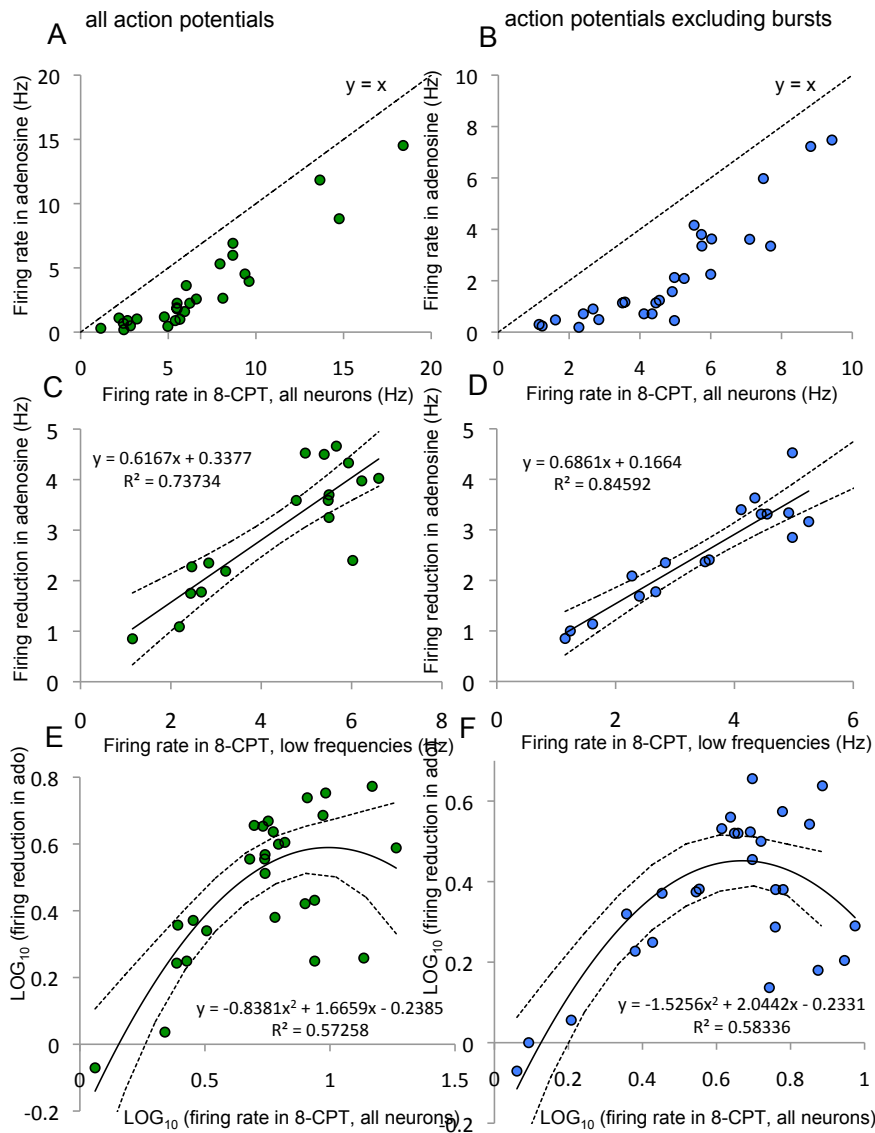


**Fig 5.5** Summary of adenosine mediated suppression of firing. (A) Firing frequency in 8-CPT plotted against firing frequency in adenosine. (C) Firing frequency in 8-CPT vs loss of firing in adenosine (8-CPT - ado) illustrating that at low frequencies there is a strong linear trend - the amount of action potentials lost in adenosine is highly dependent on the initial frequency, dotted lines illustrate 95% confidence intervals. (E) At higher frequencies this linear trend is lost and a quadratic polynomial provides a significantly improved fit ( $R^2 = 0.57$  versus  $R^2 = 0.42$  for linear regression,  $P = 0.0085$ ) compared to a linear trend (B, D and F) When only isolated action potentials or those fired at the beginning of a burst are considered the trends remain (quadratic  $R^2 = 0.58$ , linear  $R^2 = 0.31$ ,  $P = 0.0006$ ), illustrating the lack of a frequency dependent effect on bursting. (E and F) The  $\text{LOG}_{10}$  of the firing frequencies were considered in this analysis in order to preserve a normal distribution.



Strikingly, there was very little correlation between the adenosine-mediated suppression of firing and the decrease in input resistance (linear regression,  $R^2 = 0.04$ ,  $P = 0.36$ ), or change in  $V_T - E_M$  (linear regression,  $R^2 = 0.02$ ,  $P = 0.57$ ). There was also a lack of correlation between the change in input resistance and membrane potential ( $R^2 = 0.02$ ,  $P = 0.42$ ). This potentially indicates that the changes in membrane potential and resistance are not solely mediated by the activation of a single conductance, as a large drop in input resistance did not necessarily correspond to a strong hyperpolarisation and vice versa.

Thus, the changes in  $E_M$ ,  $V_T$  and  $\tau_m$  account for little of the variation in firing suppression on their own. However, when the change in input resistance was added to the change in  $V_T - E_M$  the correlation with firing suppression increased and became significant (linear regression,  $R^2 = 0.2$ ,  $P = 0.04$ ).

This relatively weak correlation is perhaps due to the fact that the measured changes in these parameters are relatively minor yet highly amplified in the firing output of the cells. Adenosine induced a  $26 \pm 20\%$  increase in  $V_T - E_M$ , and a  $20 \pm 15\%$  decrease in  $\tau_m$  yet these changes were amplified to a  $63 \pm 18\%$  decrease in firing over a range of frequencies.

#### 5.2.4 Action potential parameters

The physiological changes observed in adenosine could potentially affect the parameters of action potentials. To test this I classified action potentials based on whether they occurred within bursts and measured three parameters – half width, amplitude and the integral at half amplitude (area).

Of these parameters only amplitude was found to be significantly affected by adenosine (Table 5.1, paired two-tailed t-test,  $P = 0.005$ ,  $n = 27$ ). The reduction in amplitude in adenosine occurred due to the increase in threshold, as there was no significant change in the peak voltage.

The properties of each action potential in periods of bursting were also examined. Action potentials occurring within bursts (i.e. 2<sup>nd</sup> – 4<sup>th</sup>) had significantly increased mean half widths (paired two-tailed t-test,  $P < 0.001$ ,  $n = 27$ ), areas (paired two-tailed t-test,  $P < 0.001$ ,  $n = 27$ ), and reduced peak amplitudes (paired two-tailed t-test,  $P < 0.001$ ,  $n = 27$ ), compared to initial action potentials. However again, only amplitude was significantly modulated by adenosine (paired two-tailed t-test,  $P = 0.007$ ,  $n = 27$ ).

	Singles			Doublets		
	Control	Adenosine	8-CPT	Control	Adenosine	8-CPT
Half-width (ms)	0.84 ± 0.14	0.84 ± 0.12	0.85 ± 0.11	1.33 ± 0.23	1.38 ± 0.23	1.37 ± 0.25
Amplitude (mV)	84.4 ± 6.7	81.9 ± 8.6*	82.9 ± 5.9	73.2 ± 7.3	70.8 ± 9.1*	72.4 ± 6.1
Area (mVms)	21.5 ± 2.7	21.9 ± 3.2	21.7 ± 2.3	26.8 ± 2.9	27.9 ± 4.6	27.7 ± 3.8

**Table 5.1** Measured action potential parameters in each pharmacological manipulation. Singles – isolated action potentials, or those at the beginning of a burst. Doublets – the second action potential in a burst. Only the amplitude was significantly changed in adenosine. \* Indicates significant change.

### 5.2.5 Action Potential Bursting

Pyramidal neurons in layer 5 of the sensory cortices can be classified electrophysiologically based on the action potential discharge in response to synaptic excitation or steps of depolarising current (McCormick *et al.*, 1985;

Kasper *et al.*, 1994). The class of pyramidal neurons that send axonal projections to sub-cortical structures preferentially fire bursts (typically 2-5) of action potentials (Chagnac-Amitai *et al.*, 1990). The generation of burst firing involves the recruitment of Ca<sup>2+</sup>-channels in the apical dendrite by back-propagating action potentials (Williams and Stuart, 1999; Schwindt and Crill, 1999). Burst firing tends to occur at frequencies that allow temporal summation of EPSPs, which can result in later EPSPs being amplified by voltage gated Na<sup>2+</sup> channel activation as the post-synaptic neuron nears action potential threshold.

Pyramidal neurons are most commonly classified as burst firing by their response to long depolarising current steps, and while to an extent burst firing can occur independently of input I observed that when stimulated with a noisy current neurons that may be classified as regular firing in response to step currents may still fire a significant proportion of action potentials in bursts. However in neurons that fired an initial burst (weakly bursting) or train of bursts (strongly bursting) in response to a step current a significantly higher proportion of action potentials led into bursts compared to regular firing neurons (regular firing =  $0.17 \pm 0.19$ , bursting =  $0.45 \pm 0.15$ , Mann-Whitney U test,  $P = 0.015$ ,  $n = 10$  regular, 8 bursting). The degree of bursting was defined as the proportion of initial spikes that were followed by a doublet within 18 msec. This window was chosen based on the time during which back-propagating action potentials show significant summation (see 5.2.9) and spikes occurring within this time window had significantly wider half widths and reduced amplitudes (see 5.2.4). The

proportion of action potentials leading to bursts was not strongly correlated with overall firing frequency (linear regression,  $R^2 = 0.16$ ,  $P = 0.06$ )

Across the whole population of neurons the application of adenosine induced a small but significant reduction (Wilcoxon Matched pairs test,  $P = 0.014$ ,  $n = 25$ ) in the proportion of action potentials leading to bursts, from  $0.25 \pm 0.21$  in control, to  $0.21 \pm 0.21$  in adenosine, and returning to  $0.24 \pm 0.19$  in 8-CPT. Although across the whole population the reduction was small, neurons could be grouped into two populations: responsive to adenosine (reduced bursting), and unresponsive to adenosine (no change in bursting). A neuron was defined as responsive to adenosine if a reduction in bursting occurred upon application of adenosine and this was reversed in 8-CPT (fig 5.6). Across all the experiments 11 neurons showed a reduction in bursting in adenosine and full or nearly-full recovery in 8-CPT (control =  $0.27 \pm 0.20$ , adenosine =  $0.16 \pm 0.13$ , 8-CPT =  $0.25 \pm 0.17$ ; one-tailed Wilcoxon matched pairs control/adenosine,  $P < 0.001$ , adenosine/8-CPT,  $P < 0.001$ ), while 14 neurons showed no response to adenosine (control =  $0.27 \pm 0.25$ , adenosine =  $0.28 \pm 0.26$ , 8-CPT =  $0.25 \pm 0.23$ ; one-tailed Wilcoxon matched pairs control/adenosine,  $P = 0.16$ , adenosine/8-CPT,  $P = 0.13$ ).

These populations did not differ significantly in age (responders =  $P22 \pm 5.0$ , non-responders =  $P24.4 \pm 5.3$ , Mann-Whitney U test  $P = 0.12$ ), resting potential (responders =  $-66.6 \pm 4$  mV, non-responders =  $-65.8 \pm 3.6$  mV, 2-tailed unpaired t-test,  $P = 0.68$ ), input resistance (responders =  $38.5 \pm 10.6$  M $\Omega$ , non-responders =  $36.5 \pm 10.3$  M $\Omega$ , 2-tailed unpaired t-test,  $P = 0.63$ ) or capacitance (responders =  $361 \pm 92$  pF, non-responders =  $406 \pm 126$  pF, 2-

tailed unpaired t-test,  $P = 0.37$ ). There was however a significantly larger total membrane hyperpolarisation ( $E_M$  in 8-CPT-  $E_M$  in adenosine) in the responding population (responders =  $4.51 \pm 1.75$  mV, non-responders =  $3.04 \pm 1.32$  mV, 1-tailed unpaired t-test,  $P = 0.014$ ), while the decrease in input resistance was larger, but not by an amount that was significant for this sample size (responders =  $8.5 \pm 4.8$  M $\Omega$ , non-responders =  $6.3 \pm 3.8$  M $\Omega$ , 1-tailed unpaired t-test,  $P = 0.11$ ). While the overall loss of firing was higher in the responding class ( $67 \pm 13\%$  compared to  $61 \pm 21\%$ ) this was largely due to the loss of the bursts themselves. When only initial action potentials were included there was less difference (responders =  $61 \pm 14\%$ , non-responders  $59 \pm 21\%$ ).

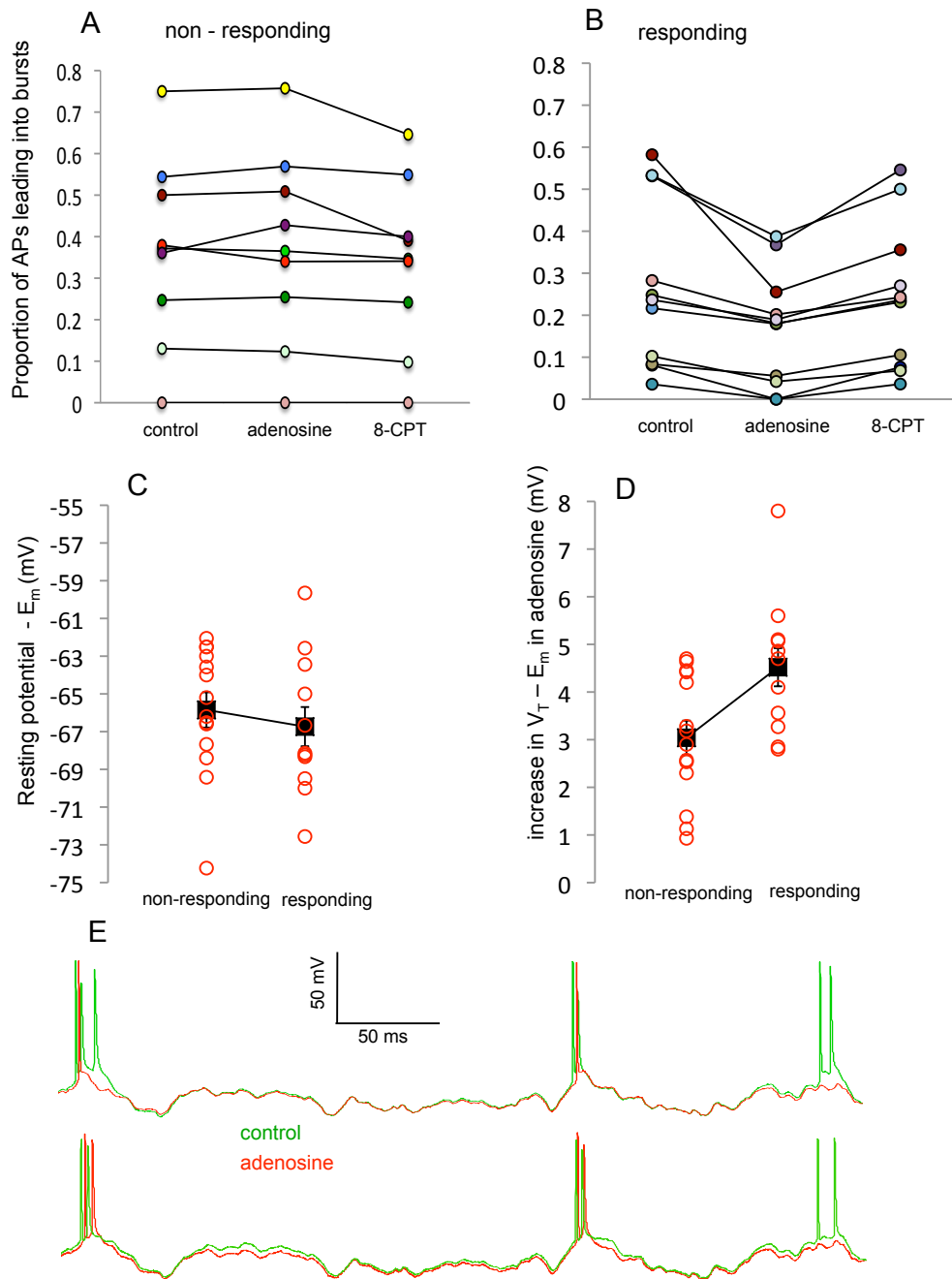


**Fig 5.6** Adenosine modulation of action potential burst firing. (A and B) 2 classes of neurons were identified based on the modulation of bursting, 11 out of 25 neurons reduced their proportion of APs leading to bursts in adenosine and recovered in 8-CPT. (C and D) These neurons did not differ in any sub-threshold parameters (C shows  $E_m$ ), but cells that lost bursts in adenosine showed a significantly increased shift in resting potential away from AP threshold (D). (E) Example voltage traces of a cell showing modulation of bursting (top) and one with no response (bottom).

Thus, while the magnitude of sub-threshold changes induced by adenosine had little correlation with the overall loss of firing – perhaps because the relatively minor sub-threshold changes were amplified by the cells' firing

reduction; there was significant correlation with the magnitude of these changes and the tendency for some neurons to reduce burst firing in adenosine.

#### 5.2.6 Increase in endogenous activation of $A_1R$ during development

The experiments in this chapter included slices taken from both (using the terminology from chapter 4) juvenile (P17-22) and mature (P28-32) cortex. As well as this, some slices were taken from rats in between these two developmental stages. In order to determine if the post-synaptic activation of  $A_1$  receptors showed the same developmental increase as the pre-synaptic activation demonstrated in chapter 4 I measured the level of endogenous  $A_1R$  activation as the ratio of the difference in membrane potential or input resistance between the control condition and 8-CPT (2  $\mu\text{M}$ ) to the difference between adenosine (100  $\mu\text{M}$ ) and 8-CPT. Using these measures it was observed that the level of endogenous activation increased with post-natal development (fig 5.7b, input resistance, linear regression,  $R^2 = 0.18$ ,  $P = 0.03$ ), showing a similar trend as the synaptic experiments in chapter 4, of minimal endogenous activation at the youngest ages (P17-22), to an increased and heterogeneous tone in older slices (P28-32).

#### 5.2.7 Dendritic current injection

The above results illustrate how adenosine can produce a profound reduction in action potential firing despite only small changes in sub-threshold parameters. Even though current was injected at the soma and therefore travelled only a relatively short distance to the action potential

initiation site at the axonal initial segment, the effects of adenosine on firing were still apparent. I next decided to examine how adenosine would modulate inputs injected from a different location a significant distance from the soma, at the site of apical dendrite bifurcation (mean distance of 320  $\mu\text{m}$  from soma, range 240 – 580  $\mu\text{m}$ ).

In these experiments whole-cell recordings were established at both the soma and apical dendrite bifurcation of a single thick-tufted layer 5 pyramidal neuron. A whole-cell recording was first established at the soma, with a pipette containing 50  $\mu\text{M}$  Alexafluor-488, and then the fluorescent dendrite was whole-cell patch clamped. The noisy current protocols were injected alternately at the dendrite and the soma in order to compare the impact of adenosine modulation of spiking between the two. The membrane potential at the apical dendrite-recording electrode was significantly depolarised compared to the soma ( $E_M$  at soma =  $-67.3 \pm 3.2$  mV,  $E_M$  at dendrite =  $-62.1 \pm 2.1$  mV, paired 2-tailed t-test,  $P < 0.001$ ,  $n = 12$ ). No significant difference was observed in the amplitude of hyperpolarisation induced by adenosine between the two sites ( $2.13 \pm 1.1$  mV at the soma,  $1.97 \pm 1.1$  mV at the dendrite, paired 2-tailed t-test,  $P = 0.84$ ,  $n = 12$ ). Similarly no difference was observed in the effect of the endogenous tone (defined as the depolarisation between control and 8-CPT) between the soma and dendrite (fig 5.7a,  $1.64 \pm 1.01$  mV at the soma,  $1.73 \pm 1.24$  mV at the dendrite, paired 2-tailed t-test,  $P = 0.42$ ,  $n = 8$ ). There was a significant correlation between the effect of tone at the soma and dendrite (fig 5.7c, linear regression,  $R^2 = 0.61$ ,  $P = 0.003$ ).



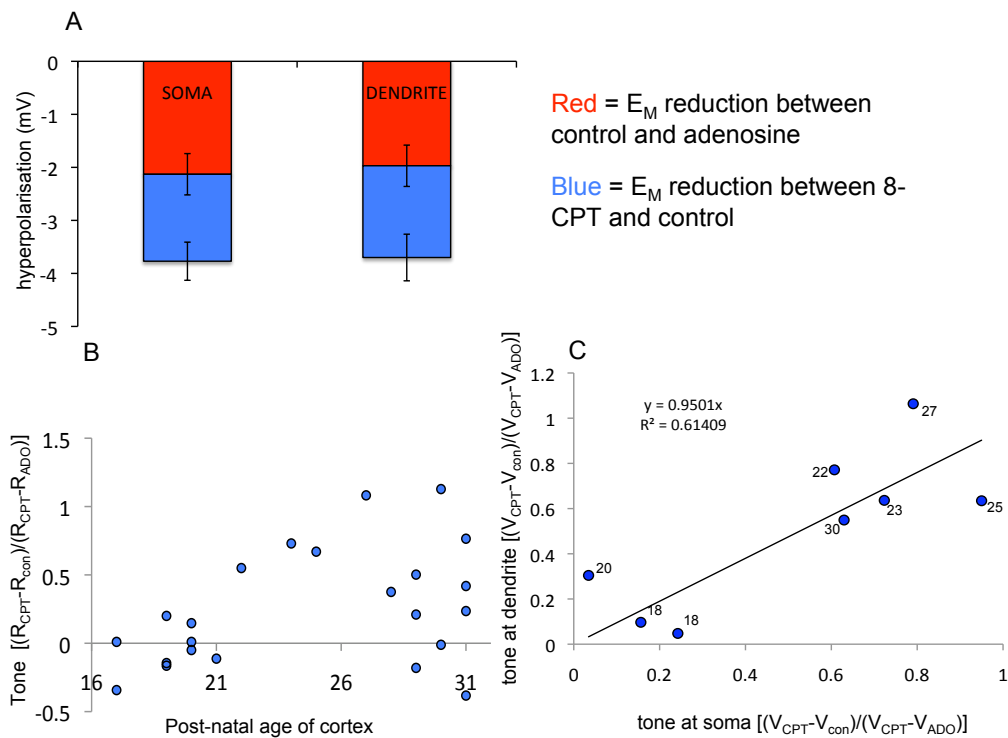


**Fig 5.7** Effects of endogenous adenosine tone across development. (A) There was no significant difference in the effect of bath-applied adenosine (red) or endogenous  $A_1$  activation revealed in 8-CPT (blue) between the soma and the dendrite. (B) The relative baseline activation of  $A_1$ R<sub>s</sub> measured via changes in input resistance in adenosine and 8-CPT. The average level of tonic activation increased and became more variable with age of cortex. (C) Baseline activation (measured from the membrane potential) was highly correlated between the soma and dendrite. Numbers indicate age of each animal.

Even though the hyperpolarisation was identical between the dendrite and soma, I was interested in how the impact of travelling down the apical dendrite would affect the modulation of current inputs by adenosine. Patch-clamp studies have demonstrated that significant attenuation of inputs occurs along dendrites of layer 5 pyramidal neurons (Williams and Stuart, 2002; Nevian *et al.*, 2007) due to current leakage from a variety of  $Ca^{2+}$ -sensitive conductances. Several of these conductances, such as  $I_h$  and GIRK are known to be modulated by the  $A_1$  receptor activation elsewhere in the brain and are thought to be distributed non-uniformly along the apical dendrite – with increasing densities in the distal direction (Stuart and

Spruston, 1998). For these reasons I hypothesised there could be a significant change in the modulation of firing outputs by adenosine for current injected at the apical dendrite compared to the soma.

For the analysis of adenosine's modulation of firing evoked by current injected into the dendrite I compared the effects of adenosine to control conditions rather than to 8-CPT as more recordings were made in control and adenosine for pair-wise statistical analysis compared with adenosine and 8-CPT (12 versus 7). However, when recordings were held long enough for 8-CPT to be applied, firing returned to levels greater than the corresponding control recordings.

For the somatic current injections the firing frequency in adenosine was  $46 \pm 10\%$  of the control frequency ( $n = 12$ ). This reduction in firing was significantly lower (paired Mann-Whitney U test,  $P = 0.02$ ) than the effects of adenosine on firing evoked by dendritic current injections (which reduced to  $26 \pm 12\%$  of control,  $n = 12$ , fig 5.8a). There was no significant difference (unpaired 2-tailed t-test,  $P = 0.266$ ,  $n = 12$ ) in the control firing frequencies induced by current injections in the soma ( $5.8 \pm 2.7$  Hz) and in the dendrite ( $5.5 \pm 2$  Hz). However the firing frequency in adenosine was significantly lower (unpaired 2-tailed t-test,  $p = 0.013$ ,  $n = 7$ ) for dendritic current injection ( $1.7 \pm 1$  Hz) compared to somatic injection ( $2.5 \pm 1.8$  Hz).

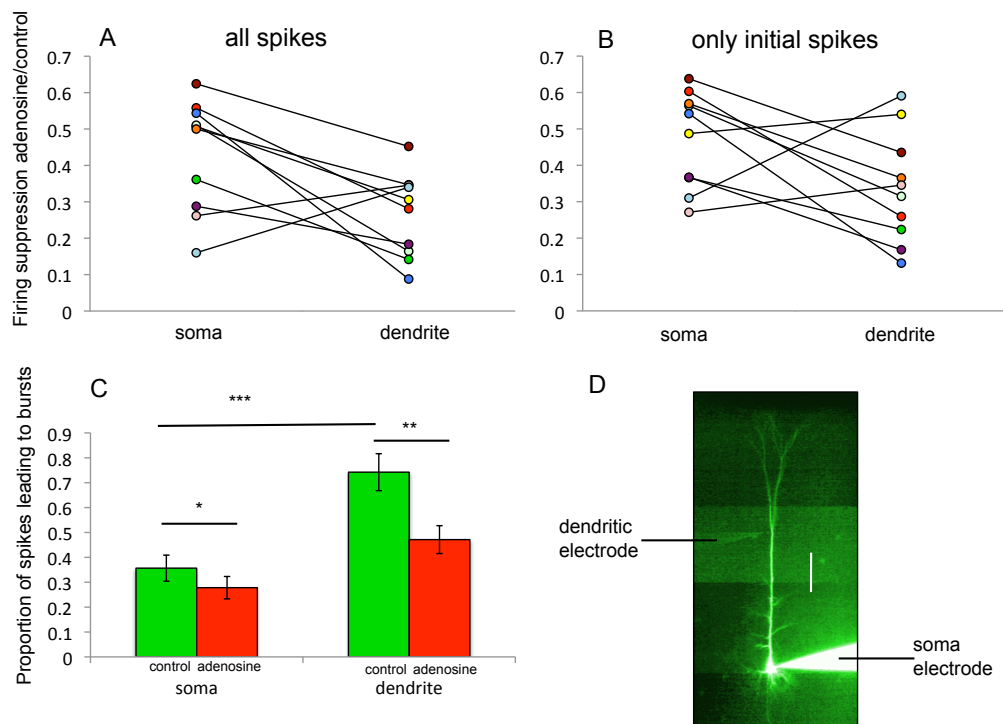


**Fig 5.8** Increased suppression of firing by adenosine for current injected from the apical dendrite. (A) Pair-wise comparisons of firing suppression of somatic and dendritic injections. Significantly more spikes were lost when current was injected at the dendrite. (B) This effect persisted, although to a lesser extent when APs fired in bursts were discounted. (C) More bursting occurred when current was injected at the dendrite and there was an increased loss of this bursting in adenosine (green = control, red = adenosine). (D) Picture of alexa-488 filled neuron with recording electrodes at soma and dendritic bifurcation. No alexa-488 was included in the dendritic pipette to facilitate visualisation of dye filled dendrite. Scale bar = 100 $\mu$ m.

These data include all action potentials, however it was noticeable that there was an increase in the proportion of action potentials leading to bursts when current was injected in the apical dendrite (dendrite =  $0.73 \pm 0.24$ , soma =  $0.35 \pm 0.18$ , Wilcoxon matched pairs,  $P < 0.001$ ,  $n = 12$ ). This has been reported elsewhere (Schwindt and Crill, 1999) and may be due to the depolarisation of the dendrite, which is known to enhance burst firing by eliciting calcium potentials in the dendrite (Williams and Stuart, 1999).

Upon application of adenosine, in contrast to the somatic current injections, all neurons showed a reduction in burst firing when injected with current

from the dendrite (reducing from  $0.73 \pm 0.24$  to  $0.45 \pm 0.3$ , one-tailed Wilcoxon matched pairs,  $P = 0.004$ ,  $n = 12$ ). 8-CPT was applied following adenosine on 7 occasions and resulted in a recovery of burst firing. The increased suppression of firing at the dendrite affected both bursting and initial action potentials - when only initial action potentials were included, the loss of firing remained higher for current injected from the dendrite (reducing to  $0.43 \pm 0.17$  at the soma, and  $0.26 \pm 0.12$  at the dendrite, one-tailed Wilcoxon matched pairs,  $P = 0.042$ ,  $n = 12$ , fig 5.8b).

### 5.2.8 $I_h$ sag reduced in adenosine

The lack of correlation between the membrane potential and input resistance changes in adenosine may indicate the involvement of multiple conductances modulated by the  $A_1$  receptor. I therefore tested whether the sag response to hyperpolarising current (indicative of HCN channel activation) was modulated by adenosine. Sag was defined as,  $V_s - V_b / V_{\min} - V_b$ , giving a ratio that is relatively independent of both input resistance changes and, over the ranges used, amplitude of current injection (fig 5.9a).

At the soma the sag reduced significantly, from  $0.25 \pm 0.06$  in control to  $0.19 \pm 0.04$  in adenosine, recovering to  $0.25 \pm 0.06$  in 8-CPT (control/adenosine paired 1-tailed t-test,  $P < 0.001$ ,  $n = 11$ , adenosine/8-CPT, paired 1-tailed t-test,  $P = 0.019$ ,  $n = 6$ ).

Estimating the voltage response accurately at the dendritic electrode is often difficult when current is injected from that same electrode due to uncertainties in the compensation of series resistance. This is less of a

problem at the soma due to the larger pipette tips. Thus to accurately measure the sag at the dendrite I used the dendritic recording of current injected at the soma. This sag was significantly higher than at the soma (dendrite =  $0.56 \pm 0.04$ , soma =  $0.24 \pm 0.06$ , paired two-tailed t-test,  $P < 0.001$ ,  $n = 10$ ), but was reduced by a similar margin in adenosine (to  $0.51 \pm 0.06$ , paired one-tailed t-test,  $P = 0.002$ ,  $n = 10$ ).

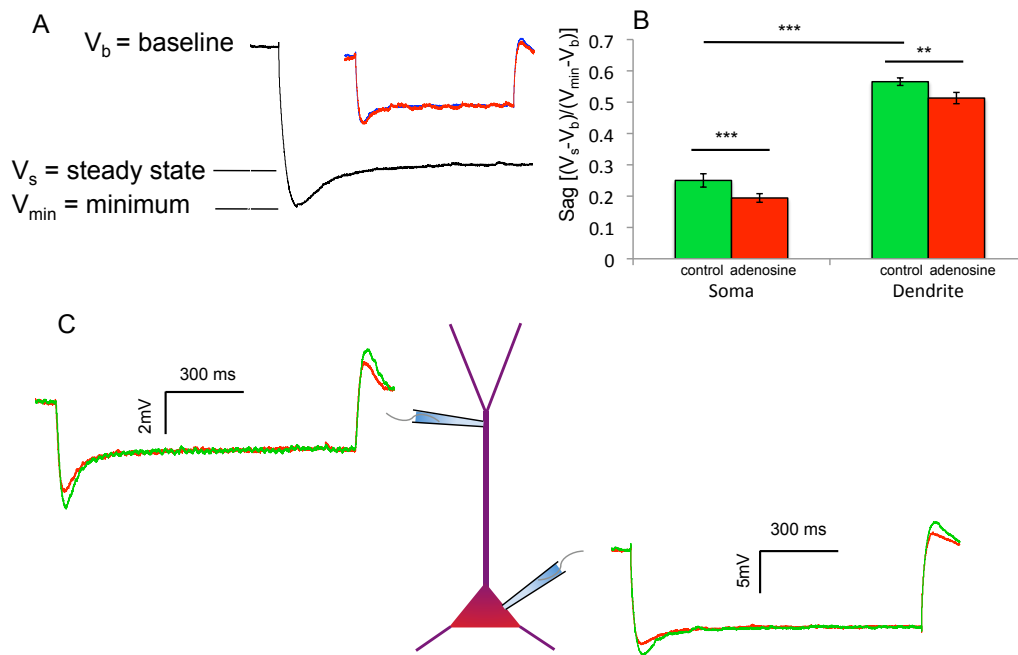


**Fig 5.9** Adenosine mediated reduction of  $I_h$  sag at soma and apical dendrite. (A) Measurement of sag. This ratio was independent of input resistance and the amplitude of current injection over the ranges (-100 to -500 pA) injected. Inset shows normalised overlaid voltage responses to -100 (red) and -300 pA (blue) illustrating no change in sag ratio. (B) Sag was significantly higher at the apical dendrite, but reduced by similar extents in adenosine at soma and dendrite. (C) Illustration of the experimental set up (green = control, red = adenosine).

### 5.2.9 Action Potential Back-propagation

The back-propagation of action potentials into the dendrites assists the integration of synaptic inputs and the induction of synaptic plasticity in cortical pyramidal neurons (Sjostrom and Hausser, 2006). The extent to which action potentials back-propagate may also play a role in the

generation of dendritic calcium spikes and burst firing (Williams and Stuart, 2000). Action potential back-propagation in CA1 pyramidal neurons is known to be modulated by muscarinic receptor activation (Tsubokawa and Ross, 1997). However Tsubokawa and Ross used stimuli evoked at regular intervals, whereas it is known (Williams and Stuart, 2000) that the extent of back-propagation is heavily dependent on the pattern of stimuli used.

Therefore I examined the extent to which adenosine modulated the back-propagation of action potentials evoked from my physiological like inputs. The dendritic electrode provided clean access to the dendritic voltage during the somatic current injection recordings (fig 5.10d).

Dendritic recordings taken at the site of apical dendrite bifurcation (240-580  $\mu\text{m}$ ) showed dramatic attenuation of back-propagating single action potentials (defined as action potentials arriving  $<18$  msec after the previous action potential). Mean amplitude underwent a significant (paired one-tailed t-test,  $P < 0.001$ ,  $n = 12$ ) attenuation from  $84.4 \pm 6.7$  mV measured at the soma (following voltage filtering) to  $24.9 \pm 11.6$  mV at the apical dendrite recording electrode. As well as the attenuation in amplitude, back-propagating action potentials (BAPs) showed significantly increased widths. BAPs were measured at their base rather than half-width to facilitate comparison between singles and bursts (which have  $\geq 2$  peaks). The width at AP base increased significantly (paired t-test,  $P < 0.001$ ,  $n = 12$ ) from  $1.7 \pm 0.2$  ms at the soma, to  $13.9 \pm 4$  ms at the apical dendrite bifurcation.

High frequency action potential bursts tend to summate supra-linearly as they back-propagate into the apical dendrite of pyramidal neurons

(Williams and Stuart, 2000). I also observed this phenomenon in my recordings and in order to account for the summation, the burst was treated as a single event. Back-propagating bursts of action potentials reached significantly higher peak voltages than isolated spikes ( $-3.55 \pm 14.75$  mV at the dendrite, compared to  $-25.67 \pm 13.85$  mV at the soma, Wilcoxon matched pairs,  $P < 0.001$ ,  $n = 11$ ).

The application of adenosine ( $100 \mu\text{M}$ ) resulted in a significant increase in the membrane filtering of BAPs, however the extent of the changes differed between single spikes and bursts. For single isolated spikes the addition of adenosine resulted in a significant narrowing of BAP width (from  $13.9 \pm 4$  ms to  $10.2 \pm 2.6$  ms,  $P = 0.006$ , paired two-tailed t-test,  $n = 11$ ) and integral (from  $136.4 \pm 76.1$  mVms to  $108.4 \pm 52.8$  mVms,  $P = 0.01$ , paired two-tailed t-test,  $n = 11$ ). However adenosine had no significant effect on the amplitude of single BAPs (from  $24.8 \pm 11.6$  mV to  $24.4 \pm 13.8$  mV, paired two-tailed t-test,  $P = 0.776$ ,  $n = 11$ ). Thus adenosine produced a significant narrowing of BAPs, without affecting peak amplitude (fig 5.10).

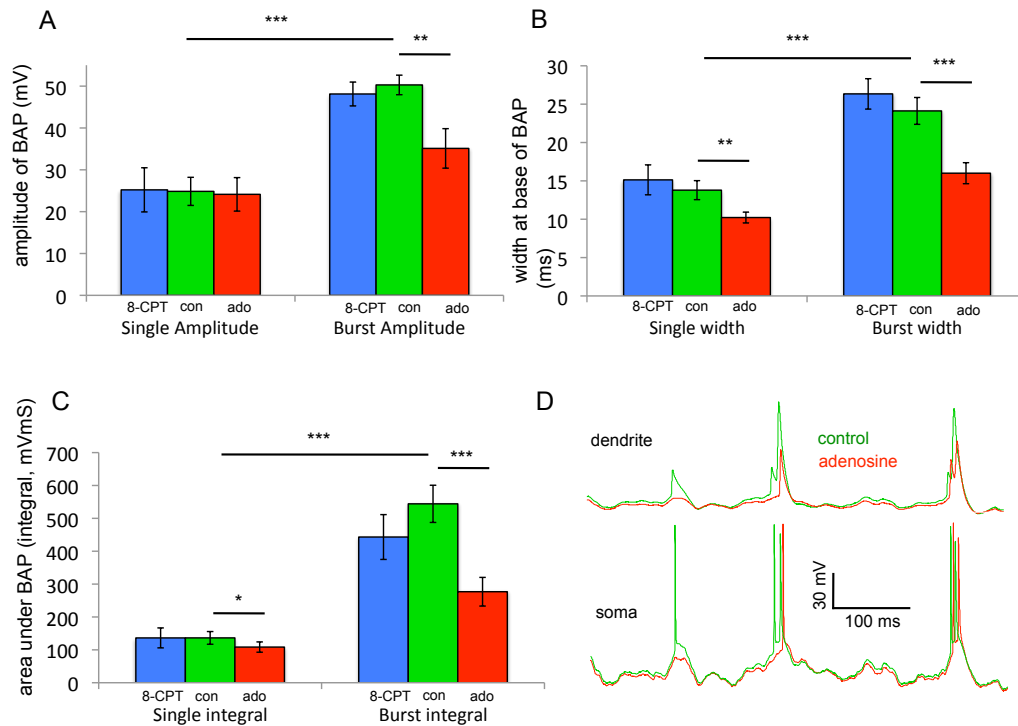


**Fig 5.10** Increased attenuation of back-propagating action potentials (BAPs) in adenosine. (A) Bursts of BAPs summated in the dendrite. Adenosine significantly reduced the amplitude of bursts but not isolated BAPs. (B and C) The width and area under BAPs was significantly reduced in adenosine for both bursts and isolated BAPs. (D) Example trace of somatic action potentials and back propagations in dendrite in control (green) and adenosine (red). Adenosine reduced the amplitude of summated bursts, but not single APs.

The mean reduction in BAP bursts was higher than for single spikes and showed increased variation between neurons. The mean amplitude of BAP bursts was significantly reduced in adenosine (from  $50.3 \pm 12.6$  mV in control to  $35.1 \pm 16.4$  mV in adenosine, Wilcoxon matched pairs,  $P < 0.001$ ,  $n = 11$ ). Similarly the BAP width (from  $23.2 \pm 5.9$  ms,  $P < 0.001$ , paired two-tailed t-test,  $n = 11$ ) and integral (from  $544 \pm 198$  mVmS to  $276 \pm 129$  mVmS, paired two-tailed t-test,  $P < 0.001$ ,  $n = 11$ ) were also significantly reduced.

In 7 of the experiments, following adenosine wash 8-CPT ( $2 \mu\text{M}$ ) was added to the bath solution, before the experimental protocols were repeated. The BAP parameters in 8-CPT return to values similar to those in control conditions (fig 5.10).



### 5.3 Discussion

I have demonstrated that, through a combination of hyperpolarisation, an increase in action potential threshold and a reduction in input resistance, adenosine can powerfully suppress the firing of thick-tufted layer 5 pyramidal neurons. This study is to our knowledge the first investigation demonstrating post-synaptic actions for adenosine in the neocortex.

Although adenosine induced relatively small changes in membrane properties the effects were amplified in a dramatic reduction in firing of 63%.

This firing reduction was however not conserved across all frequencies. At low (1-7 Hz) initial firing frequencies adenosine induced a linear reduction in firing. At higher frequencies adenosine showed a diminished capacity to suppress firing. This saturation is notable because adenosine is known to be released in the cortex in response to high-frequency seizure activity (Dale and Frenguelli, 2009). These results suggest that it may have an only limited capacity to reduce firing through post-synaptic mechanisms in such situations.

The neurons in this study were selected under visual identification and identified using a DAB staining protocol as thick-tufted pyramidal neurons. Nevertheless I identified significant heterogeneity in the capacity for adenosine to reduce action potential bursting. These actions on bursting correlated with the magnitude of subthreshold changes (fig 5.6 c, d). Thick-tufted pyramidal neurons project to different regions of the brain including the superior colliculus, basal pons and spinal cord (Molnar and Cheung,

2006). It would be of significant interest to learn how these bursting properties and their modulation by adenosine correlate to the projection targets of these neurons.

In the previous chapter I demonstrated that an increased activation of  $A_1$  receptors during post-natal development plays a significant role in EPSP amplitude and variability at connections between these neurons. Here I show that this shift also occurs at post-synaptic  $A_1$  receptors (fig 5.7b).

However it does not appear that the shift is solely responsible for the change in membrane excitability seen during development. The decline in input resistance, in conjunction with the synaptic changes, may aid the pyramidal neuron network in transmitting information at higher frequencies later in post-natal development (Etherington and Williams, 2011).

By conducting dual recordings at the soma and apical dendrite I was able to demonstrate that contrary to my initial hypothesis adenosine maintained a similar extent of action between the two regions. There is evidence that the expression of both GIRK and HCN channels increases along the apical dendrite in these neurons, and that there is significant attenuation of voltage signals along its length. However, while I observed an increased  $I_h$  sag at the dendrite, it was reduced in adenosine by a similar proportion at both the soma and dendrite, and there was no change in the hyperpolarisation induced by adenosine between the soma and dendrite. These observations may be explained by a reduced expression of  $A_1$  receptors in the dendrite, and indeed Ochiishi *et al.*, 1999 demonstrate, using electron photomicrographs, that while  $A_1R$  immunoreactivity is strong in layer 5

pyramidal cell bodies, in dendrites immunoreactivity is weaker and more heterogeneous.

In spite of the identical sub-threshold actions at the apical dendrite and soma my results demonstrate that adenosine exerted a more powerful suppression of firing when current was injected at the apical dendrite. This may be explained by the increased distance the dendritic current must travel to the axon.

The back-propagation of action potentials into pyramidal dendrites is thought to play important roles in signalling the activity state of the neuron. The reliability of dendritic back-propagation is heavily history dependent (Williams and Stuart, 2000). This occurs due to the supralinear summation of high-frequency bursts of action potentials. My data demonstrates that this summation is weakened in the presence of adenosine. While the amplitude of isolated BAPs was maintained in adenosine, back-propagating bursts showed a significantly reduction (fig 5.10a).

There is evidence that back-propagating action potentials are important for the induction of long-term plasticity (Markram *et al.*, 1997; Czarnecki *et al.*, 2007). In this manner adenosine may modify the dominant direction of long-term plasticity at synapses located along the apical dendritic tree.

Considering adenosine's importance in the modulation of sleep in the cortex (Porkka-Heiskanen *et al.*, 2002) this hypothesis suggests a direction for future research.

The data provide further support for the utility of the EIF model, with refractory properties, in the accurate prediction of spike times. There is an extensive body of literature examining minimal models that predict sub-threshold dynamics and spiking outputs. These models are of importance because they are mathematically tractable and therefore suitable for analyses of network dynamics. Much of this previous research, in an effort to simplify the analysis has neglected the complex modulatory environment that neurons are subjected to *in vivo*. My results here show that, in the case of adenosine at least, these modulatory actions can be well captured within the parameters of these quantitative models. Finally, adenosine's variable impact of burst firing highlights the importance of considering these heterogeneities when investigating effects emerging at the level of the network.

## 6. General Discussion

The research documented in this thesis demonstrates that adenosine can produce profound changes in the properties of synaptic transmission and action potential firing in the thick-tufted layer 5 pyramidal neurons of the rat somatosensory cortex. In chapter 3 I demonstrate that adenosine powerfully suppresses synaptic transmission through a pre-synaptic mechanism. In chapter 4 I extend these findings to provide evidence that increased endogenous pre-synaptic A<sub>1</sub> receptor activation is plays a significant role in the early post-natal developmental changes that have been observed at this synapse. In chapter 5 I show that, as well as suppressing synaptic transmission adenosine also induces post-synaptic changes in membrane excitability, which acts to reduce both the frequency and temporal pattern of action potential firing in these neurons.

Given the magnitude of these changes and the pervasiveness of A<sub>1</sub> receptor activation by endogenous adenosine it is evident that the action of adenosine on these neurons is likely to have powerful implications for the dynamics of network activity in the neocortex and thus a number of physiological processes. While the actions of A<sub>1</sub> receptors have been documented at synapses and neurons across the brain, my results present a comprehensive picture of how this activation changes the functional properties of information transfer at a single identified neuron and synaptic pathway. This detailed examination will provide the groundwork for further study of adenosine's release, regulation and actions in the neocortex.

However the results as they stand already raise various important implications.

### 6.1 Adenosine and sleep in the neocortex

Increases in extracellular adenosine concentration in the brain are known to promote sleep, while blocking the effects of adenosine is known to promote wakefulness (Bjorness and Greene, 2009). However the exact mechanisms by which adenosine modulates sleep remain poorly understood. Several areas of the brain are thought to be important, including the inhibition of cholinergic neurons in the basal forebrain by adenosine (Arrigoni *et al.*, 2006), and the hyperpolarisation of thalamic neurons, which results in increased bursting behaviour (Pape, 1992). Some recent studies suggest that changes in adenosine levels in the neocortex are also likely to play a significant role, and my results suggest mechanisms through which this may occur. While A<sub>1</sub> receptors are known to be expressed on neocortical pyramidal neurons data has been lacking on the functional impacts of A<sub>1</sub> receptor activation on synaptic transmission and action potential firing on these neurons therefore the results presented in this thesis have important implications for our understanding of how adenosine regulates sleep.

Slow-wave sleep is characterised by synchronised bursts of synaptic induced depolarisations and action potential firing in neurons interspersed by periods of low synaptic drive (Sanchez-Vives and McCormick, 2000). The power of this slow-wave activity increases with sleep deprivation in wild-type but not mice lacking the A<sub>1</sub> receptor (Bjorness and Greene, 2009).

Other evidence also suggests that adenosine can modulate the power of

slow-wave activity during sleep (the LFP or EEG correlate of up and down-states). However there are conflicting reports as to precisely how this occurs. Both A<sub>1</sub> receptor agonists (CPA, Benington *et al.*, 1995) and antagonists (8-CPT, Schmitt *et al.*, 2012) have been shown to enhance slow-wave power. It is possible that these conflicting results reflect the different scales of measurement and regions of the brain that were probed, with the Benington study using cortical EEG, while Schmitt used hippocampal LFP.

My results demonstrate that adenosine transforms synaptic transmission at this synapse from being dominated by short-term depression to weak facilitation (figure 3.4). There is recent theoretical evidence (De Pitta *et al.*, 2011) that an increase in short-term facilitation can indeed aid the generation of slow oscillatory activity due to an increased tendency for neuronal firing at the transition of Down to Up-states. Experiments in slices of ferret cortex have also observed an increase in short-term facilitation during up-states (Reig and Sanchez-Vives, 2007). This raises the possibility that an agent affecting pre-synaptic transmitter release, such as adenosine, may be involved in the transition from down to up-state activity.

Another intriguing aspect of adenosines modulation of these neurons is the reduction in the proportion of action potentials being fired in bursts in a sub-population of cells (figure 5.6). During sleep these neurons have a tendency to fire short bursts of action potentials during up-states.

It is therefore interesting that in this study burst firing was modulated only in a sub-population of neurons studied. It is possible that this reflects a means by the network of switching the pattern of activity during periods of

high extracellular adenosine concentration by increasing the relative influence of the cells that did not reduce bursting in adenosine. However more research would be required to examine this hypothesis. An alternative explanation for the differential modulation of bursting may be linked to the fact that the dendritic back-propagation of bursts of action potentials was severely reduced in many neurons (figure 5.10). These dendritic back-propagations are believed to play an important role in the direction of long-term plasticity changes at synapses on the dendrite. Thus it is possible that the altered temporal pattern of action potentials observed in adenosine in some neurons may have a different impact on long-term plasticity changes than in neurons where the temporal pattern of action potentials remained the same in adenosine. More research is required to first examine whether these changes in back-propagation affect plasticity and second to determine whether the differential effect on bursting between neurons translates into altered effects of adenosine on plasticity.

One of the most surprising aspects of this research was the observation that reciprocal synapses were just as likely to differ in the degree of tonic activation of A<sub>1</sub> receptors by endogenous adenosine as synapses from different individuals (figure 4.8). This result tells us that the level of A<sub>1</sub> receptor activation can be regulated locally. During sleep deprivation the extracellular concentration of adenosine is known to rise in the cortex (Porkka-Heiskanen *et al.*, 2000). However it has been previously unclear the extent to which this rise varies locally. The biosensor experiments in this thesis suggested that there is no global rise in extracellular adenosine



during development (figure 4.7) even though the average level of A<sub>1</sub> receptor activation rises at the synapse. I found no evidence of any change in the properties of A<sub>1</sub> receptors during development (figure 4.3 and 4.4), and the concentration response data suggests that it is only the extracellular concentration of adenosine at the synapse that changes during development (figure 4.5). With respect to sleep these results raise the possibility that during sleep deprivation it is adenosine increases at key synapses that may drive the increased power in the delta (1-4 Hz) frequency during slow-wave sleep EEGs.

The increased delta power may reflect an increased proportion of the network engaging in slow-wave activity. Recent evidence suggests that slow-wave oscillations can occur sporadically during restful waking periods (Vyazovskiy *et al.*, 2011). Although it is as yet unclear the mechanism by which these neurons transfer into this sleep-like activity, the research highlights the fact that important aspects of sleep can occur at the local level. That tonic adenosine can similarly be regulated locally raises the possibility that increases in endogenous adenosine at individual synapses may help provide the drive for these local transitions to sleep-like oscillatory behaviour.

### 6.2 Adenosine and homeostatic modulation

ATP and adenosine play essential roles in energy maintenance in all living cells and both play key roles in extracellular signalling. The ubiquity of adenosine across the brain allows it to play a key role in many physiological

processes. One role that is currently subject to intensive research is in homeostatic plasticity at synapses and neurons.

Homeostatic plasticity acts as a counterpoint to Hebbian plasticity in the brain in order to prevent runaway changes in synaptic strength and neuronal firing (Turrigiano, 1999). Several forms of homeostatic plasticity are known to exist in the rodent neocortex, such as the activity dependent regulation of intrinsic neuronal properties, the balancing of inhibitory and excitatory inputs, metaplasticity (adjusting the ability of synapses to undergo plasticity) and synaptic scaling.

While the research in this thesis has not directly investigated the role of adenosine in homeostatic plasticity changes, one result in particular may have important implications for this field of research. My data indicates that the synaptic effects of adenosine are subject to highly local spatial regulation. The data illustrated in figure 4.8 indicates that A<sub>1</sub> receptor activation can vary significantly between reciprocal synapses. This raises the possibility that synapses connecting different neurons to the same pre-synaptic neuron may also be subject to differential regulation by the adenosine tone – a scenario that could allow neurons to use the local adenosine tone to control action potential firing via synaptic scaling (Dias *et al.*, 2013).

### 6.3 Tonic and phasic A<sub>1</sub> receptor activation

One of the most striking findings of this research was the extent to which the extent to which the level of endogenous A<sub>1</sub> receptor activation can differ

between synapses while the overall effect of A<sub>1</sub> receptor activation at the synapse (measured as the EPSP amplitude ratio between 100μM adenosine, and 2μM 8-CPT) showed little difference between synapses or across development. These factors meant that the effect of applied adenosine was largely dependent on the level of tonic endogenous activation of A<sub>1</sub> receptors i.e. on occasions when the effect of applied adenosine (compared to control) was small, the application of 8-CPT revealed this to be due to the already high level of A<sub>1</sub> receptor activation in control.

There is experimental evidence (Pascual *et al.*, 2005) that suggests astrocytes can release ATP (rapidly metabolised to adenosine) in two different modes – tonic release that results in persistent synaptic suppression, and phasic release, which modulates synapses as a result of activity-dependent recruitment of astrocytes. While I did not investigate the circumstances of phasic ATP (adenosine) release, the heterogeneity in tonic A<sub>1</sub> receptor activation across synapses meant that the impact of bath-applied adenosine (analogous to phasic release) could be qualitatively different across different connections with respect to the impact on synaptic dynamics. For example connections that were recorded with a large tone of endogenous adenosine tended to display EPSP trains with sustained amplitudes or slight facilitation and the addition of bath-applied adenosine suppressed each EPSP by roughly the same amount (e.g. mature connection, fig 4.5). Connections with a low endogenous adenosine tone tended to exhibit significant short-term depression, resulting in a much more

significant depression of the initial EPSPs in a train (e.g. juvenile connection, fig 4.5).

Given the computation potential in the expression of synaptic dynamics (Abbott and Regehr, 2004) this phenomenon suggests that activity-dependent phasic adenosine release may be able to act in several distinct ways upon a synapses, depending on the initial level of tonic adenosine.

#### 6.4 Modelling the effects of neuromodulation

One of the major aims of this thesis was to determine the extent to which simple models can reliably capture the synaptic and neuronal changes produced by adenosine. I have shown that the change in dynamics could be reliably captured as a reduction in the fraction of resources utilised in a phenomenological model of synaptic dynamics and that adenosine induced small changes in the sub-threshold parameters of an integrate-and-fire model that could precisely predict action potential firing.

In recent years neuronal firing and fast synaptic transmission have been subject to a great degree of quantitative study and a lot of emphasis has been placed on the generation of models that can accurately account for the intricacies of these phenomena at the minimum level of complexity (Tsodyks and Markram, 1997; Varela *et al.*, 1997; Fourcaud-Trocme *et al.*, 2003; Badel *et al.*, 2008). Less emphasis has been placed on quantitative characterisations of neuromodulatory processes, partly due to the relative lack of data on the release and diffusion of these molecules in neural tissue. Several recent studies have however shown that some of these aspects of

neuromodulation can be captured quantitatively (Klyuch *et al.*, 2011) and incorporated into models of neuronal computation and plasticity (Chorley and Seth, 2011).

My research demonstrates that aspects of the synaptic and action potential firing impacts of neuromodulation can be captured by parameter modifications of simple existing tractable models. Often, the effects of neuromodulators are generalised when considered in quantitative network models (De Pitta *et al.*, 2011). The data in this thesis illustrates that these modulatory effects must be considered with respect to the complex history dependence of synaptic transmission and action potential firing in individual neurons.

## 7. Conclusions and Future Perspectives

### 7.1 Conclusions

Neurons communicate under the constant influence of a wide variety of modulatory chemicals that subtly alter the way in which information is integrated within the neuron and transferred across the synapse. If we are to understand how networks of neurons interact to produce the complex emergent dynamics observed at larger scales in the brain it will be necessary to understand how the action of modulators affects this information at the level of individual neurons and synapses. It is clear that given the enormous complexity of these circuits an important part of this understanding will arrive only from quantitative analyses of these modulatory interactions.

In recent years many aspects of neocortical micro-circuitry and synaptic transmission have been elucidated using paired intracellular recordings taken from isolated brain slices. I aimed in this body of work to examine how adenosine modulates the properties of communication at one location in this circuit. By focusing on a single neuron I have been able to provide a more detailed analysis of adenosine's actions than has often been presented in past research. In doing so I have been able to demonstrate that aspects of adenosine's actions can be accurately quantified in simple tractable models. The intention has not been to develop complex biophysical models that account for mechanistic intracellular interactions but rather to accurately reproduce the modulatory changes using the minimal level of quantitative

description in order to best facilitate future analyses at the level of the circuit.

My results demonstrate that the dramatic reduction of firing observed in response to naturalistic current inputs can be captured within the parameters of a simple rEIF model derived from a dynamic I-V curve measured during ongoing activity (chapter 5). At connections between thick-tufted layer 5 pyramidal neurons I have shown that adenosine produces a dramatic shift in synaptic dynamics that can be captured as a reduction only in the probability of release in a simple model. By conducting experiments across three developmental periods I have shown that increased activation of  $A_1$  receptors by endogenous adenosine is responsible for the well-known changes in synaptic dynamics and the reliability of transmission that occur during post-natal development (chapter 4). While assumptions of simple binomial independence in transmitter release have previously been used to describe the variability of transmission at cortical synapses I have presented evidence that when  $A_1$  receptors are activated failures of release do not occur independently and binomial model based analysis can no longer describe the variability in transmitter release (chapter 3).

Through this body of work I have demonstrated that to understand the role of neuromodulation requires a consideration of how information is transferred in neural circuits. When compared to studies conducted on neurons in other parts of the CNS adenosine produced a relatively minor hyperpolarisation and reduction in input resistance in thick-tufted layer 5

pyramidal neurons. However these changes were sufficient to cause a large suppression of firing output. By using naturalistic noisy inputs I have also shown how adenosine can alter burst firing in some neurons as well as selectively suppressing the dendritic back-propagation of bursts of action potentials. This is likely to have profound implications for network dynamics and long-term plasticity. Likewise, by conducting paired recordings I have been able to demonstrate that adenosine alters the reliability of synaptic transmission in a complex manner than will require more work to fully understand.

I have deliberately placed more focus on the physiological outcomes of adenosine modulation as opposed to the biophysical mechanisms behind the modulation. Much previous research has focused on detailing the intracellular pathways that are activated in response to adenosine receptor activation, my aim has been to contextualise the effects of adenosine within an active area of research into the functional properties of neocortical synaptic transmission and microcircuitry. Although some care should be taken when extrapolating *in vitro* electrophysiology to the situation *in vivo* (where ongoing neuronal activity will increase membrane conductances and alter synaptic transmission) the major principals, if not the exact quantification of model parameters, will hold.

## 7.2 Future perspectives

In this work I have focused on one network of pyramidal neurons in layer 5. These neurons provide outputs to other regions of the brain and play a vital role in the generation of up-states during sleep (Beltramo *et al.*, 2013). To



gain a full picture of how adenosine modulates neocortical network dynamics it will be important to fully understand how neurons and synapses are modulated across the neocortical microcircuit. I have conducted preliminary experiments demonstrating that adenosine pre-synaptically suppresses glutamergic synapses onto inhibitory interneurons (both fast spiking and adapting) in layer 5. I have also identified a small suppression of GABAergic synapses onto pyramidal neurons. Interneurons in the neocortex display a diverse variety of morphological, electrophysiological and molecular properties that are not yet completely understood. Nevertheless it is vital that these preliminary investigations are taken further to learn more about how the modulation of different pathways interacts to affect neural activity at the level of the network. Eventually, with a complete picture of how adenosine modulates the different neurons and canonical synaptic pathways in the neocortex, the utilisation of quantitative models could help probe what causative roles adenosine plays in driving network activity on larger scales.

In chapter 3 I presented evidence that the variability of synaptic transmission during  $A_1$  receptor activation cannot be captured by a simple binomial model of independent release. In control conditions, however, the model prediction of quantal amplitude was close to that measured from aEPSPs indicating that the release statistics matched predictions that assume independent release. More experimental and modelling work is required to fully understand how the variability in transmission develops in adenosine. It would also be interesting to extend this work to other pre-

synaptic modulators such as acetylcholine (via muscarinic receptors) and GABA (via GABA<sub>B</sub> receptors) to examine whether they can induce the same changes in the variability in transmitter release.

In chapter 4 I presented evidence that the developmental changes in synaptic dynamics and reliability at thick-tufted layer 5 pyramidal synapses are mediated by an increased tone of endogenous adenosine. This raises the obvious question of where the increased adenosine comes from and how the larger tone is maintained at the synapse. Recent publications have presented diverging pictures as to how this tone arrives in the extracellular environment, whether directly from neurons (Lovatt *et al.*, 2012) or via the metabolism of ATP released from astrocytes (Schmitt *et al.*, 2012). Also, given the efficiency with which adenosine is itself metabolised once in the extracellular environment, the regulation of enzymes involved in the metabolism of adenosine are likely to play a key role in the maintenance of the tone. Experiments utilising genetic inhibition of key enzymes could provide insights into the mechanisms that regulate the endogenous tone that I have observed.

In chapter 5 my observations that adenosine selectively suppresses the back-propagation of bursts of action potentials raises questions as to what impact this will have on the induction of long-term plasticity. The direction of long-term plasticity in layer 5 pyramidal neurons has been shown to depend on the temporal pattern of back-propagating action potentials (Czarnecki *et al.*, 2007) with high-frequency bursts inducing potentiation (LTP) and isolated spikes inducing depression (LTD). Adenosine is likely to

modify these rules and thus may play an important role in homeostatic plasticity, which is thought to be an important function of sleep – a hypothesis that is subject to active debate (Born and Feld, 2012).

Recent advances in optogenetics have led to the development of optically activated GPCRs (optoXRs, Airan *et al.*, 2009). Although still in their infancy the development of optically activated receptors that mimic adenosine receptor activation at particular locations on specific neurons would offer unparalleled temporal control over experiments probing adenosine's role in network dynamics. However given the highly local nature of endogenous A<sub>1</sub> receptor activation that I have observed in this work, care would have to be taken in the interpretation of experiments using optical stimulation.

Adenosine acts as a ubiquitous modulator of neural activity across the brain. Although it has not seen the same intensity of research interest as brainstem modulators it is perhaps just as important to the functioning of a healthy brain. It is striking, given the depth of research into neocortical functionality in recent years that research into adenosine has been largely absent in this area. Great challenges remain in understanding how adenosine interacts with neurons in the neocortex – both in terms of its release and regulation in the extracellular space and also its direct actions on neurons and synapses. It is likely that, given the complexity of the neocortical circuit and the diversity in neuronal architecture, quantitative modelling will play a key role in helping understand fully the roles adenosine plays in this region of the brain. This has become increasingly recognised in the study of neocortical function as a whole and it is now time

to begin integrating the subtle actions of neuromodulators into this research.

## 8. References

Abbott L. F., Varela J. A., Sen K., and Nelson S. B. (1997). Synaptic depression and cortical gain control. *Science* **275**, 220-224.

Abbott L. F., and Regehr W. G. (2004). Synaptic computation. *Nature* **431**, 796-803.

Airan R. D., Thompson K. R., Fenno L. E., Bernstein H., and Deisseroth K. (2009). Temporally precise in vivo control of intracellular signalling. *Nature* **458**, 1025-1029.

Arrigoni E., Chamberlin N. L., Saper C. B., and McCarley R. W. (2006). Adenosine inhibits basal forebrain cholinergic and noncholinergic neurons in vitro. *Neuroscience* **140**, 403-413.

Badel L., Lefort S., Brette R., Petersen C. C., Gerstner W., and Richardson M. J. (2008). Dynamic I-V curves are reliable predictors of naturalistic pyramidal-neuron voltage traces. *J Neurophysiol* **99**, 656-666.

Barth A. L., and Poulet J. F. Experimental evidence for sparse firing in the neocortex. *Trends Neurosci* **35**, 345-355.

Beierlein M., Gibson J. R., and Connors B. W. (2000). A network of electrically coupled interneurons drives synchronized inhibition in neocortex. *Nat Neurosci* **3**, 904-910.

Beltramo R., D'Urso G., Dal Maschio M., Farisello P., Bovetti S., Clovis Y., Lassi G., Tucci V., De Pietri Tonelli D., and Fellin T. (2013) Layer-specific excitatory circuits differentially control recurrent network dynamics in the neocortex. *Nat Neurosci* **16**, 227-234.

Benington J. H., Kodali S. K., and Heller H. C. (1995). Stimulation of A1 adenosine receptors mimics the electroencephalographic effects of sleep deprivation. *Brain Res* **692**, 79-85.

Berger T., Larkum M. E., and Luscher H. R. (2001). High I(h) channel density in the distal apical dendrite of layer V pyramidal cells increases bidirectional attenuation of EPSPs. *J Neurophysiol* **85**, 855-868.

Bjorness T. E., and Greene R. W. (2009). Adenosine and sleep. *Curr Neuropharmacol* **7**, 238-245.

Bjorness T. E., Kelly C. L., Gao T., Poffenberger V., and Greene R. W. (2009). Control and function of the homeostatic sleep response by adenosine A1 receptors. *J Neurosci* **29**, 1267-1276.

- Blazynski C. (1987). Adenosine A1 receptor-mediated inhibition of adenylate cyclase in rabbit retina. *J Neurosci* **7**, 2522-2528.
- Boison D. (2006). Adenosine kinase, epilepsy and stroke: mechanisms and therapies. *Trends Pharmacol Sci* **27**, 652-658.
- Boison D. (2008). Adenosine as a neuromodulator in neurological diseases. *Curr Opin Pharmacol* **8**, 2-7.
- Born J., and Feld G. B. (2012) Sleep to upscale, sleep to downscale: balancing homeostasis and plasticity. *Neuron* **75**, 933-935.
- Bremaud A., West D. C., and Thomson A. M. (2007). Binomial parameters differ across neocortical layers and with different classes of connections in adult rat and cat neocortex. *Proc Natl Acad Sci U S A* **104**, 14134-14139.
- Briggs F. (2010) Organizing principles of cortical layer 6. *Front Neural Circuits* **4**, 3.
- Bruno R. M., and Simons D. J. (2002). Feedforward mechanisms of excitatory and inhibitory cortical receptive fields. *J Neurosci* **22**, 10966-10975.
- Callaway J. C., and Ross W. N. (1995). Frequency-dependent propagation of sodium action potentials in dendrites of hippocampal CA1 pyramidal neurons. *J Neurophysiol* **74**, 1395-1403.
- Canals M., Marcellino D., Fanelli F., Ciruela F., de Benedetti P., Goldberg S. R., Neve K., Fuxe K., Agnati L. F., Woods A. S., et al. (2003). Adenosine A2A-dopamine D2 receptor-receptor heteromerization: qualitative and quantitative assessment by fluorescence and bioluminescence energy transfer. *J Biol Chem* **278**, 46741-46749.
- Caporale N., and Dan Y. (2008). Spike timing-dependent plasticity: a Hebbian learning rule. *Annu Rev Neurosci* **31**, 25-46.
- Cass C. E., Young J. D., and Baldwin S. A. (1998). Recent advances in the molecular biology of nucleoside transporters of mammalian cells. *Biochem Cell Biol* **76**, 761-770.
- Chagnac-Amitai Y., Luhmann H. J., and Prince D. A. (1990). Burst generating and regular spiking layer 5 pyramidal neurons of rat neocortex have different morphological features. *J Comp Neurol* **296**, 598-613.
- Chauvette S., Volgushev M., and Timofeev I. Origin of active states in local neocortical networks during slow sleep oscillation. *Cereb Cortex* **20**, 2660-2
- Cheetham C. E., and Fox K. Presynaptic development at L4 to l2/3 excitatory synapses follows different time courses in visual and somatosensory cortex. *J Neurosci* **30**, 12566-12571.

Chen C. C., Abrams S., Pinhas A., and Brumberg J. C. (2009). Morphological heterogeneity of layer VI neurons in mouse barrel cortex. *J Comp Neurol* **512**, 726-746.

Choi S., and Lovinger D. M. (1997). Decreased probability of neurotransmitter release underlies striatal long-term depression and postnatal development of corticostriatal synapses. *Proc Natl Acad Sci U S A* **94**, 2665-2670.

Chorley P., and Seth A. K. (2011) Dopamine-signaled reward predictions generated by competitive excitation and inhibition in a spiking neural network model. *Front Comput Neurosci* **5**, 21.

Clark B. D., Kurth-Nelson Z. L., and Newman E. A. (2009). Adenosine-evoked hyperpolarization of retinal ganglion cells is mediated by G-protein-coupled inwardly rectifying K<sup>+</sup> and small conductance Ca<sup>2+</sup>-activated K<sup>+</sup> channel activation. *J Neurosci* **29**, 11237-11245.

Compte A., Sanchez-Vives M. V., McCormick D. A., and Wang X. J. (2003). Cellular and network mechanisms of slow oscillatory activity (<1 Hz) and wave propagations in a cortical network model. *J Neurophysiol* **89**, 2707-2725.

Constantinople C. M., and Bruno R. M. (2011) Effects and mechanisms of wakefulness on local cortical networks. *Neuron* **69**, 1061-1068.

Connors B. W., and Gutnick M. J. (1990). Intrinsic firing patterns of diverse neocortical neurons. *Trends Neurosci* **13**, 99-104.

Craig C. G., and White T. D. (1993). N-methyl-D-aspartate- and non-N-methyl-D-aspartate-evoked adenosine release from rat cortical slices: distinct purinergic sources and mechanisms of release. *J Neurochem* **60**, 1073-1080.

Crunelli V., Lorincz M. L., Errington A. C., and Hughes S. W. (2011) Activity of cortical and thalamic neurons during the slow (<1 Hz) rhythm in the mouse in vivo. *Pflugers Arch* **463**, 73-88.

Cunha R. A. (2005). Neuroprotection by adenosine in the brain: From A(1) receptor activation to A (2A) receptor blockade. *Purinergic Signal* **1**, 111-134.

Cunha R. A., Milusheva E., Vizi E. S., Ribeiro J. A., and Sebastiao A. M. (1994). Excitatory and inhibitory effects of A1 and A2A adenosine receptor activation on the electrically evoked [3H]acetylcholine release from different areas of the rat hippocampus. *J Neurochem* **63**, 207-214.

- Cunha R. A., and Sebastiao A. M. (1991). Extracellular metabolism of adenine nucleotides and adenosine in the innervated skeletal muscle of the frog. *Eur J Pharmacol* **197**, 83-92.
- Czarnecki A., Birtoli B., and Ulrich D. (2007). Cellular mechanisms of burst firing-mediated long-term depression in rat neocortical pyramidal cells. *J Physiol* **578**, 471-479.
- Dale N., Hatz S., Tian F., and Llaudet E. (2005). Listening to the brain: microelectrode biosensors for neurochemicals. *Trends Biotechnol* **23**, 420-428.
- Dale N., and Frenguelli B. G. (2009). Release of adenosine and ATP during ischemia and epilepsy. *Curr Neuropharmacol* **7**, 160-179.
- de Mendonca A., Sebastiao A. M., and Ribeiro J. A. (2000). Adenosine: does it have a neuroprotective role after all? *Brain Res Brain Res Rev* **33**, 258-274.
- De Pitta M., Volman V., Berry H., and Ben-Jacob E. (2011) A tale of two stories: astrocyte regulation of synaptic depression and facilitation. *PLoS Comput Biol* **7**, e1002293.
- Defelipe J., Markram H., and Rockland K. S. (2012) The neocortical column. *Front Neuroanat* **6**, 22.
- Dias R. B., Rombo D. M., Ribeiro J. A., Henley J. M., and Sebastiao A. M. (2013) Adenosine: setting the stage for plasticity. *Trends Neurosci* **36**, 248-257.
- Diekelmann S., and Born J. The memory function of sleep. *Nat Rev Neurosci* **11**, 114-126.
- Diogenes M. J., Neves-Tome R., Fucile S., Martinello K., Scianni M., Theofilas P., Lopatar J., Ribeiro J. A., Maggi L., Frenguelli B. G., et al. Homeostatic Control of Synaptic Activity by Endogenous Adenosine is Mediated by Adenosine Kinase. *Cereb Cortex*.
- Dixon A. K., Gubitza A. K., Sirinathsinghji D. J., Richardson P. J., and Freeman T. C. (1996). Tissue distribution of adenosine receptor mRNAs in the rat. *Br J Pharmacol* **118**, 1461-1468.
- Dunwiddie T. V., and Diao L. (1994). Extracellular adenosine concentrations in hippocampal brain slices and the tonic inhibitory modulation of evoked excitatory responses. *J Pharmacol Exp Ther* **268**, 537-545.
- Dunwiddie T. V., and Haas H. L. (1985). Adenosine increases synaptic facilitation in the in vitro rat hippocampus: evidence for a presynaptic site of action. *J Physiol* **369**, 365-377.



- Dunwiddie T. V., and Masino S. A. (2001). The role and regulation of adenosine in the central nervous system. *Annu Rev Neurosci* **24**, 31-55.
- Edwards F. A., Gibb A. J., and Colquhoun D. (1992). ATP receptor-mediated synaptic currents in the central nervous system. *Nature* **359**, 144-147.
- Etherington S. J., and Williams S. R. (2011) Postnatal development of intrinsic and synaptic properties transforms signaling in the layer 5 excitatory neural network of the visual cortex. *J Neurosci* **31**, 9526-9537.
- Faber D. S., and Korn H. (1991). Applicability of the coefficient of variation method for analyzing synaptic plasticity. *Biophys J* **60**, 1288-1294.
- Feldmeyer D., Lubke J., Silver R. A., and Sakmann B. (2002). Synaptic connections between layer 4 spiny neurone-layer 2/3 pyramidal cell pairs in juvenile rat barrel cortex: physiology and anatomy of interlaminar signalling within a cortical column. *J Physiol* **538**, 803-822.
- Feldmeyer D., Lubke J., and Sakmann B. (2006). Efficacy and connectivity of intracolumnar pairs of layer 2/3 pyramidal cells in the barrel cortex of juvenile rats. *J Physiol* **575**, 583-602.
- Feldmeyer D., and Radnikow G. (2009). Developmental alterations in the functional properties of excitatory neocortical synapses. *J Physiol* **587**, 1889-1896.
- Fellin T., Halassa M. M., Terunuma M., Succol F., Takano H., Frank M., Moss S. J., and Haydon P. G. (2009). Endogenous nonneuronal modulators of synaptic transmission control cortical slow oscillations in vivo. *Proc Natl Acad Sci U S A* **106**, 15037-15042.
- Fontanez D. E., and Porter J. T. (2006). Adenosine A1 receptors decrease thalamic excitation of inhibitory and excitatory neurons in the barrel cortex. *Neuroscience* **137**, 1177-1184.
- Fourcaud-Trocme N., Hansel D., van Vreeswijk C., and Brunel N. (2003). How spike generation mechanisms determine the neuronal response to fluctuating inputs. *J Neurosci* **23**, 11628-11640.
- Fredholm B. B. (2010) Adenosine receptors as drug targets. *Exp Cell Res* **316**, 1284-1288.
- Fredholm B. B., Irenius E., Kull B., and Schulte G. (2001). Comparison of the potency of adenosine as an agonist at human adenosine receptors expressed in Chinese hamster ovary cells. *Biochem Pharmacol* **61**, 443-448.
- Fuhrmann G., Segev I., Markram H., and Tsodyks M. (2002). Coding of temporal information by activity-dependent synapses. *J Neurophysiol* **87**, 140-148.

- Gessi S, Merighi S, Varani K, Leung E, Mac Lennan S, and Borea P. A. (2008). The A3 adenosine receptor: an enigmatic player in cell biology. *Pharmacol Ther* **117**, 123-140.
- Gil Z., Connors B. W., and Amitai Y. (1997). Differential regulation of neocortical synapses by neuromodulators and activity. *Neuron* **19**, 679-686.
- Gonzalez-Burgos G., Kroener S., Zaitsev A. V., Povysheva N. V., Krimer L. S., Barrionuevo G., and Lewis D. A. (2008). Functional maturation of excitatory synapses in layer 3 pyramidal neurons during postnatal development of the primate prefrontal cortex. *Cereb Cortex* **18**, 626-637.
- Greene R. W., and Haas H. L. (1985). Adenosine actions on CA1 pyramidal neurones in rat hippocampal slices. *J Physiol* **366**, 119-127.
- Gu Q. (2002). Neuromodulatory transmitter systems in the cortex and their role in cortical plasticity. *Neuroscience* **111**, 815-835.
- Gur M., and Snodderly D. M. (2008). Physiological differences between neurons in layer 2 and layer 3 of primary visual cortex (V1) of alert macaque monkeys. *J Physiol* **586**, 2293-2306.
- Gvilia I., Suntsova N., Angara B., McGinty D., and Szymusiak R. (2011). Maturation of sleep homeostasis in developing rats: a role for preoptic area neurons. *Am J Physiol Regul Integr Comp Physiol* **300**, R885-894.
- Hardingham N. R., Read J. C., Trevelyan A. J., Nelson J. C., Jack J. J., and Bannister N. J. (2010) Quantal analysis reveals a functional correlation between presynaptic and postsynaptic efficacy in excitatory connections from rat neocortex. *J Neurosci* **30**, 1441-1451.
- Haas H. L., and Selbach O. (2000). Functions of neuronal adenosine receptors. *Naunyn Schmiedeberg's Arch Pharmacol* **362**, 375-381.
- Hasselmo M. E. (1995). Neuromodulation and cortical function: modeling the physiological basis of behavior. *Behav Brain Res* **67**, 1-27.
- Hempel C. M., Hartman K. H., Wang X. J., Turrigiano G. G., and Nelson S. B. (2000). Multiple forms of short-term plasticity at excitatory synapses in rat medial prefrontal cortex. *J Neurophysiol* **83**, 3031-3041.
- Hestrin S., and Armstrong W. E. (1996). Morphology and physiology of cortical neurons in layer I. *J Neurosci* **16**, 5290-5300.
- Horton J. C., and Adams D. L. (2005). The cortical column: a structure without a function. *Philos Trans R Soc Lond B Biol Sci* **360**, 837-862.

- Huang C. H., Bao J., and Sakaba T. (2010) Multivesicular release differentiates the reliability of synaptic transmission between the visual cortex and the somatosensory cortex. *J Neurosci* **30**, 11994-12004.
- Hubel D. H., and Wiesel T. N. (1962). Receptive fields, binocular interaction and functional architecture in the cat's visual cortex. *J Physiol* **160**, 106-154.
- Huston J. P., Haas H. L., Boix F., Pfister M., Decking U., Schrader J., and Schwarting R. K. (1996). Extracellular adenosine levels in neostriatum and hippocampus during rest and activity periods of rats. *Neuroscience* **73**, 99-107.
- Iwasaki S., Momiyama A., Uchitel O. D., and Takahashi T. (2000). Developmental changes in calcium channel types mediating central synaptic transmission. *J Neurosci* **20**, 59-65.
- Iwasaki S., and Takahashi T. (2001). Developmental regulation of transmitter release at the calyx of Held in rat auditory brainstem. *J Physiol* **534**, 861-871.
- Kampa B. M., Letzkus J. J., and Stuart G. J. (2006). Cortical feed-forward networks for binding different streams of sensory information. *Nat Neurosci* **9**, 1472-1473.
- Kampa B. M., Letzkus J. J., and Stuart G. J. (2006). Requirement of dendritic calcium spikes for induction of spike-timing-dependent synaptic plasticity. *J Physiol* **574**, 283-290.
- Karlen S. J., and Krubitzer L. (2006). The evolution of the neocortex in mammals: intrinsic and extrinsic contributions to the cortical phenotype. *Novartis Found Symp* **270**, 146-159; discussion 159-169.
- Kasper E. M., Larkman A. U., Lubke J., and Blakemore C. (1994). Pyramidal neurons in layer 5 of the rat visual cortex. I. Correlation among cell morphology, intrinsic electrophysiological properties, and axon targets. *J Comp Neurol* **339**, 459-474.
- Katzel D., Zemelman B. V., Buetfering C., Wolfel M., and Miesenbock G. (2011) The columnar and laminar organization of inhibitory connections to neocortical excitatory cells. *Nat Neurosci* **14**, 100-107.
- Kawamura M., Jr., Ruskin D. N., and Masino S. A. (2011) Metabolic autocrine regulation of neurons involves cooperation among pannexin hemichannels, adenosine receptors, and KATP channels. *J Neurosci* **30**, 3886-3895.
- Klyuch B. P., Richardson M. J., Dale N., and Wall M. J. (2011) The dynamics of single spike-evoked adenosine release in the cerebellum. *J Physiol* **589**, 283-295.

- Landolt H. P. (2008). Sleep homeostasis: a role for adenosine in humans? *Biochem Pharmacol* **75**, 2070-2079.
- Latini S., and Pedata F. (2001). Adenosine in the central nervous system: release mechanisms and extracellular concentrations. *J Neurochem* **79**, 463-484.
- Levy R. B., Reyes A. D., and Aoki C. (2006). Nicotinic and muscarinic reduction of unitary excitatory postsynaptic potentials in sensory cortex; dual intracellular recording in vitro. *J Neurophysiol* **95**, 2155-2166.
- Lovatt D., Xu Q., Liu W., Takano T., Smith N. A., Schnermann J., Tieu K., and Nedergaard M. (2012). Neuronal adenosine release, and not astrocytic ATP release, mediates feedback inhibition of excitatory activity. *Proc Natl Acad Sci U S A* **109**, 6265-6270.
- Letzkus J. J., Kampa B. M., and Stuart G. J. (2006). Learning rules for spike timing-dependent plasticity depend on dendritic synapse location. *J Neurosci* **26**, 10420-10429.
- Loebel A., Silberberg G., Helbig D., Markram H., Tsodyks M., and Richardson M. J. (2009). Multiquantal release underlies the distribution of synaptic efficacies in the neocortex. *Front Comput Neurosci* **3**, 27.
- Li Y., and Burke R. E. (2002). Developmental changes in short-term synaptic depression in the neonatal mouse spinal cord. *J Neurophysiol* **88**, 3218-3231.
- Li Y., Fan S., Yan J., Li B., Chen F., Xia J., Yu Z., and Hu Z. (2011) Adenosine modulates the excitability of layer II stellate neurons in entorhinal cortex through A1 receptors. *Hippocampus* **21**, 265-280.
- Llaudet E., Botting N. P., Crayston J. A., and Dale N. (2003). A three-enzyme microelectrode sensor for detecting purine release from central nervous system. *Biosens Bioelectron* **18**, 43-52.
- London M., and Hausser M. (2005). Dendritic computation. *Annu Rev Neurosci* **28**, 503-532.
- Lubke J., and Feldmeyer D. (2007). Excitatory signal flow and connectivity in a cortical column: focus on barrel cortex. *Brain Struct Funct* **212**, 3-17.
- Lund J. S. (1973). Organization of neurons in the visual cortex, area 17, of the monkey (*Macaca mulatta*). *J Comp Neurol* **147**, 455-496.
- Lupica C. R., Proctor W. R., and Dunwiddie T. V. (1992). Presynaptic inhibition of excitatory synaptic transmission by adenosine in rat hippocampus: analysis of unitary EPSP variance measured by whole-cell recording. *J Neurosci* **12**, 3753-3764.

- Markram H. (1997). A network of tufted layer 5 pyramidal neurons. *Cereb Cortex* **7**, 523-533.
- Markram H. (2006). The blue brain project. *Nat Rev Neurosci* **7**, 153-160.
- Markram H., Lubke J., Frotscher M., Roth A., and Sakmann B. (1997). Physiology and anatomy of synaptic connections between thick tufted pyramidal neurones in the developing rat neocortex. *J Physiol* **500 (Pt 2)**, 409-440.
- Markram H., Lubke J., Frotscher M., and Sakmann B. (1997). Regulation of synaptic efficacy by coincidence of postsynaptic APs and EPSPs. *Science* **275**, 213-215.
- Markram H., Toledo-Rodriguez M., Wang Y., Gupta A., Silberberg G., and Wu C. (2004). Interneurons of the neocortical inhibitory system. *Nat Rev Neurosci* **5**, 793-807.
- Markram H., Wang Y., and Tsodyks M. (1998). Differential signaling via the same axon of neocortical pyramidal neurons. *Proc Natl Acad Sci U S A* **95**, 5323-5328.
- Marshall L., Helgadottir H., Molle M., and Born J. (2006). Boosting slow oscillations during sleep potentiates memory. *Nature* **444**, 610-613.
- McCool B. A., and Farroni J. S. (2001). A1 adenosine receptors inhibit multiple voltage-gated Ca<sup>2+</sup> channel subtypes in acutely isolated rat basolateral amygdala neurons. *Br J Pharmacol* **132**, 879-888.
- McCormick D. A., Connors B. W., Lighthall J. W., and Prince D. A. (1985). Comparative electrophysiology of pyramidal and sparsely spiny stellate neurons of the neocortex. *J Neurophysiol* **54**, 782-806.
- McCormick D. A., and Contreras D. (2001). On the cellular and network bases of epileptic seizures. *Annu Rev Physiol* **63**, 815-846.
- Methippara M. M., Kumar S., Alam M. N., Szymusiak R., and McGinty D. (2005). Effects on sleep of microdialysis of adenosine A1 and A2a receptor analogs into the lateral preoptic area of rats. *Am J Physiol Regul Integr Comp Physiol* **289**, R1715-1723.
- Meyer H. S., Schwarz D., Wimmer V. C., Schmitt A. C., Kerr J. N., Sakmann B., and Helmstaedter M. (2011) Inhibitory interneurons in a cortical column form hot zones of inhibition in layers 2 and 5A. *Proc Natl Acad Sci U S A* **108**, 16807-16812.
- Miledi R. (1966). Strontium as a substitute for calcium in the process of transmitter release at the neuromuscular junction. *Nature* **212**, 1233-1234.

- Molnar Z., and Cheung A. F. (2006). Towards the classification of subpopulations of layer V pyramidal projection neurons. *Neurosci Res* **55**, 105-115.
- Mountcastle V. B., Davies P. W., and Berman A. L. (1957). Response properties of neurons of cat's somatic sensory cortex to peripheral stimuli. *J Neurophysiol* **20**, 374-407.
- Nevian T., Larkum M. E., Polsky A., and Schiller J. (2007). Properties of basal dendrites of layer 5 pyramidal neurons: a direct patch-clamp recording study. *Nat Neurosci* **10**, 206-214.
- Noudoost B., and Moore T. (2011) The role of neuromodulators in selective attention. *Trends Cogn Sci* **15**, 585-591.
- Ochiishi T., Chen L., Yukawa A., Saitoh Y., Sekino Y., Arai T., Nakata H., and Miyamoto H. (1999). Cellular localization of adenosine A1 receptors in rat forebrain: immunohistochemical analysis using adenosine A1 receptor-specific monoclonal antibody. *J Comp Neurol* **411**, 301-316.
- Packer A. M., and Yuste R. (2011) Dense, unspecific connectivity of neocortical parvalbumin-positive interneurons: a canonical microcircuit for inhibition? *J Neurosci* **31**, 13260-13271.
- Palchykova S., Winsky-Sommerer R., Shen H. Y., Boison D., Gerling A., and Tobler I. (2010). Manipulation of adenosine kinase affects sleep regulation in mice. *J Neurosci* **30**, 13157-13165.
- Pangrsic T., Potokar M., Stenovc M., Kreft M., Fabbretti E., Nistri A., Pryazhnikov E., Khiroug L., Giniatullin R., and Zorec R. (2007). Exocytotic release of ATP from cultured astrocytes. *J Biol Chem* **282**, 28749-28758.
- Pankratov Y., Lalo U., Verkhratsky A., and North R. A. (2006). Vesicular release of ATP at central synapses. *Pflugers Arch* **452**, 589-597.
- Pape H. C. (1992). Adenosine promotes burst activity in guinea-pig geniculocortical neurones through two different ionic mechanisms. *J Physiol* **447**, 729-753.
- Pascual O., Casper K. B., Kubera C., Zhang J., Revilla-Sanchez R., Sul J. Y., Takano H., Moss S. J., McCarthy K., and Haydon P. G. (2005). Astrocytic purinergic signaling coordinates synaptic networks. *Science* **310**, 113-116.
- Perin R., Berger T. K., and Markram H. (2011) A synaptic organizing principle for cortical neuronal groups. *Proc Natl Acad Sci U S A* **108**, 5419-5424.
- Polsky A., Mel B. W., and Schiller J. (2004). Computational subunits in thin dendrites of pyramidal cells. *Nat Neurosci* **7**, 621-627.

- Porkka-Heiskanen T., Strecker R. E., Thakkar M., Bjorkum A. A., Greene R. W., and McCarley R. W. (1997). Adenosine: a mediator of the sleep-inducing effects of prolonged wakefulness. *Science* **276**, 1265-1268.
- Porkka-Heiskanen T., Strecker R. E., and McCarley R. W. (2000). Brain site-specificity of extracellular adenosine concentration changes during sleep deprivation and spontaneous sleep: an in vivo microdialysis study. *Neuroscience* **99**, 507-517.
- Porkka-Heiskanen T., Alanko L., Kalinchuk A., and Stenberg D. (2002). Adenosine and sleep. *Sleep Med Rev* **6**, 321-332.
- Poskanzer K. E., and Yuste R. (2011) Astrocytic regulation of cortical UP states. *Proc Natl Acad Sci U S A* **108**, 18453-18458.
- Pozo K., and Goda Y. (2010) Unraveling mechanisms of homeostatic synaptic plasticity. *Neuron* **66**, 337-351.
- Proctor W. R., and Dunwiddie T. V. (1987). Pre- and postsynaptic actions of adenosine in the in vitro rat hippocampus. *Brain Res* **426**, 187-190.
- Rakic P. (2008). Confusing cortical columns. *Proc Natl Acad Sci U S A* **105**, 12099-12100.
- Ralevic V., and Burnstock G. (1998). Receptors for purines and pyrimidines. *Pharmacol Rev* **50**, 413-492.
- Rebola N., Sebastiao A. M., de Mendonca A., Oliveira C. R., Ribeiro J. A., and Cunha R. A. (2003). Enhanced adenosine A2A receptor facilitation of synaptic transmission in the hippocampus of aged rats. *J Neurophysiol* **90**, 1295-1303.
- Reig R., and Sanchez-Vives M. V. (2007). Synaptic transmission and plasticity in an active cortical network. *PLoS One* **2**, e670.
- Rex C. S., Kramar E. A., Colgin L. L., Lin B., Gall C. M., and Lynch G. (2005). Long-term potentiation is impaired in middle-aged rats: regional specificity and reversal by adenosine receptor antagonists. *J Neurosci* **25**, 5956-5966.
- Reyes A., and Sakmann B. (1999). Developmental switch in the short-term modification of unitary EPSPs evoked in layer 2/3 and layer 5 pyramidal neurons of rat neocortex. *J Neurosci* **19**, 3827-3835.
- Romand S., Wang Y., Toledo-Rodriguez M., and Markram H. (2011) Morphological development of thick-tufted layer v pyramidal cells in the rat somatosensory cortex. *Front Neuroanat* **5**, 5.

- Richardson M. J., and Silberberg G. (2008). Measurement and analysis of postsynaptic potentials using a novel voltage-deconvolution method. *J Neurophysiol* **99**, 1020-1031.
- Rubio-Garrido P., Perez-de-Manzo F., Porrero C., Galazo M. J., and Clasca F. (2009). Thalamic input to distal apical dendrites in neocortical layer 1 is massive and highly convergent. *Cereb Cortex* **19**, 2380-2395.
- Salgado H., Garcia-Oscos F., Martinolich L., Hall S., Restom R., Tseng K. Y., and Atzori M. (2012) Pre- and postsynaptic effects of norepinephrine on gamma-aminobutyric acid-mediated synaptic transmission in layer 2/3 of the rat auditory cortex. *Synapse* **66**, 20-28.
- Sanchez-Vives M. V., and McCormick D. A. (2000). Cellular and network mechanisms of rhythmic recurrent activity in neocortex. *Nat Neurosci* **3**, 1027-1034.
- Schiller J., Major G., Koester H. J., and Schiller Y. (2000). NMDA spikes in basal dendrites of cortical pyramidal neurons. *Nature* **404**, 285-289.
- Schiller J., Schiller Y., Stuart G., and Sakmann B. (1997). Calcium action potentials restricted to distal apical dendrites of rat neocortical pyramidal neurons. *J Physiol* **505 (Pt 3)**, 605-616.
- Schmitt L. I., Sims R. E., Dale N., and Haydon P. G. (2012) Wakefulness affects synaptic and network activity by increasing extracellular astrocyte-derived adenosine. *J Neurosci* **32**, 4417-4425.
- Schulte G., and Fredholm B. B. (2000). Human adenosine A(1), A(2A), A(2B), and A(3) receptors expressed in Chinese hamster ovary cells all mediate the phosphorylation of extracellular-regulated kinase 1/2. *Mol Pharmacol* **58**, 477-482.
- Schwindt P., and Crill W. (1999). Mechanisms underlying burst and regular spiking evoked by dendritic depolarization in layer 5 cortical pyramidal neurons. *J Neurophysiol* **81**, 1341-1354.
- Sebastiao A. M., Cunha R. A., de Mendonca A., and Ribeiro J. A. (2000). Modification of adenosine modulation of synaptic transmission in the hippocampus of aged rats. *Br J Pharmacol* **131**, 1629-1634.
- Sebastiao A. M., and Ribeiro J. A. (2009). Tuning and fine-tuning of synapses with adenosine. *Curr Neuropharmacol* **7**, 180-194.
- Seol G. H., Ziburkus J., Huang S., Song L., Kim I. T., Takamiya K., Huganir R. L., Lee H. K., and Kirkwood A. (2007). Neuromodulators control the polarity of spike-timing-dependent synaptic plasticity. *Neuron* **55**, 919-929.



- Silberberg G., Gupta A., and Markram H. (2002). Stereotypy in neocortical microcircuits. *Trends Neurosci* **25**, 227-230.
- Silberberg G., Grillner S., LeBeau F. E., Maex R., and Markram H. (2005). Synaptic pathways in neural microcircuits. *Trends Neurosci* **28**, 541-551.
- Silberberg G., and Markram H. (2007). Disynaptic inhibition between neocortical pyramidal cells mediated by Martinotti cells. *Neuron* **53**, 735-746.
- Simons D. J. (1978). Response properties of vibrissa units in rat SI somatosensory neocortex. *J Neurophysiol* **41**, 798-820.
- Sjostrom P. J., and Hausser M. (2006). A cooperative switch determines the sign of synaptic plasticity in distal dendrites of neocortical pyramidal neurons. *Neuron* **51**, 227-238.
- Sjostrom P. J., and Nelson S. B. (2002). Spike timing, calcium signals and synaptic plasticity. *Curr Opin Neurobiol* **12**, 305-314.
- Song S., Sjostrom P. J., Reigl M., Nelson S., and Chklovskii D. B. (2005). Highly nonrandom features of synaptic connectivity in local cortical circuits. *PLoS Biol* **3**, e68.
- Spruston N. (2008). Pyramidal neurons: dendritic structure and synaptic integration. *Nat Rev Neurosci* **9**, 206-221.
- Stout C. E., Costantin J. L., Naus C. C., and Charles A. C. (2002). Intercellular calcium signaling in astrocytes via ATP release through connexin hemichannels. *J Biol Chem* **277**, 10482-10488.
- Stuart G., and Spruston N. (1998). Determinants of voltage attenuation in neocortical pyramidal neuron dendrites. *J Neurosci* **18**, 3501-3510.
- Stuart G., Spruston N., Sakmann B., and Hausser M. (1997). Action potential initiation and backpropagation in neurons of the mammalian CNS. *Trends Neurosci* **20**, 125-131.
- Svenningsson P., Le Moine C., Fisone G., and Fredholm B. B. (1999). Distribution, biochemistry and function of striatal adenosine A2A receptors. *Prog Neurobiol* **59**, 355-396.
- Takata N., and Hirase H. (2008). Cortical layer 1 and layer 2/3 astrocytes exhibit distinct calcium dynamics in vivo. *PLoS One* **3**, e2525.
- Takigawa T., and Alzheimer C. (1999). G protein-activated inwardly rectifying K<sup>+</sup> (GIRK) currents in dendrites of rat neocortical pyramidal cells. *J Physiol* **517 ( Pt 2)**, 385-390.

Takigawa T., and Alzheimer C. (2003). Interplay between activation of GIRK current and deactivation of Ih modifies temporal integration of excitatory input in CA1 pyramidal cells. *J Neurophysiol* **89**, 2238-2244.

Thomson A. M. (2010) Neocortical layer 6, a review. *Front Neuroanat* **4**, 13.

Thomson A. M., and Lamy C. (2007). Functional maps of neocortical local circuitry. *Front Neurosci* **1**, 19-42.

Tononi G., and Cirelli C. (2006). Sleep function and synaptic homeostasis. *Sleep Med Rev* **10**, 49-62.

Trussell L. O., and Jackson M. B. (1985). Adenosine-activated potassium conductance in cultured striatal neurons. *Proc Natl Acad Sci U S A* **82**, 4857-4861.

Trussell L. O., and Jackson M. B. (1987). Dependence of an adenosine-activated potassium current on a GTP-binding protein in mammalian central neurons. *J Neurosci* **7**, 3306-3316.

Tsodyks M. V., and Markram H. (1997). The neural code between neocortical pyramidal neurons depends on neurotransmitter release probability. *Proc Natl Acad Sci U S A* **94**, 719-723.

Tsubokawa H., and Ross W. N. (1997). Muscarinic modulation of spike backpropagation in the apical dendrites of hippocampal CA1 pyramidal neurons. *J Neurosci* **17**, 5782-5791.

Turrigiano G. G. (1999). Homeostatic plasticity in neuronal networks: the more things change, the more they stay the same. *Trends Neurosci* **22**, 221-227.

Varela J. A., Sen K., Gibson J., Fost J., Abbott L. F., and Nelson S. B. (1997). A quantitative description of short-term plasticity at excitatory synapses in layer 2/3 of rat primary visual cortex. *J Neurosci* **17**, 7926-7940.

Vyazovskiy V. V., Olcese U., Hanlon E. C., Nir Y., Cirelli C., and Tononi G. (2011) Local sleep in awake rats. *Nature* **472**, 443-447.

Wall M. J., and Dale N. (2007). Auto-inhibition of rat parallel fibre-Purkinje cell synapses by activity-dependent adenosine release. *J Physiol* **581**, 553-565.

Wang Y., Markram H., Goodman P. H., Berger T. K., Ma J., and Goldman-Rakic P. S. (2006). Heterogeneity in the pyramidal network of the medial prefrontal cortex. *Nat Neurosci* **9**, 534-542.

Wang Y., Toledo-Rodriguez M., Gupta A., Wu C., Silberberg G., Luo J., and Markram H. (2004). Anatomical, physiological and molecular properties of

Martinotti cells in the somatosensory cortex of the juvenile rat. *J Physiol* **561**, 65-90.

Williams S. R., and Atkinson S. E. (2007). Pathway-specific use-dependent dynamics of excitatory synaptic transmission in rat intracortical circuits. *J Physiol* **585**, 759-777.

Williams S. R., and Stuart G. J. (1999). Mechanisms and consequences of action potential burst firing in rat neocortical pyramidal neurons. *J Physiol* **521 Pt 2**, 467-482.

Williams S. R., and Stuart G. J. (2000). Backpropagation of physiological spike trains in neocortical pyramidal neurons: implications for temporal coding in dendrites. *J Neurosci* **20**, 8238-8246.

Williams S. R., and Stuart G. J. (2002). Dependence of EPSP efficacy on synapse location in neocortical pyramidal neurons. *Science* **295**, 1907-1910.

Wu L. G., and Saggau P. (1997). Presynaptic inhibition of elicited neurotransmitter release. *Trends Neurosci* **20**, 204-212.

Yoshimura M., Doi A., Mizuno M., Furue H., and Katafuchi T. (2005). In vivo and in vitro patch-clamp recording analysis of the process of sensory transmission in the spinal cord and sensory cortex. *J Physiol Anthropol Appl Human Sci* **24**, 93-97.

Zimmermann H. (2000). Extracellular metabolism of ATP and other nucleotides. *Naunyn Schmiedebergs Arch Pharmacol* **362**, 299-309.

Zucker R. S., and Regehr W. G. (2002). Short-term synaptic plasticity. *Annu Rev Physiol* **64**, 355-405.